Promoter of the Project:

CONSTRUCTION ENGINEERING AND MANAGEMENT DEPARTMENT
CIVIL ENGINEERING FACULTY
WARSAW UNIVERSITY OF TECHNOLOGY
POLAND

Partners of the Project:

REYKJAVIK UNIVERSITY
ICELAND

TECHNICAL UNIVERSITY OF DARMSTADT
GERMANY

ASSOCIATION OF BUILDING SURVEYORS
AND CONSTRUCTION EXPERTS
UNITED KINGDOM

POLISH ASSOCIATION OF BUILDING MANAGERS
POLAND

CHARTERED INSTITUTE OF BUILDING
UNITED KINGDOM

AWBUD S.A.
POLAND

ISBN: 978-83-947920-4-6

M24: MECHANICS OF MATERIALS AND STRUCTURES FOR CONSTRUCTION MANAGERS

This book is a result of the project carried out within the framework of ERASMUS+ programme.

Project number: 2015-1-PL01-KA202-016454

MECHANICS OF MATERIALS AND STRUCTURES FOR CONSTRUCTION MANAGERS

THIS BOOK IS ELEMENT OF:

CONSTRUCTION MANAGERS' LIBRARY

CONSTRUCTION MANAGERS' LIBRARY, ERASMUS+ 2015-1-PL01-KA202-016454

MECHANICS OF MATERIALS AND STRUCTURES FOR CONSTRUCTION MANAGERS

Kazimierz Józefiak

Magda Kruk

Fabian Linnebacher

Daniela Löw

Christoph Motzko

Artur Zbiciak

Germany, Poland, 2017

This project has been funded with support from the European Commission.
This publication [communication] reflects the views only of the author , and the Commission cannot be held responsible for any use which may be made of the information contained therein.

Editors:
PhD. Eng. Paweł Nowak,
MSc. Eng. Jerzy Rosłon

Cover design:
PhD. Eng. Paweł Nowak
MSc. Eng. Jerzy Rosłon

ISBN 978-83-947920-4-6

Print and cover:
POLCEN Sp. z o.o.
ul. Nowogrodzka 31, lok. 333
00-511 Warszawa
www.polcen.com.pl
(księgarnia internetowa)

This manual is part of the Construction Managers' Library – a set of books related to the wide area of management in construction. The books were created within the Leonardo da Vinci (LdV) projects No: PL/06/B/F/PP/174014; 2009-1-PL1-LEO05-05016, 2011-1-PL1-LEO05-19888, and ERASMUS+ project No: 2015-1-PL01-KA202-016454, entitled: "COMMON LEARNING OUTCOME FOR EUROPEAN MANAGERS IN CONSTRUCTION, phases I, II, III and IV – CLOEMC)". Warsaw University of Technology, Civil Engineering Faculty, Department of Construction Engineering and Management was the Promoter of the Projects.

The following organisations were Partners in the CLOEMC I Project:

- Association of Building Surveyors and Construction Experts (Belgium),
- Universidad Politécnica de Valencia (Spain),
- Chartered Institute of Building Ireland (Ireland),
- Polish Association of Building Managers (Poland),
- Polish British Construction Partnership Sp. z o.o. (Poland),
- University of Salford (Great Britain),
- Chartered Institute of Building (Great Britain).

The objective of this project was to create first, seven manuals conveying all the information necessary to develop civil engineering skills in the field of construction management.

The following manuals have been developed in CLOEMC I (in the brackets you will find an estimate of didactic hours necessary for mastering the contents of a given manual):

M1: PROJECT MANAGEMENT IN CONSTRUCTION (100),
M2: HUMAN RESOURCE MANAGEMENT IN CONSTRUCTION (100),
M3: PARTNERING IN CONSTRUCTION (100),
M4: BUSINESS MANAGEMENT IN CONSTRUCTION ENTERPRISE(100),
M5: REAL ESTATE MANAGEMENT (100),
M6: ECONOMY AND FINANCIAL MANAGEMENT IN CONSTRUCTION (240),
M7: CONSTRUCTION MANAGEMENT (100).

The manuals created for the purposes of the library are available in three languages: Polish, Spanish and English. The manuals may be used as didactic materials for students of postgraduate courses and regular studies in all three languages. Graduates from the courses will receive a certificate, which is recognized by all organisations – members of the AEEBC, association of construction managers from over a dozen European countries.

Polish representative in the AEEBC is the Polish Association of Building Managers, in Warsaw.

Partners of the CLOEMC II project were:

- Technische Universität Darmstadt (Germany),

- Universida de do Minho (Portugal),
- Chartered Institute of Building (Great Britain),
- Association of European Building Surveyors and Construction Experts (Belgium),
- Polish British Construction Partnership (Poland),

Within the second part of the project the following manuals were developed:
M8: RISK MANAGEMENT (130)
M9: PROCESS MANAGEMENT – LEAN CONSTRUCTION (90),
M10: COMPUTER METHODS IN CONSTRUCTION (80),
M11: PPP PROJECTS IN CONSTRUCTION (80),
M12: VALUE MANAGEMENT IN CONSTRUCTION (130),
M13: CONSTRUCTION PROJECTS – GOOD PRACTICE (80),
The manuals were prepared in four languages: Polish, Portuguese, German and English.
Partners of the CLOEMC III project were:
- Technische Universität Darmstadt (Germany),
- Universida de do Minho (Portugal),
- Chartered Institute of Building (Great Britain),
- Thomas More Kempen University (Belgium),
- Association of European Building Surveyors and Construction Experts (Belgium),
- Polish Association of Building Managers (Poland).

Within the third part of the project the following manuals were developed:
M14: DUE-DILIGENCE IN CONSTRUCTION (100),
M15: MOTIVATION AND PSYCHOLOGY ASPECTS IN CONSTRUCTION INDUSTRY (100),
M16: PROFESSIONALISM AND ETHICS IN CONSTRUCTION (100),
M17: SUSTAINABILITY IN CONSTRUCTION (100),
M18: HEALTH AND SAFETY IN CONSTRUCTION (100),
M19: MANAGING BUILDING PATHOLOGY AND MAINTENANCE (100).
The manuals were prepared in five languages: Polish, Portuguese, German, French and English.
Partners of the CLOEMC IV project were:
- Technische Universität Darmstadt (Germany),
- Reykjavik University (Iceland),
- Chartered Institute of Building (Great Britain),
- AWBUD S.A. (Poland),
- Association of European Building Surveyors and Construction Experts (Belgium/Great Britain),
- Polish Association of Building Managers (Poland).

Within the fourth part of the project the following manuals were developed:
M20: REVITALISATION AND REFURBISHMENT IN CONSTRUCTION (100),
M21: BUILDING INFORMATION MODELING – BIM (120),
M22: OPTIMISATION OF CONSTRUCTION PROCESSES (120),
M23: DIVERSITY MANAGEMENT IN CONSTRUCTION (100),
M24: MECHANICS OF MATERIALS AND STRUCTURES FOR CONSTRUCTION MANAGERS (120),
M25: CSR - CORPORATE SOCIAL RESPONSIBILITY IN CONSTRUCTION (100).

The manuals were prepared in three languages: Polish, German and English (and additionally English version with summary in Icelandic language).

The scope of knowledge presented in the manuals is necessary in activities of managers - construction engineers, managing undertakings in the conditions of the modern market economy. The manuals are approved by the European AEEBC association as a basis for recognising manager qualifications. Modern knowledge in the field of management in construction, presented in the manuals, is one of prerequisites to obtain EurBE (European Building Expert) cards, a professional certificate documenting the qualification level of a construction manager in EU. The manuals are designated for managers - construction engineers, students completing postgraduate studies "Management in construction" and students completing construction studies. Postgraduate studies got a recognised program, and graduates receive certificates recognised by 17 national organisations, members of AEEBC.

More information:
- about the project: www.cloemcIV.il.pw.edu.pl
- about the EURBE CARD: www.aeebc.org

TABLE OF CONTENTS:

LEARNING OUTCOMES
(P. NOWAK)

This manual should be considered as gentle reminder of the mechanics of materials and structures issues for construction managers. It shows basics of the mechanics with examples for systemizing the knowledge acquired during studies.

First chapter of the manual underlines importance of the soil treatment and its properties. It shows classification of soli, physical and mechanical parameters, consolidation rules and calculations methods of shear strength of the soil.

Reader of the second chapter will know basics of structural mechanics, including types of planar linear structural elements, load and support idealization. There are many different types of structures with variety of shapes and materials used, which makes them complex for analyze and design. It is common to use simplifications by grouping elements with the same patterns or carrying similar type of loads. Then any complex structure can be split into simple structural elements. It is important for an engineer to recognize the various types of elements composing a structure and to be able to classify them as to the form and function. This process is called "structure idealization". Construction managers should know how to calculate basic tensions in the most common elements: the axial force, shear force, bending moment or the torque (twisting moment) in, at least, straight rods or columns.

Authors of the chapter 3 shows practical applications of the theory and discussed elements of shallow and deep foundations (relation of the structures and the soil), as well as present calculations for formworks (especially fresh concrete pressure), as the most popular element of the site.

Chapter 4 consists set of case studies case studies / exercises showing mathematical solutions of the chosen problems of mechanics of materials and structures.

CHAPTER 1
OUTLINE OF SOIL MECHANICS (A. ZBICIAK, K. JÓZEFIAK)

1.1 INTRODUCTION TO SOIL MECHANICS PROBLEMS

Soils, in the geotechnical sense, can be regarded as engineering materials. The physical characteristics of soils can be determined by experiment, and the application of methods of analysis enables these properties to be used to predict their likely behaviour under defined working conditions. But unlike other engineering materials such as metals and concrete, over which control can be exercised during manufacture, soils are naturally occurring materials, which more often than not have to be used in their natural condition. Even when some kind of processing is possible, either in-situ or by using excavated material, the soil can be modified only to a limited extent by relatively simple procedures on site [13].

The variety of soils is very wide indeed, and no two sites have identical soil conditions. It is therefore necessary to evaluate the physical properties and engineering behaviour of the soils present at every site that is developed in any way. Many of the procedures used for determining soil characteristics consist of empirical methods derived from practical experience [13].

Soils contain three components: solid, liquid, and gas. The solid components of soils are the product of weathered rocks. The liquid component is usually water, and the gas component is usually air. The gaps between the solid particles are called voids. The voids may contain air, water, or both. The soil structure in shown schematically in Figure 1.1. The total volume (V) and the total weight (W) of the specimen can be measured in the laboratory. Next, let us separate the three components of the soil as shown on the right-hand side of the Figure 1.1. The solid particles are gathered in one region such that there are no voids in between, as shown in the figure (this can only be done theoretically). The volume of this component is V_s and its weight is W_s. The second component is water, whose volume is V_w and whose weight is W_w. The third component is the air, which has a volume V_a and a very small weight that can be assumed to be zero. Note that the volume of voids (V_V) is the sum of V_a and V_w. Therefore, the

total volume is $V = V_v + V_s = V_a + V_w + V_s$. Also, the total weight $W = W_w + W_s$ [16].

When load is applied to a soil mass some part of the load is transferred to water and some to solid particles. Thus, the external load causes the rise of water pressure and the rise of stress within solid particles. The first is called pore pressure and the latter – effective stress.

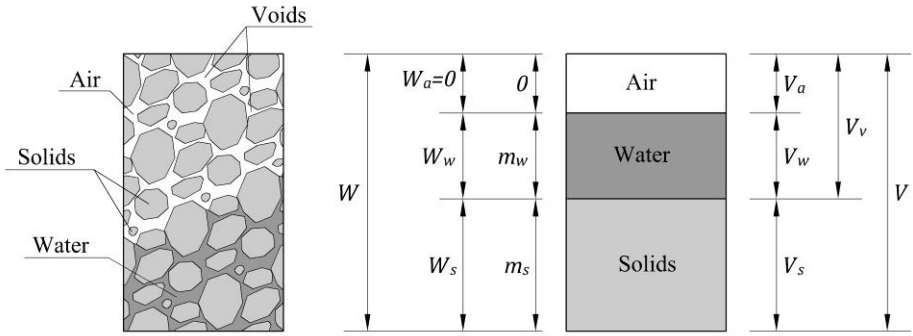

Fig. 1.1. Schematics of three-phase soil structure [16].

There are several ways in which water is held in cohesive soils, which contain clay minerals existing as plate-like particles of less than 2 μm across. The shape and very small size of these particles, together with their chemical composition, enables them to combine with or hold onto water by several complex means. A simplified illustration of the zones of water surrounding a clay particle is obtained by considering the following five categories of water, indicated in Figure 1.2 [13]:

1. Adsorbed water held on the surface of the particle by powerful forces of electrical attraction and virtually in a solid state. This layer is of very small thickness, perhaps of the order of 0.005 μm. This water cannot be removed by oven drying at 110°C, and may, therefore, be considered to be part of the solid soil grain.
2. Water which is not so tightly held and can be removed by oven drying, but not by air drying (hygroscopic moisture).
3. Capillary water, held by surface tension, generally removable by air drying.
4. Gravitational water, which can move in the voids between soil grains and is removable by drainage.

5. Chemically combined water, in the form of water of hydration within the crystal structure. Except for gypsum and some tropical clays, this water is not generally removable by oven drying.

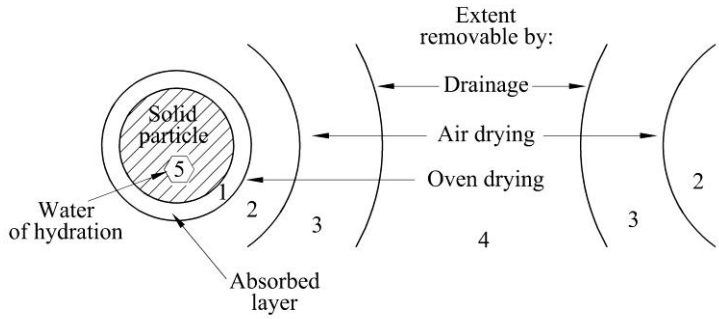

Fig. 1.2. Representation of categories of water surrounding clay particles [13].

For the purpose of routine soil testing, moisture content relates only to the water that is removable by oven drying at 105–110°C. The water of category 1 above is not taken into account in the determination of moisture content and will not be referred to again in that context [13].

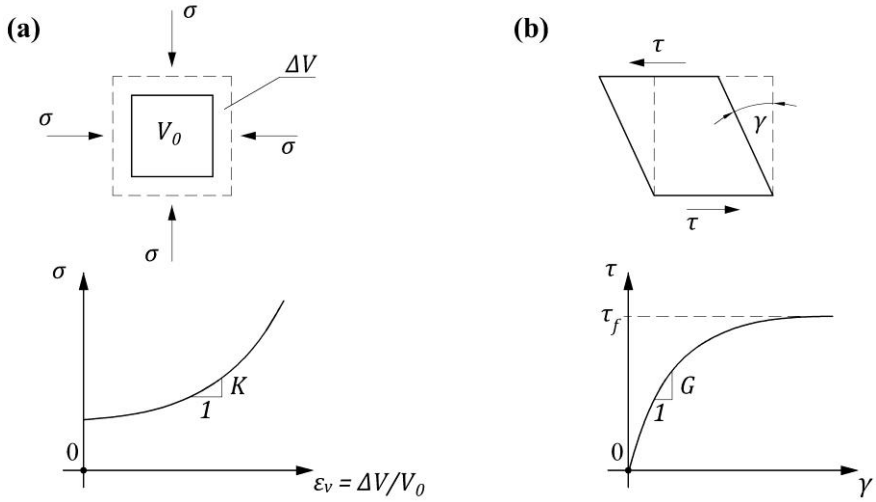

Fig. 1.3. Non-linear behaviour of a granular material.

Unlike for typical structural elements (e.g. beams, plates or trusses), for geotechnical structures, non-linear material behaviour has to be taken into account even in the elastic range. Figure 1.3a shows diagrammatically non-linear de-

pendency of bulk modulus K, whose value is related to volume strain level. Also, non-linear behaviour is seen for the pure shear stress state as shown in Figure 1.3b. In that figure, non-dilatant state is shown. The dilatancy phenomena will be explained in the next chapters.

Let us point out the essential features of soil behaviour related to soil strength:

1. External loads and water pressures interact with each other to produce a stress that is effective in controlling soil behaviour.
2. Soil is compressible. Volume changes occur as the grains rearrange themselves and the void space changes.
3. Soil shearing is basically frictional so that strength increases with normal stress and with depth in the ground. We will find out that soil stiffness with normal stress and depth.
4. Combining these basic features of soil behaviour leads to the observation that soil strength and stiffness decrease with increasing water pressure and with increasing water content.
5. Soil compression and distortion are generally not fully recoverable on unloading, so soil is essentially inelastic. This is a consequence of the mechanism of compression by rearrangement of the grains. They do not 'un-rearrange' on unloading.

Figure 1.4 illustrates a range of geotechnical structures. Except for the foundations, the retaining walls and the tunnel lining all are made from natural geological materials. In slopes and retaining walls the soils apply the loads as well as provide strength and stiffness. Geotechnical engineering is simply the branch of engineering that deals with structures built of, or in, natural soils and rocks. The subject requires knowledge of strength and stiffness of soils and rocks, methods of analyses of structures and hydraulics of groundwater flow. Use of natural soil and rock makes geotechnical engineering different from many other branches of engineering and more interesting. The distinction is that most engineers can select and specify the materials they use, but geotechnical engineers must use the materials that exist in the ground and they have only very limited possibilities for improving their properties. This means that an essential part of geotechnical engineering is a ground investigation to determine what materials are present and what their properties are. Since soils and rocks were formed by natural geological processes, knowledge of geology is essential for geotechnical engineering [5].

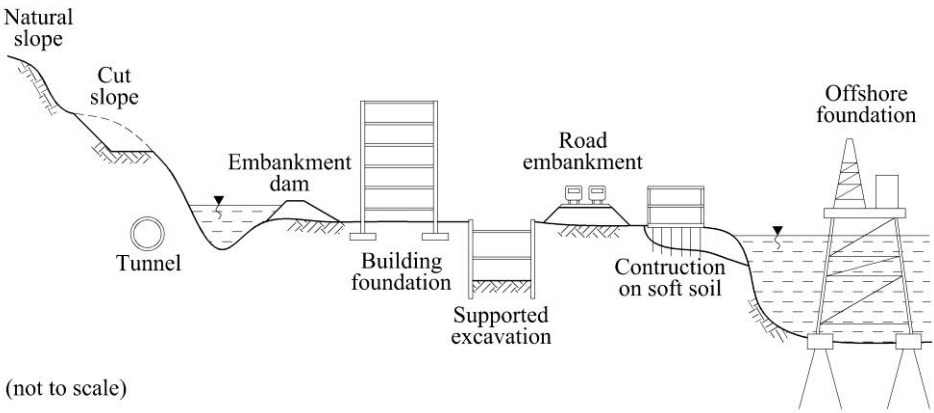

Fig. 1.4. Examples of geotechnical structures [5].

1.2 GENERAL CLASSIFICATION OF SOIL

1.2.1 Particle size limits and soil names

Basic soils are soil with uniform grading as they consist of particles of only one size range [1, 2]. Particle size fraction are shown in Table 1.1. Most soils are composite and consist of principal and secondary fractions. They are designated by a noun (main term) describing the principal fraction and by one or more adjectives (qualifying terms) describing the secondary fraction (e.g. gravely sand: grSa, silty clay: siCl, sandy silty clay: sasiCl) [1]. The principal fraction in terms of mass determines the engineering properties of the soil. It may be given in capital letters for clarity. Secondary and further fractions do not determine but will affect the engineering properties of the soil. [1].

The designation for soil consisting principally of organic matter are summarized in Table 1.2. Organic soils are generally considered as weak soils, not suitable for engineering purposes.

Table 1.1. Particle size fractions according to [1].

Soil fractions	Sub-fractions	Symbols	Particle sizes [mm]
Very coarse soil	Large boulder	LBo	> 630
	Boulder	Bo	200 ÷ 630
	Cobble	Co	63 ÷ 200
Coarse soil	Gravel: Coarse gravel Medium gravel Fine gravel	Gr CGr MGr FGr	2.0 ÷ 63 20 ÷ 63 6.3 ÷ 20 2.0 ÷ 6.3
	Sand: Coarse sand Medium sand Fine sand	Sa CSa MSa FSa	0.063 ÷ 2.0 0.63 ÷ 2.0 0.2 ÷ 0.63 0.063 ÷ 0.2
Fine soil	Silt: Coarse silt Medium silt Fine silt	Si FSi MSi FSi	0.02 ÷ 0.063 0.02 ÷ 0.063 0.0063 ÷ 0.02 0.002 ÷ 0.0063
	Clay	Cl	≤ 0.002

Table 1.2. Identification and description of organic soil according to [1]

Term	Description
Fibrous peat	Fibrous structure, easily recognizable plant structure, retains some strength
Pseudo-fibrous peat	Recognizable plant structure, no strength of apparent plant material
Amorphous peat	No visible plant structure, mushy consistency
Gyttja	Decomposed plant and animal remains; may contain inorganic constituents
Humus	Plant remains, living organisms and their excretions together with inorganic constituents; form the topsoil

1.2.2 Determination of particle size distribution

Mechanical analysis is the determination of the size range of particles present in a soil, expressed as a percentage of the total dry weight. Two methods generally are used to find the particle-size distribution of soil: sieve analysis and hydrometer analysis [16].

A set of standardized sieves is used for the analysis. Each sieve is 200 mm in diameter and 50 mm in height. The opening size of the sieves ranges from 0.075 mm for sieve No. 200 to 4.75 mm for sieve No. 4. A dry soil specimen is shaken through the sieves for 10 minutes. The percent by weight of soil passing each sieve is plotted as a function of the grain diameter (corresponding to a sieve number). It is customary to use a logarithmic horizontal scale on this plot [16].

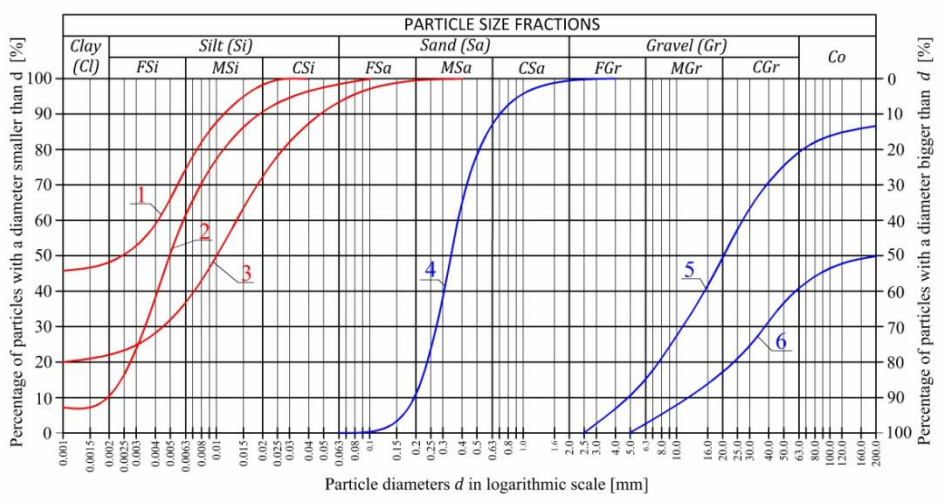

Fig. 1.5. Examples of particle size distribution curves.

Sieve analysis cannot be used for clay and silt particles because they are too small (<0.075 mm in diameter) and they will be suspended in air for a long time during shaking. The grain-size distribution of the fine particles can be obtained using hydrometer analysis. The basis of hydrometer analysis is that when soil particles are dispersed in water, they will settle at different velocities because of their different sizes. A dry soil specimen weighing 50 g is mixed thoroughly with water and placed in a graduated 1000-mL glass flask. A floating instrument called a hydrometer is placed in the flask to measure the specific gravity of the mixture in the vicinity of the hydrometer centre. In a 24-hour period the time t and the corresponding depth L are recorded [16].

Example particle size distribution curves are shown in Figure 1.5. The method of determination of soil name according to the standard [1] is shown in Figure 1.6.

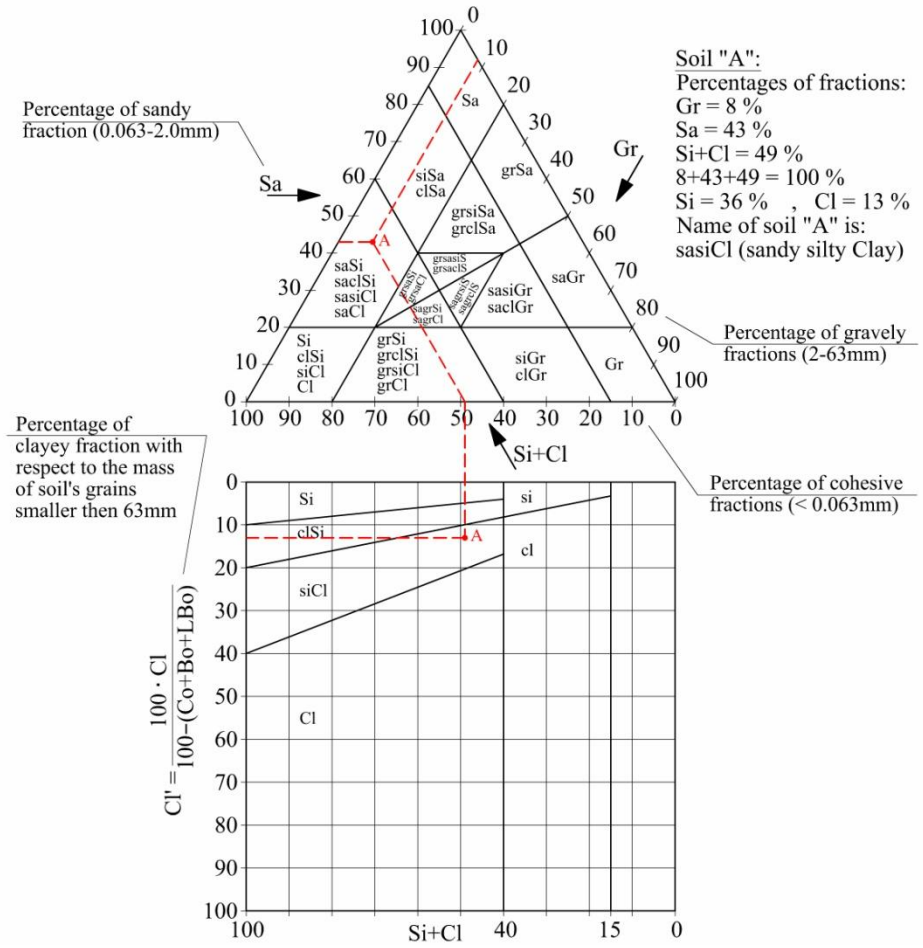

Fig. 1.6. Determination of soil name according to [1, 2].

1.3 PHYSICAL AND MECHANICAL PARAMETERS OF SOIL

1.3.1 Introduction

As a three-phase material, soil has to be characterized by more parameters then 'common' engineering materials like, for example, steel. In this section soil physical and mechanical parameters are defined according to [3, 4]. Please note that the weight, mass and density are related by gravity constant g and can be used interchangeably:

$$W = g \cdot m \tag{1.1}$$

$$\gamma = g \cdot \rho \tag{1.2}$$

where $g \approx 9.81 \frac{m}{s^2}$ is gravitational acceleration, $\rho \left[\frac{kg}{m^3}\right]$ – density, $m[kg]$ – mass, $W[N]$ – weight, $\gamma \left[\frac{N}{m^3}\right]$ – unit weight.

In this section we are going to use symbols for masses and volumes introduced in Figure 1.1. Also we are going to use SI unit system.

1.3.2 Moisture content and degree of saturation

Soil moisture content or water content is defined as

$$\omega = \frac{W_w}{W_s} \cdot 100 = \frac{m_w}{m_s} \cdot 100 \tag{1.3}$$

where we get ω in percent.

Table 1.3 presents ranges of values of natural water content (ω_n), that is water content of natural soil deposits. Note that organic soils like peat can contain more water than solids and thus water content higher than 100%.

Degree of saturation is the ratio of the volume of water to the volume of voids, defined as follows:

$$S_r = \frac{V_w}{V_v} \tag{1.4}$$

Table 1.3. Approximate values of natural water content [19, 24].

Soil type	ω_n
Granular soils (non-cohesive)	3 ÷ 28 %
Cohesive soils (plastic)	5 ÷ 50 %
Peat	25 ÷ 1500 %

1.3.3 Unit weight and density of soil

Bulk density (or 'wet' density) of soil is defined as

$$\rho = \frac{m}{V} \tag{1.5}$$

where $m = m_s + m_w$ and **unit weight of soil** (bulk unit weight) is defined as

$$\gamma = \frac{W}{V} = \frac{g \cdot \rho}{V} \tag{1.6}$$

Particle density of soil, that is density of soil solids is defined as

$$\rho_s = \frac{m_s}{V_s} \tag{1.7}$$

and particle unit weight or **unit weight of the soil solids**

$$\gamma_s = \frac{W_s}{V_s} = \frac{g \cdot \rho_s}{V_s} \tag{1.8}$$

Dry density of soil is defined as:

$$\rho_d = \frac{\mathrm{m_s}}{V} \tag{1.9}$$

and **dry unit weight** of soil

$$\gamma_d = \frac{W_s}{V} = \frac{g \cdot \rho_s}{V} \tag{1.10}$$

For a dry soil sample (without any voids filled with water) $W_w = 0$ and $W = W_s$. This means that a dry unit weight is a bulk unit weight of a dried soil. It is useful to relate various soil properties to a unit weight which a soil sample would have had without any water in it because we can eliminate water content from considerations.

In laboratory bulk density of soil can be determined using a measured cylinder to cut a soil sample.

Table 1.4. Typical values of particle density and particle unit weight [19, 24].

Soil type	Particle density	Particle unit weight
Clay	$2{,}71 \div 2{,}78\ Mg/m^3$	$26{,}59 \div 27{,}27\ kN/m^3$
Silt	$2{,}66 \div 2{,}67\ Mg/m^3$	$26{,}09 \div 26{,}19\ kN/m^3$
Sand	$2{,}65\ Mg/m^3$	$26{,}0\ kN/m^3$
Organic soils	$1{,}40 \div 2{,}60\ Mg/m^3$	$13{,}73 \div 25{,}51\ kN/m^3$

Particle density of soil is usually assumed from known results of laboratory tests available in literature as it doesn't change so much for common kinds of soil. Typical values of particle density and particle unit weight are summarised in Table 1.4.

1.3.4 Porosity and void ratio

Porosity is defined as

$$n = \frac{V_v}{V} \tag{1.11}$$

Void ratio is defined as

$$e = \frac{V_v}{V_s} \tag{1.12}$$

Relation between porosity and void ratio can be derived as follows:

$$e = \frac{V_v}{V_s} = \frac{V_v}{V - V_v} = \frac{\frac{V_v}{V}}{\frac{V}{V} - \frac{V_v}{V}} = \frac{n}{1-n} \tag{1.13}$$

We can also obtain a formula for porosity

$$n = \frac{e}{1+e} \tag{1.14}$$

In practice, to calculate porosity or void ratio, at first we need to determine soil particle density and dry density. Then we can use a relationship between porosity and the densities, which is derived as follows:

$$n = \frac{V_v}{V} = \frac{V - V_s}{V} = 1 - \frac{m_s}{V\rho_s} = 1 - \frac{\rho_d}{\rho_s} = \frac{\rho_s - \rho_d}{\rho_s} \tag{1.15}$$

Substituting Equation (1.15) into (1.13) we obtain

$$e = \frac{\rho_s - \rho_d}{\rho_d} \tag{1.16}$$

1.3.5 Soil consistency and Atterberg limits

Consistency is a term used to indicate the degree of firmness of cohesive soils. The consistency of natural cohesive soil deposits is expressed qualitatively by such terms as very soft, soft, stiff, very stiff and hard [16]. It is clear that the moisture (water) content has a great effect on a clayey soil, especially in terms of its response to applied loads.

Consider a very wet clay specimen that looks like slurry (fluid). In this liquid state the clay specimen has no strength (i.e., it cannot withstand any type of loading). Consider a potter's clay specimen that has a moderate amount of moisture. This clay is in its plastic state because in this state we can actually make shapes out of the clay knowing that it will not spring back as elastic materials do [16]. If we let this plastic clay dry out for a short time (i.e., so that it is not totally dry), it will lose its plasticity because if we try to shape it now, many cracks will appear, indicating that the clay is in its semisolid state. If the specimen dries out further, it reaches its solid state, where it becomes exceedingly brittle [16].

The liquid limit is obtained in the laboratory using a simple device Casagrande Liquid Limit Device that includes a shallow brass cup and a hard base against which the cup is bumped repeatedly using a crank-operated mechanism. The cup is filled with a clay specimen (paste), and a groove is cut in the paste using a standard tool [16]. The liquid limit w_L is the moisture content at which the shear strength of the clay specimen is so small that the soil "flows" to close the aforementioned groove at a standard number of blows. [16].

However, the Casagrande method is not recommended by Euro code 7 [4]. According to the standard liquid limit should be determined using a cone penetrometer method described in the code CEN ISO/TS 17892-12.

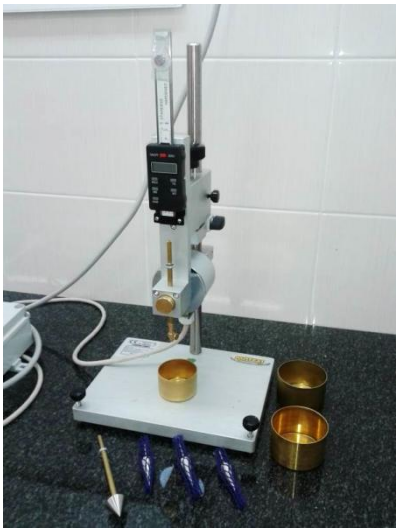

Fig. 1.7. An example cone penetrometer device used for determination of liquid limit according to [3] (Faculty of Civil Engineering at Warsaw University of Technology).

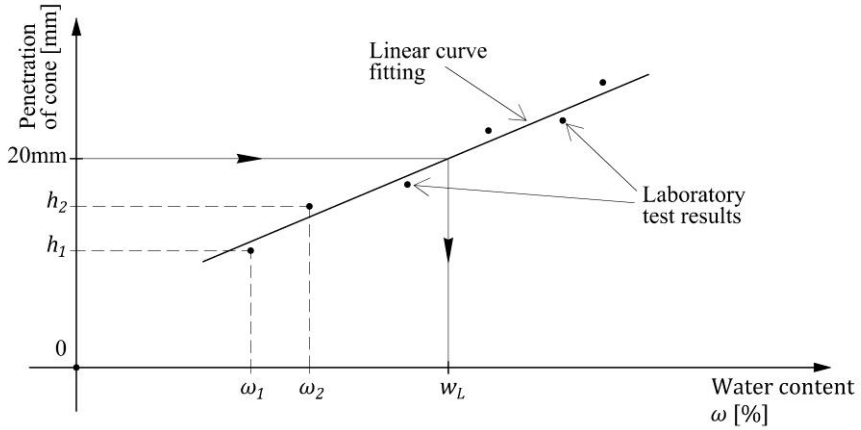

Fig. 1.8. Determination of liquid limit from cone penetrometer test results (for cone mass 80 grams and cone tip angle 30°).

In this method properly prepared soil 'paste' is put into a normalized cup. A cone with standardized dimensions, shape and mass is positioned over the soil cup with cone's tip touching soil's smoothened surface. Then the cone is released, free-falls into the soil paste and blocked again after 5 seconds. The depth of penetration is read. Several penetration are carried out with different water

contents of soil paste. For a cone with a mass of 80 grams and a cone tip angle of 30 degrees liquid limit is the water content at which the cone's penetration is equal to 20 mm. An example of cone penetrometer device is shown in Figure 1.7. Determination of liquid limit based on laboratory test results is shown in Figure 1.8.

The plastic limit is defined as the moisture content at which a soil crumbles when rolled down into threads 3 mm in diameter. To do that, use your hand to roll a round piece of clay against a glass plate. Being able to roll a moist piece of clay is an indication that it is now in its plastic state. By rolling the clay against the glass, it will lose some of its moisture moving toward its semisolid state. Crumbling of the thread indicates that it has reached its semisolid state. The moisture content w_P of the thread at that stage can be measured to give us the plastic limit, which is the verge between the plastic and semisolid states [16].

In its semisolid state, soil has some moisture. As a soil loses more moisture, it shrinks. When shrinking ceases, the soil has reached its solid state. Thus, the moisture content at which a soil ceases to shrink is the shrinkage limit, which is the verge between the semisolid and solid states [16].

The moisture range between plastic limit and liquid limit is known as the plasticity index:

$$I_P = w_L - w_P \tag{1.17}$$

Liquidity index, denoted by I_L (Lambe and Whitman, 1967) is defined as

$$I_L = \frac{w_n - w_P}{w_L - w_P} = \frac{w_n - w_P}{I_P} \tag{1.18}$$

Relative consistency, denoted by C_r (Terzaghi and Peck, 1948) or I_C (Euro code 7) is defined as

$$C_r \equiv I_C = \frac{w_L - w_n}{w_L - w_P} = \frac{w_L - w_n}{I_P} \tag{1.19}$$

Note that $I_C = 1 - I_L$. Standard [1] introduces terms describing soil consistency based on values of relative consistency. The terms along with Atterberg limits are summarized in Figure 1.9.

Soil consistency can also be determined approximately using macroscopic analysis as described in Table 1.5.

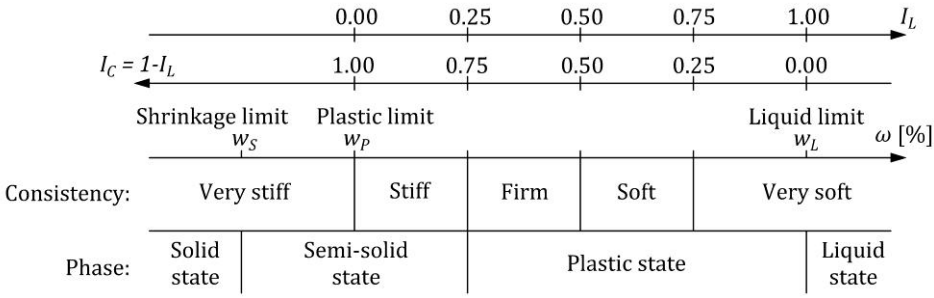

Fig. 1.9. Visualization of Atterberg limits [13, 16]

Table 1.5. Description of cohesive soil consistency [2]

Relative consistency I_C [-]	**Description of soil consistency**	**Manual approximate identification**
< 0,25	Very Soft	Exudes between the fingers when squeezed in the hand
0,25 – 0,50	Soft	Can be moulded by light finger pressure
0,50 – 0,75	Firm	Can be rolled in the hand to 3 mm thick threads without breaking or crumbling
0,75 – 1,00	Stiff	Crumbles and breaks when rolled to 3 mm thick threads but is sufficiently moist to be moulded to a lump again
> 1,00	Very Stiff	Has dried out and is mostly light coloured. It can no longer be moulded but crumbles under pressure. It can be indented by the thumbnail.

1.3.6 Relative density (density index)

Consider a uniform sand layer that has an in-situ void ratio e. It is possible to tell how dense this sand is if we compare its in-situ void ratio with the maximum and minimum possible void ratios of the same sand [16].

Relative density parameter is defined only for non-cohesive (granular) soils (e.g. sands or gravels) and only for natural soil deposits as

$$D_r = \frac{e_{max} - e}{e_{max} - e_{min}} \equiv I_D \tag{1.20}$$

If soil is in its densest possible state $e = e_{min}$ and $D_r = 1.0$. On the other hand, if $e = e_{max}$ density index $D_r = 0.0$ and it describes the loosest possible condition. Void ratio e without any indexes is the void ratio of a soil deposit. So, to calculate relative density, void ratio (density) of a soil deposit has to be also determined in a field test.

Relative density parameter can also be defined by soil sample volumes as follows:

$$D_r = \frac{e_{max} - e}{e_{max} - e_{min}} = \frac{\frac{V_{v,max}}{V_s} - \frac{V_v}{V_s}}{\frac{V_{v,max}}{V_s} - \frac{V_{v,min}}{V_s}} = \frac{V_{v,max} - V_v}{V_{v,max} - V_{v,min}} = \frac{(V_{max} - V_s) - (V - V_s)}{(V_{max} - V_s) - (V_{min} - V_s)} \tag{1.21}$$

so

$$D_r = \frac{V_{max} - V}{V_{max} - V_{min}} \tag{1.22}$$

Relative density of soil is commonly determined in a field test called dynamic probing according to the European standard [4]. However, the parameter can be also obtained in a laboratory on a disturbed sample of dried granular soil. It is beneficial to analyse this simple test as it is explicitly related to relative density definition and thus gives better understanding of the parameter. First, dried granular soil is poured into a steel cylinder from the lowest possible height. A funnel is used to achieve this. In this way a loosest possible state is achieved and the volume of the cylinder filled with that loose sand is the maximum possible volume. To obtain the minimum possible volume the soil in the cylinder is compacted by vibration. Having V_{max} and V_{min} determined it is possible to calculate e_{max}, e_{min} and D_r.

Standard [2] introduces terms describing the density state of a granular soil deposit. These are shown in Table 1.6.

Table 1.6. Description of soil related to density index [2].

Relative density [%]	**Description of soil deposit**
0-15	Very loose
15-35	Loose
35-65	Medium
65-85	Dense
85-100	Very dense

1.3.7 Compaction of soil

Soil compaction is defined as the method of mechanically increasing the density of soil by reducing volume of air as shown in Figure 1.10.

With proper compaction, the soil becomes stronger (higher shear strength), less compressible when subjected to external loads (i.e., less future settlement), and less permeable, making the soil a good construction material for highway embankments, ramps, earth dams, dikes, backfill for retaining walls and bridge abutments, and many other applications.

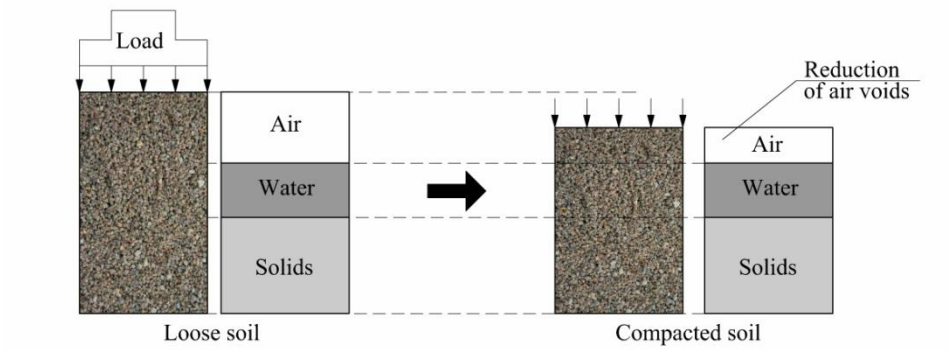

Fig. 1.10. Schematics of soil compaction

Optimum water content is the soil's water content at which the soil can be compacted most effectively by a given compaction effort. It is determined in a laboratory or field compaction test. In the laboratory, so-called Proctor com-

paction test is carried out, in which the soil is compacted in three or five layers in a cylindrical mould of a normalized size. Every layer is compacted by an appropriate number of blows of a rammer free-falling from a specified height. The number of blows for each layer, rammer falling height and mass, number of layers and mould's volume are given to achieve assumed compaction effort (i.e. specified compaction energy for a unit volume of soil in the mould). This compaction effort depends on the type and performance of equipment used for compaction of a geotechnical structure at a building side. The soil with different water contents is compacted as described above and for every compactor procedure a pair of water content ω and dry density ρ_d is obtained as shown in Figure 1.11. The maximum of the curve fitted between the laboratory test points gives information regarding optimum water content and maximum dry density which can be achieved by applying a given compaction effort.

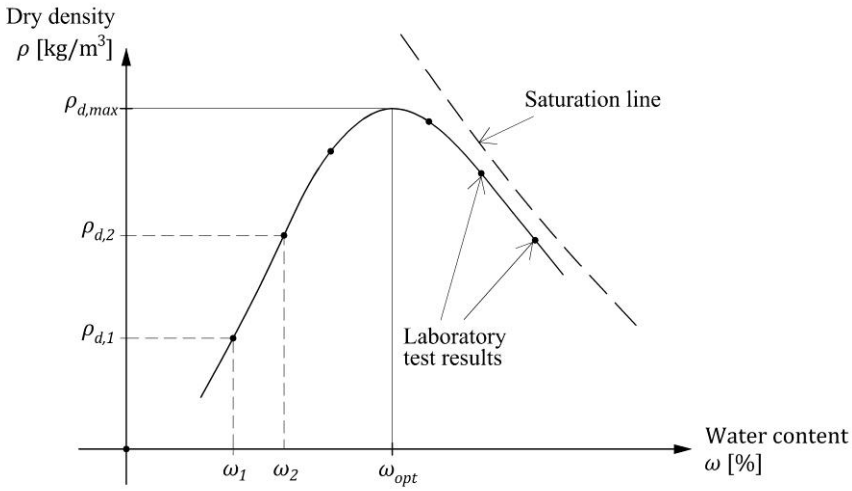

Fig. 1.11. Relationship between water content and dry density obtained in a Proctor compaction test

The dashed curve visualizes the state when volume of air voids is equal to zero ($S_r = 1.0$). This curve can be obtained from a theoretical formula describing the soil's dry density function at a constant volume of air voids (derivation can be found in [16]):

$$\rho_d(w) = \frac{1-\frac{V_a}{100}}{\frac{1}{\rho_S}+\frac{w}{100}} \tag{1.23}$$

in which $V_a = 0\%$ should be substituted, where: V_a – ratio of air void volume to the total volume [%].

Relative compaction is defined as

$$R_C \equiv I_S = \frac{\rho_{d-field}}{\rho_{d-max}} \tag{1.24}$$

A type of Proctor device used in laboratories is shown in Figure 1.12.

Fig. 1.12. Proctor's device used in geotechnical laboratory (Faculty of Civil Engineering at Warsaw University of Technology).

1.4 IN-SITU STRESS STATE IN SOIL

1.4.1 Introduction

In-situ or overburden stress in soil is an effective stress state which exists in a soil deposit before any construction of an engineering structure is considered. Overburden stress is related to self-weight of soil layers.

In a real design condition loads from the whole engineering structure induce stress in the soil mass through foundations. This additional loading can be taken into account in a simplified way, by introducing the superposition principle. In such a case the stress state caused by a building should be added to the initial overburden stress state existing in a soil mass.

1.4.2 Effective stress principle

When water is present within the soil strata, we need to distinguish between the stress and effective stress.

The strength and compressibility of the soil depend on the effective stresses that exist within the soil grains.

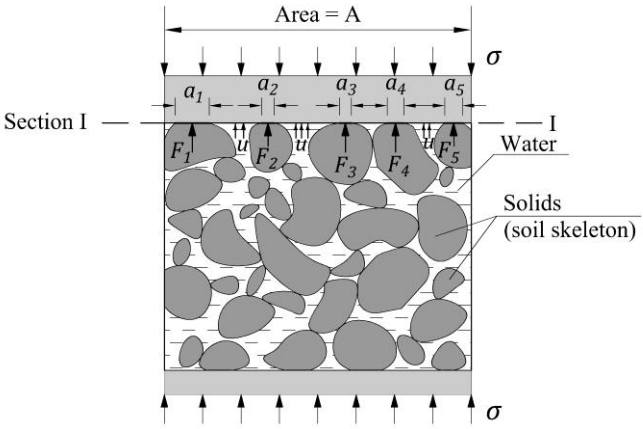

Fig. 1.13. Visualisation of effective stresses [16].

Effective stress is related to forces which are induced on soil solids (soil skeleton). According to the schematics shown in Figure 1.13 in section I-I we define the effective stress as

$$\sigma' = \frac{F_1+F_2+F_3+F_4+F_5}{A} \tag{1.25}$$

where $F_1, \dots, F_5$ are the normal components of contact forces between the soil grains and section I-I., and A is the total cross-sectional area of the soil sample. From force equilibrium at Section I-I we obtain

$$\sigma\, A = \sigma' A + u\,[A - (a_1 + a_2 + a_3 + a_4 + a_5)] \tag{1.26}$$

where u is pore-water pressure (that is the pressure of water within the soil sample), and the sum of $a_1, \dots, a_5$ is the contact area between the soil grains and section I-I. This contact area is very small compared to the total area A so we can assume

$$a_1 + a_2 + a_3 + a_4 + a_5 \approx 0 \tag{1.27}$$

Therefore,

$$\sigma A = \sigma' A + uA \approx 0 \tag{1.28}$$

so

$$\sigma = \sigma' + u \tag{1.29}$$

Equation (1.29) is the effective stress principle which was formulated by Terzaghi in 1936. It can be generalized for a three-dimensional stress state

$$\boldsymbol{\sigma} = \boldsymbol{\sigma}' + u\boldsymbol{I} \tag{1.30}$$

We assume that soil located under the groundwater table is fully saturated, that is all voids between the soil grains are filled with water (no air). Also, we assume that the soil above the groundwater table is dry.

1.4.3 Vertical in-situ soil stresses

In general, if there is no ground water table, effective vertical in-situ soil stress can be calculated as

$$\sigma_{z\rho} = \sigma'_{z\rho} = \sum_{i=1}^{n} g\rho_i h_i = \sum_{i=1}^{n} \gamma_i h_i \tag{1.31}$$

where n – number of soil layers, h_i – thickness of an i-th layer, $g \approx 9.81\frac{m}{s^2}$ – gravitational acceleration.

However, there are a few special cases, in which ground water table should be taken into account. These cases are shown in Figures 1.14 and 1.15.

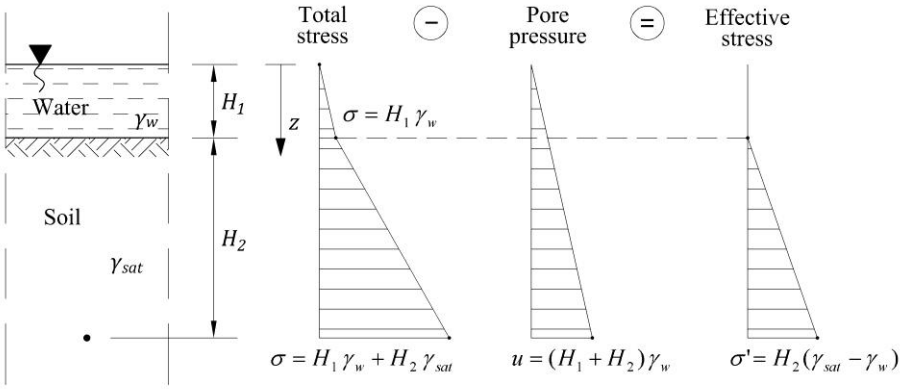

Fig. 1.14. Calculation of vertical in-situ stresses [16].

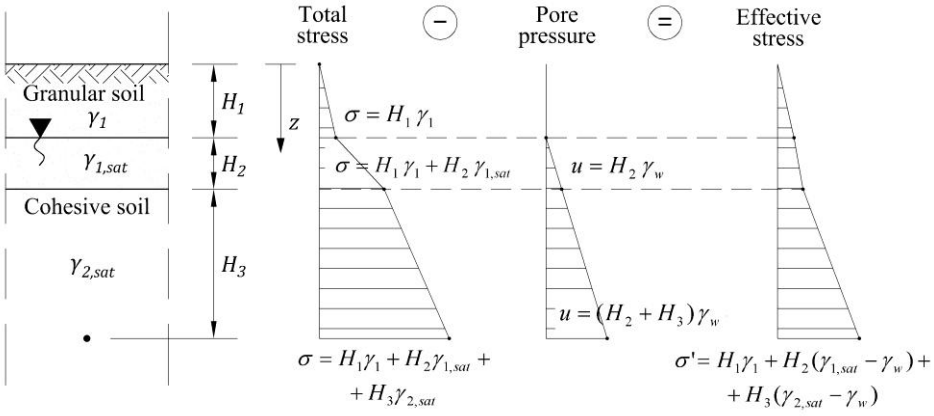

Fig. 1.15. Calculation of vertical in-situ stresses [16].

1.4.4 Horizontal in-situ soil stresses

Horizontal effective in-situ stress is calculated as

$$\sigma'_{x\rho} = \sigma'_{y\rho} = K_0 \, \sigma'_{z\rho} \tag{1.32}$$

where K_0 – coefficient of lateral earth pressure at rest.

Assuming that the soil is a linear elastic material, from theory of elasticity we can obtain:

$$K_0 = \frac{\nu}{1-\nu} \tag{1.33}$$

This approximation can be applied only for cohesive soils.

In case of overconsolidated soil deposits (for example consolidated – i.e. loaded - in the past by glaciers or dunes) K_0 coefficient can be estimated from Schmidt's formula

$$K_0 = (1 - \sin\phi') \cdot OCR^{\sin\phi'} \tag{1.34}$$

where ϕ' - effective internal friction angle, OCR – overconsolidation ratio

$$OCR = \frac{\sigma'_c}{\sigma'_0} \tag{1.35}$$

where σ'_c - overburden stress which existed in a soil layer in the past (for example caused by glaciation), σ'_0 - overburden stress in a soil layer at present.

For a normally consolidated soil $OCR = 1.0$ and

$$K_0 = (1 - \sin\phi') \tag{1.36}$$

Relationship (1.36) is called Jaky's formula and can be used for normally consolidated granular soils.

1.4.5 Capillary Rise

Soil pores are interconnected and they form a net of irregular tiny tubes. Due to the capillary phenomenon, water will rise above the water table through these tubes, forming a partially saturated zone of capillary rise. The height, above the water table to which the soil is partially saturated is called the capillary rise. This height is dependent on the grain size and soil type. In coarse soils capillary rise is very small, but in clays it can be over 10 m [16].

The pore pressure below the water table is considered positive and increases linearly with depth as discussed earlier. Above the water table, however, pore water pressure is negative (suction) and increases linearly, in absolute value, with the height above the water table [16].

$$\mathrm{u} \approx -\frac{S\%}{100}\gamma_w h_w \tag{1.37}$$

The soil within the zone of capillary rise becomes substantially stronger because of the negative pore water pressure. Negative pore water pressure causes an

increase in the effective stress: $\sigma' = \sigma - (-u) = \sigma + u$, hence the increase in strength. This is a direct consequence of the principle of effective stress [16].

An example problem of determination horizontal overburden stress state in a soil deposit taking into account capillary rise is shown in the "case problem" section below.

1.5 CONSOLIDATION

1.5.1 General principle

The process of consolidation in soil can be explained using a spring-piston analogy. The analogy was first introduced by Terzaghi and Peck in 1948. The simplified version of the model was described by Taylor (1948). The analogy also visualises the effective stress principle introduced in the previous section.

Consider a cylindrical container fitted with a watertight but frictionless piston of negligible mass, of area $A = 1m^2$, and provided with a drainage valve connected to a small-bore outlet tube. The container is filled with water, and between the piston and the base is an elastic compression spring (see Figure 1.17). Initially the system is in equilibrium with the valve closed and no load on the piston. The spring is not compressed and there is no excess pressure in the water. A weight of 200 N is now applied to the piston (see Figure 1.17). Water is not allowed to escape, so the piston cannot move down and the spring is not compressed.

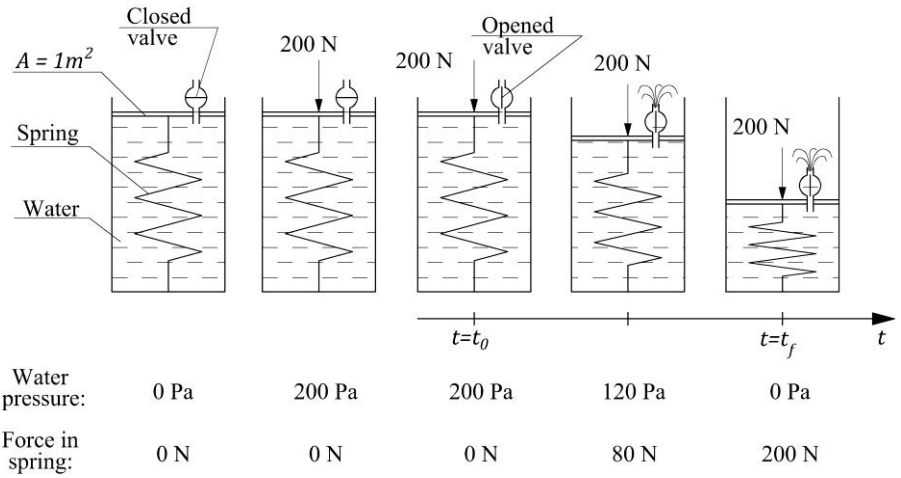

Fig. 1.17. Piston and spring analogy for soil consolidation process [14].

The downward force is therefore supported by an upward force on the piston due to an additional pressure in the water. This pressure, called the excess hydrostatic pressure, is equal to 200/A = 200 Pa. At a certain instant (time $t = t_0$), the drainage valve is opened and the timer clock is started. Water can now begin to escape from the cylinder (see Figure 1.17), but only slowly because of the small bore of the outlet tube. The piston sinks slowly, resulting in progressively more load being carried by the spring and less by the pressure of the water. Finally the spring is fully compressed by the applied force and carries the whole of the load. There is now no excess pressure in the water, equilibrium is restored and movement has ceased (see right-hand side of Figure 1.17). The loads carried by the spring and by the water at various time intervals from the start are shown in Figure 1.7. When equilibrium is reached, compression is 100% complete [14].

The behaviour of the mechanical model described above is analogous to the behaviour of soils during the consolidation process. The stress induced by the externally applied load is known as the 'total stress' and is denoted by $\boldsymbol{\sigma}$. The pressure in the water in the voids between solid particles in a soil is known as the 'pore water pressure' (p.w.p.), or pore pressure, and is denoted by u, or sometimes u_w [14]. The force in the spring is called the effective stress and denoted by $\boldsymbol{\sigma'}$.

When an external load is applied to a saturated clay soil ($S_r = 1.0$), the entire load is at first carried by the additional pore water pressure that is induced, re-

ferred to as the 'excess pore water pressure', which is equal to the total applied stress [14].

The process of consolidation shouldn't be confused with the process of compaction, where the change in volume is caused by the reduction of air voids in an unsaturated soil sample. The consolidation is related to saturated soil, and the change in volume is cause be the reduction of voids filled with ground water. Settlement of foundations is connected with the process of consolidation.

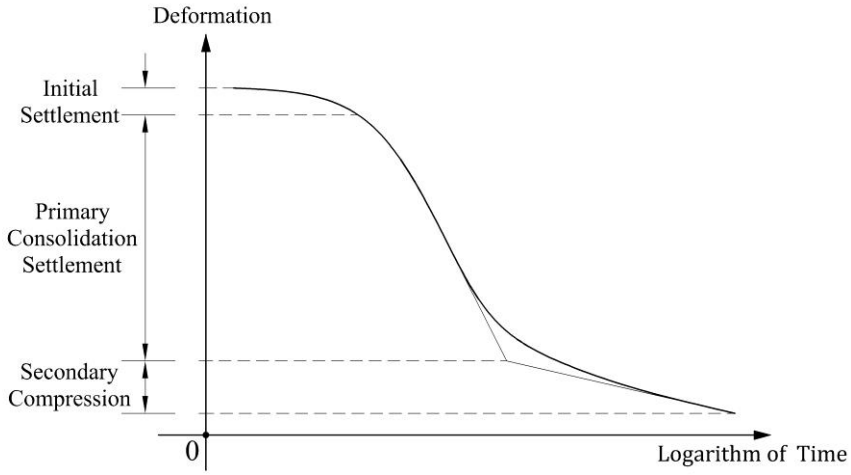

Fig. 1.18. Typical consolidation curve obtained from one loading stage of an oedometer or isotropic triaxial consolidation test [16].

In soil mechanics two problems are being solved simultaneously: one is related to the deformation of the soil skeleton (soil solids) and the second is described by the equations of fluid mechanics (specifically Darcy's law that describes the flow of a fluid through a porous medium).

1.5.2 Oedometer consolidation test

The consolidation characteristics of a soil can be measured in the laboratory using the one-dimensional consolidation test [16]. A cylindrical specimen of soil measuring 75 mm in diameter and approximately 15 mm in thickness is enclosed in a metal ring and subjected to staged static loads. Each load stage lasts 24 hours, during which changes in thickness are recorded. The load is doubled with each stage up to the required maximum (e.g.: 100, 200, 400, 800 kPa)

[16]. Figure 1.18 shows an example of the settlement versus time curve obtained from one loading stage. Three types of deformations are noted in the figure: initial compression, primary consolidation settlement, and secondary compression or creep. Initial compression is caused by the soil's elastic response to applied loads. Primary consolidation settlement is caused by the dissipation of the excess pore pressure generated by load application (the process generally called consolidation).

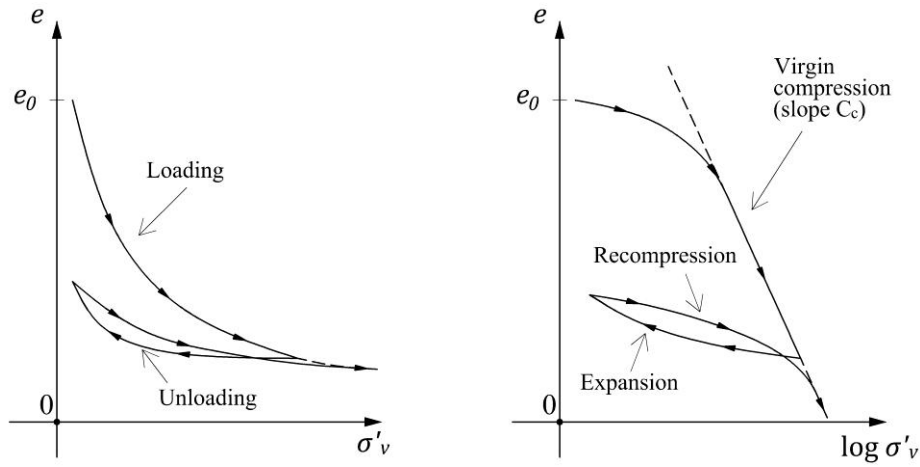

Fig. 1.19. Consolidation curves showed on linear and semi logarithmic plot.

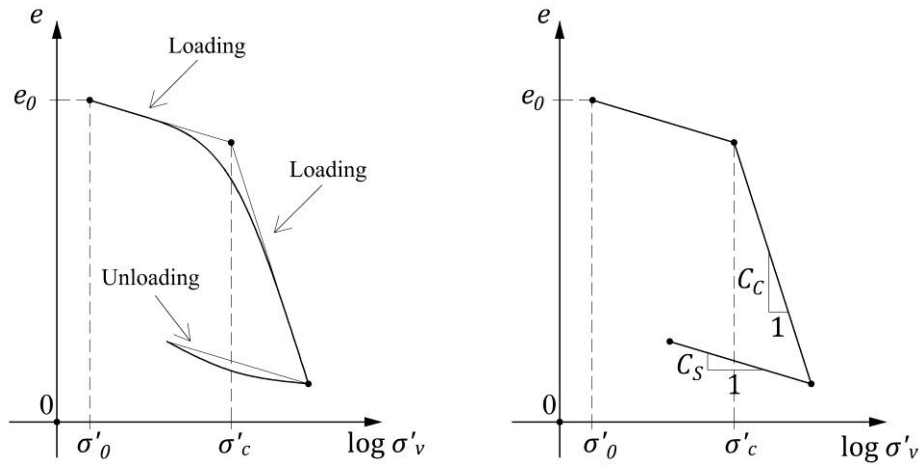

Fig. 1.20. Oedometer or triaxial consolidation curves: void ratio vs log σ_v and its idealization [16]

Secondary compression is caused by the time-dependent deformation behaviour of soil particles, which is not related to excess pore pressure dissipation. Primary consolidation settlement is our focus in this section [16].

Enclosing the soil specimen in a circular metal ring is done to suppress lateral strains. The specimen is sandwiched between two porous stones and kept submerged during all loading stages; thus, the specimen is allowed to drain from top and bottom [16].

After every loading stage, when the change in height of the specimen stops changing, we know that the excess pore pressure is zero and the load divided by the sample cross-sectional area is equal to the effective stress. Plotting the measurements of the effective stress and void ratio at the end of every consolidation stage we obtain a non-linear relationship shown on the left-hand side of Figure 1.19. This relationship is piecewise linear when plotted on a semi logarithmic graph as shown in Figure 1.19 and 1.20.

The void ratio versus logarithm vertical effective-stress relationship (e–log σ'_v) is obtained from the changes in thickness at the end of each load stage of a one-dimensional consolidation test. An example of an e–log σ'_v curve is shown in Figure 1.20.

Now define a preconsolidation pressure σ'_c as the maximum past pressure to which a clay layer has been subjected throughout time. A normally consolidated (NC) clay is defined as a clay that has a present (in situ) vertical effective stress σ'_0 equal to its preconsolidation pressure σ'_c. An overconsolidated (OC) clay is defined as a clay that has a present vertical effective stress of less than its preconsolidation pressure. Finally, define an overconsolidation ratio (OCR) as the ratio of the preconsolidation pressure to the present vertical effective stress (see Equation 1.33) [16].

The preconsolidation pressure is located near the point where the e–log(σ'_v) curve changes in slope, as shown in Figure 1.20. Other consolidation parameters, such as the compression index (C_c) and swelling index (C_s), are also obtained from the e–log(σ'_v) curve. The compression index is the slope of the loading portion, in the e-log(σ'_v) curve, and the swelling index is the slope of the unloading portion, as indicated in Figure 1.20 [16]. These parameters are used to calculate settlement of shallow foundations as described in the next sections.

1.6 SHEAR STRENGTH OF SOIL

1.6.1 Introduction

The term shear strength, as applied to soils, is not a fundamental property of a soil in the same way as, for instance, the compressive strength is a property of concrete. On the contrary, shear strength is related to the conditions prevailing in-situ, and can also vary with time. The value measured in the laboratory is likewise dependent upon the conditions imposed during the test and in some instances upon the duration of the test. The aspects of shear strength dealt with in this section can be divided into four categories [14].

1. The shear resistance of free-draining non-cohesive soils (i.e. sands and gravels), which is virtually independent of time.
2. The drained shear strength of cohesive soils, which depends upon the rate of displacement being slow enough to permit full drainage to take place during shear.
3. The long-term or residual drained shear strength of soils such as over-consolidated clays, for which a slow rate of displacement and a large displacement movement are required.

4. The shear strength of very soft cohesive soils under undrained conditions, i.e. in which shearing is applied relatively quickly [14].

The shear strength of soil is the shear resistance offered by the soil to overcome applied shear stresses. Shear strength is to soil as tensile strength to steel. When you design a steel truss for a bridge, for example, you have to make sure that the tensile stress in any truss element is less than the tensile strength of steel, with some safety factor. Similarly, in soil mechanics one has to make sure that the shear stress in any soil element underlying a shallow foundation, for example, is less than the shear strength of that particular soil, with some safety factor [16].

In soils the shear strength, τ_f , is a function of the applied normal effective stress, σ'_n. The Mohr–Coulomb failure criterion provides a relationship between the two:

$$\tau_f = c' + \sigma'_n \tan \phi' \tag{1.38}$$

where: $c'[kPa]$ - effective cohesion of the soil, $\phi'[deg]$ - effective internal friction angle of the soil. These two parameters are termed the strength parameters of a soil. They can be obtained from laboratory and field tests [16].

Short-term or 'immediate' shear strength of soils measured under fast rates of loading is related only to cohesion resistance and called undrained shear strength, denoted by c_u $[kPa]$.

1.6.2 Direct shear test

The shearbox test is the simplest, the oldest and the most straightforward procedure for measuring the shear strength of soils in terms of total or effective stresses. It is also the easiest to understand. In principle the shearbox test is an 'angle of friction' test, in which one portion of soil is made to slide along another by the action of a steadily increasing horizontal shearing force, while a constant load is applied normal to the plane of relative movement. These conditions are achieved by placing the soil in a rigid metal box, square in plan, consisting of two halves. The lower half of the box can slide relative to the upper half when pushed (or pulled) by a motorised drive unit, while a yoke supporting a load hanger provides the normal pressure. The usual shearbox apparatus provides no control of drainage and no provision for measuring pore water pressure. It is therefore not suitable for carrying out undrained tests, and its usual application is restricted to drained tests in which effective stresses are equal to total stresses. During the shearing process the applied shearing force is steadily increased. The resulting relative displacement of the two portions of the specimen, and the applied force, are both measured at suitable intervals so that a load–displacement curve can be drawn. The vertical movement of the top

surface of the specimen, which indicates changes of volume, is also measured and enables changes in density and voids ratio during shear to be evaluated [14].

Most commercial shearbox machines are still based on the displacement control principle (see Figure 1.21) and today provide a wide range of displacement speeds, from a few millimetres per minute to about 10,000 times slower. Electronic control using thyristors provides steplessly variable speed control throughout a similar range [14].

In order to carry out a slow 'drained' shear test, provision is made for the specimen to be consolidated before shearing and for further drainage to take place during shear at a suitably slow rate of displacement, so that the consolidated-drained (effective) shear strength parameters (c' and ϕ') can be determined. The use of reversing attachments enables a specimen to be re-sheared a number of times in order to determine the drained residual shear strength [14].

The shear strength envelope obtained from a set of drained tests is typically of the form shown in Figure 1.22. The envelope is approximately linear, the inclination to the horizontal axis being the angle of shear resistance in terms of effective stress, ϕ'. The intercept with the shear stress axis gives the apparent cohesion in terms of effective stress, denoted by c' .

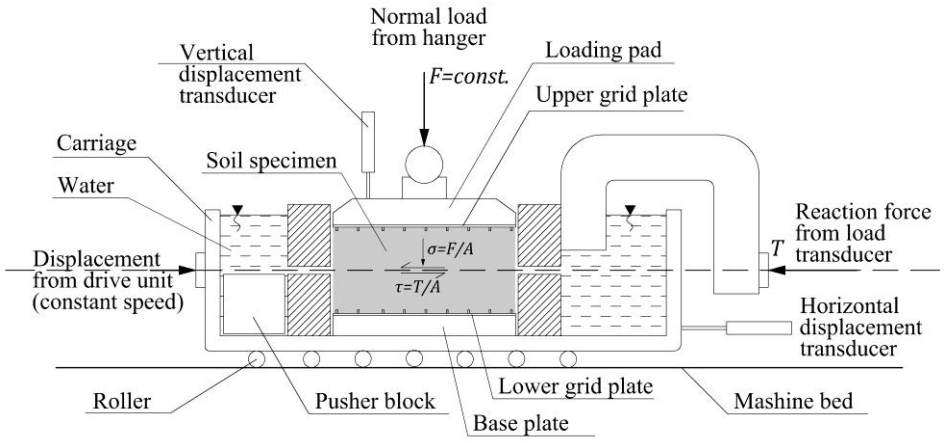

Fig. 1.21. Shear box schematics [14]

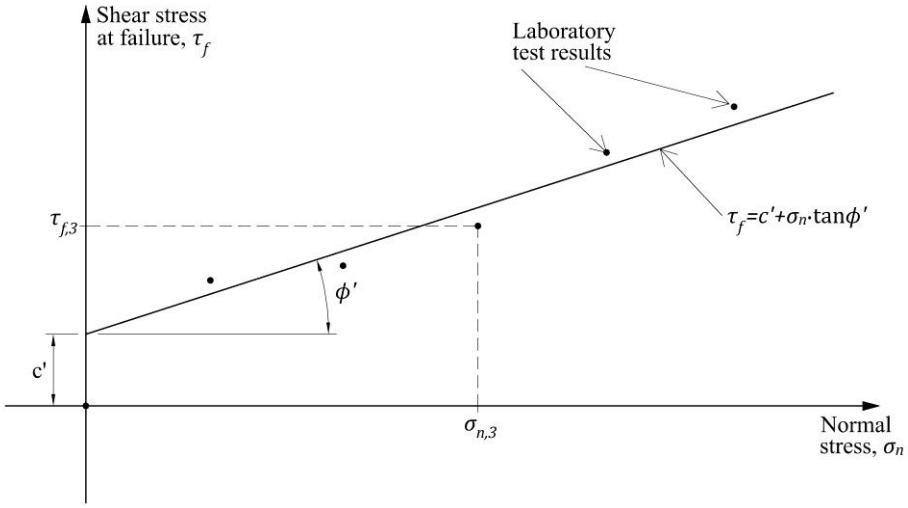

Fig. 1.22. Typical shear strength envelope from a set of drained shearbox tests [14].

1.6.3 Triaxial compression tests

The triaxial compression test is used to determine the shear strength of soil and to determine the stress–strain behaviour of the soil under different confining pressures. The test involves a cylindrical soil sample that is subjected to a uniform confining pressure from all sides and then subjected to an additional vertical load until failure. Figure 1.23 shows the triaxial test apparatus schematically. The cylindrical soil sample can have different dimensions. A typical triaxial soil specimen is 5 cm in diameter and about 15 cm in height. The sample is situated on top of the pedestal that is part of the base of the triaxial chamber, as shown in Figure 1.23.

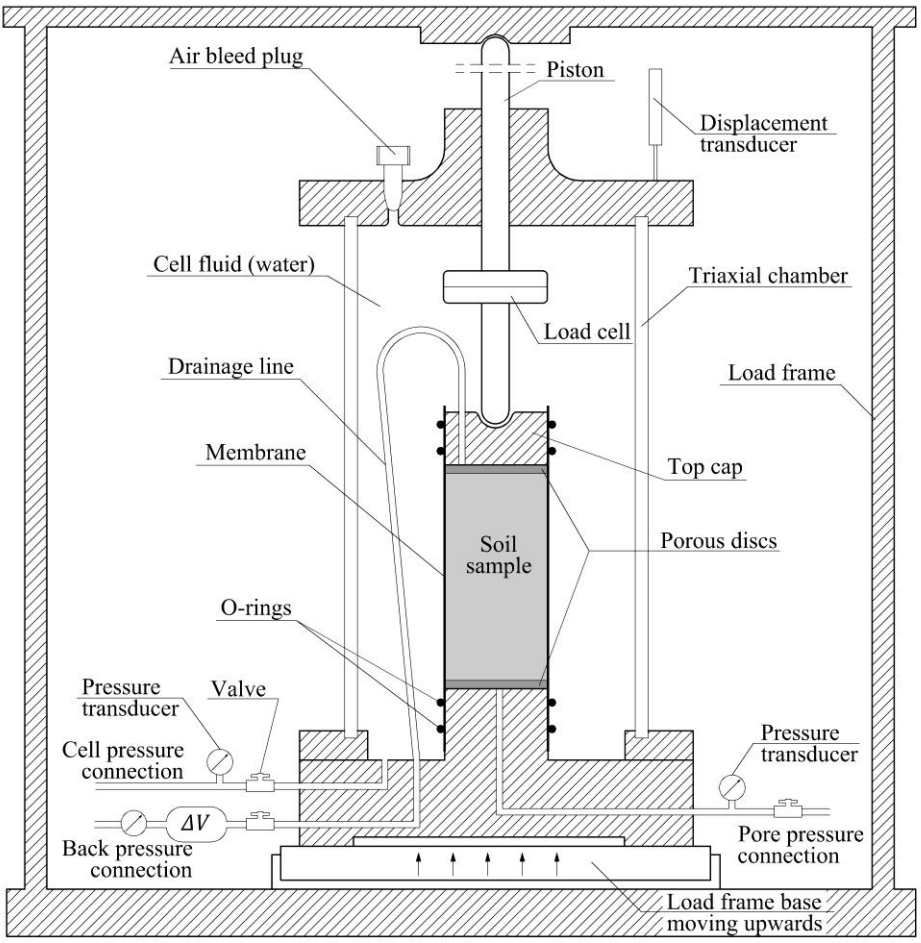

Fig. 1.23. Triaxial compression cell schematics [14, 15, 16].

A loading plate is then placed on top of the specimen. The pedestal, the soil specimen, and the top loading plate are carefully enclosed in a thin rubber membrane. O-rings are used to prevent the confining fluid from entering the soil specimen. Finally, the triaxial chamber is positioned on top of the base, the loading ram is lowered to the position shown in Figure 1.23, and the triaxial chamber is filled with water [16].

As noted in Figure 1.23, two drainage tubes connect the top and bottom of the soil specimen to the outside of the triaxial chamber. These tubes have valves that are used to control drainage into the soil specimen. A third tube leads to the

space inside the triaxial chamber, which is usually filled with water. This tube is used to pressurize the confining fluid (water) using pressurized air and a pressure regulator [16].

There are three types of triaxial compression tests: CD, CU, and UU. Each triaxial test consists of two stages: Stage I is the conditioning stage, during which the initial stress condition of the soil specimen is established; stage II is the shearing stage, during which a deviator stress is applied until failure. The designation of a triaxial test consists of two letters, the first letter describes stage I and the second describes stage II. Stage I can be either consolidated (C) or unconsolidated (U), and stage II can be either drained (D) or undrained (U). A triaxial CD test means that the soil specimen is allowed to consolidate in stage I of the triaxial test, and during stage II the specimen is allowed to drain while being sheared. On the other hand, a triaxial CU test means that the soil specimen is allowed to consolidate in stage I, and during stage II the specimen is not allowed to drain while being sheared. Finally, the UU test means that the specimen is not allowed to consolidate in stage I and is not allowed to drain during shearing [16].

The consolidated–drained (TXCD) triaxial test is used to obtain the effective strength parameters of soils. First, a soil specimen is saturated by circulating deaired water through the specimen, from bottom to top, utilizing the two drainage tubes shown in Figure 1.23. After the specimen is fully saturated, the triaxial test is done in two stages: a stress initialization stage and a shearing stage. In the first stage a confining pressure is applied via the confining fluid. Because the soil specimen is fully saturated, excess pore water pressure will be generated (approximately equal to confining pressure). The soil specimen is allowed to consolidate by opening the two drainage valves throughout this stage. That will allow the excess pore water pressure to dissipate gradually and the specimen to consolidate. The volume of the dissipated water can be measured using a special volume change apparatus. The volume of the dissipated water is equal to the volume change of the specimen because the specimen is fully saturated. The volumetric strain can be calculated by dividing the volume change by the initial volume of the specimen [16].

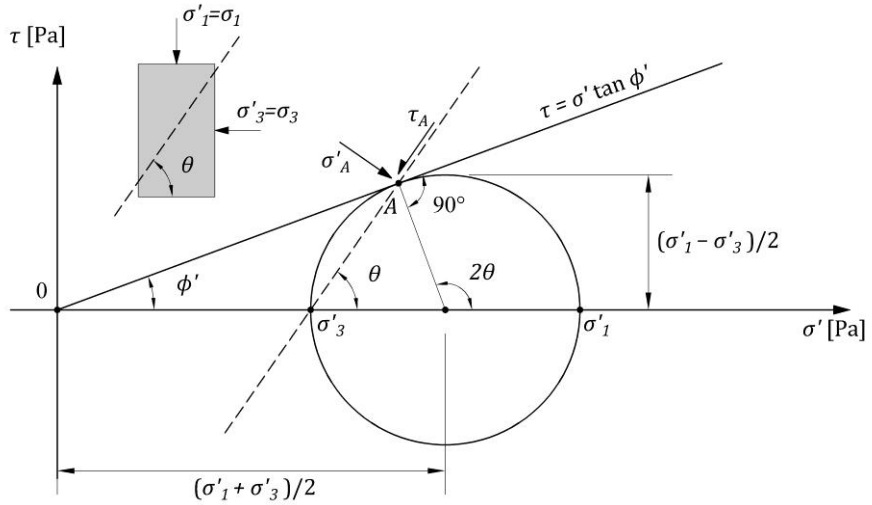

Fig. 1.24. Determination of the Mohr-Coulomb failure criterion for sand based a CD triaxial test results [16]

In the shearing stage of the CD test a deviator stress $\Delta\sigma_d = \sigma_1 - \sigma_3$ is applied very slowly while the drainage valves are opened, to ensure that no excess pore water pressure is generated. Consequently, the effective stresses are equal to the total stresses during this stage of the CD test. Because of its stringent loading requirements, the CD test may take days to carry out, making it an expensive test [16].

We need only one CD test to determine the strength parameters of sand (because $c' = 0$). From the peak deviator stress measured $(\sigma_1 - \sigma_3)_f$, we can plot Mohr's circle, which describes the stress state of the soil specimen at failure as shown in Figure 1.24. The Mohr–Coulomb failure criterion can be obtained by drawing a line that is tangent to Mohr's circle and passing through the origin. The slope of the Mohr–Coulomb failure criterion is the effective (or drained) friction angle ϕ' of the soil [16].

For clays the cohesion intercept, c', is not equal to zero. Therefore, we will need to have the results of at least two CD triaxial tests on two identical specimens subjected to two different confining pressures. From the measured peak deviator stress $(\sigma_1 - \sigma_3)_f$ of these tests, we can plot Mohr's circles that describe the stress states of the soil specimens at failure, as shown in Figure 1.25. The Mohr–Coulomb failure criterion in this case can be obtained by drawing a line that is tangent to the two Mohr's circles.

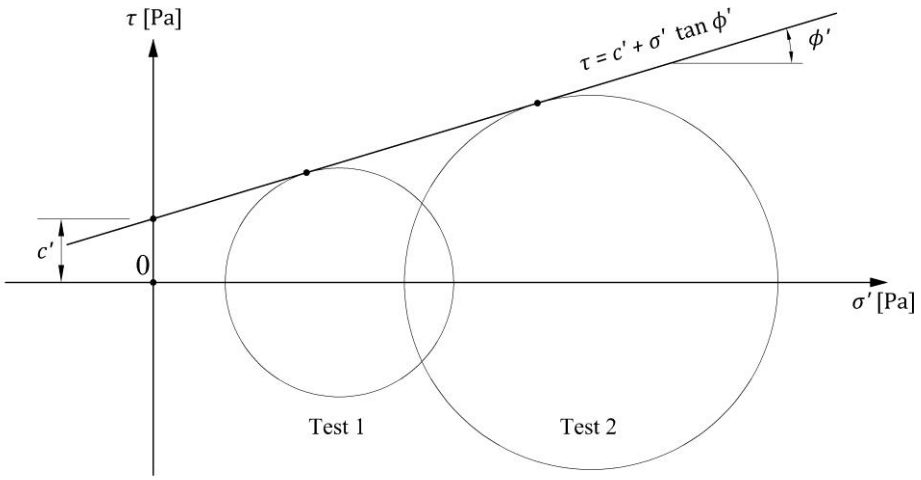

Fig. 1.25. Determination of internal friction angle and cohesion from two triaxial compression tests [16]

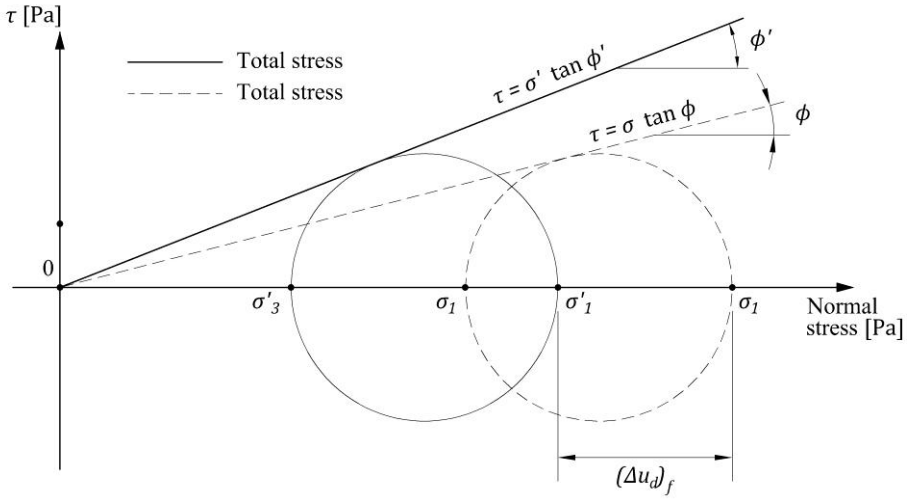

Fig. 1.26. Total and effective-stress Mohr–Coulomb failure criteria from CU triaxial for sand [16]

The Mohr-Coulomb failure criterion will intersect with the shear stress axis at $\tau = c'$, as shown in Figure 1.25. This is the effective cohesion intercept of the clay. The slope of the Mohr–Coulomb failure criterion is the effective friction angle ϕ' of the clay sample [16].

The consolidated–undrained (TXCU) triaxial test includes two stages: stage I, the consolidation stage, and stage II, the shearing stage [16]. The first stage is the same as in the CD test. In stage II, however, the soil specimen is sheared in an undrained condition. The undrained condition is realized by closing the drainage valves, thus preventing the water from flowing out of the sample or into the sample. The undrained condition makes it possible to apply the deviator stress in a much faster manner than in the consolidated–drained triaxial test. This makes the CU test more economical than the CD test. During stage II there will be no volume change since water is not allowed to leave the specimen [16]. The excess pore water pressure is measured using a pressure transducer connected to one of the drainage tubes [16].

We need only one CU test to determine the total and effective shear strength parameters of a dense sand (because $c = c' = 0$). From the peak deviator stress measured $(\sigma_1 - \sigma_3)_f$, we can plot the total stress Mohr's circle that describes the total stress state of the soil specimen at failure, as shown in Figure 1.26. Knowing that the pore water pressure at failure is $-(\Delta u_d)_f$, we can calculate the effective stresses at failure and plot the effective-stress Mohr's circle as shown in Figure 1.26. Note that the effective-stress Mohr's circle has the same diameter as the total stress Mohr's circle. Also note that the effective-stress circle results from the total stress circle by a shift equal to $(\Delta u_d)_f$ from left to right [16]. The effective-stress Mohr–Coulomb failure criterion for sand can be obtained by drawing a line tangent to the effective-stress Mohr's circle and passing through the origin. The slope of the effective-stress Mohr–Coulomb failure criterion is the effective (or drained) friction angle ϕ' of the soil [16].

For clays, the cohesion intercept, c', is not equal to zero. Therefore, we will need to have the results of at least two CU triaxial tests on two identical specimens subjected to two different confining pressures. From the measured peak deviator stress of these tests we can plot Mohr's circles that describe the total stress state of the soil specimens at failure.

The unconsolidated–undrained (TXUU) triaxial test is usually performed on undisturbed saturated samples of fine-grained soils (clay and silt) to measure their undrained shear strength, c_u. The soil specimen is not allowed to consolidate in stage I under the confining pressure applied. It is also not allowed to drain during shearing in stage II. Identical soil specimens exhibit the same shear strength under different confining pressures [16]. The Mohr–Coulomb failure criterion is horizontal ($\phi_u = 0$) and it intersects the vertical axis at $\tau = c_u$. Note that c_u is the undrained shear strength of a soil and is equal to the radius of the total stress Mohr's circle:

$$c_u = \frac{\sigma_{1f} - \sigma_{3f}}{2} \quad (1.39)$$

The undrained shear strength is used appropriately to describe the strength of fine-grained soils subjected to rapid loading, during which drainage is not allowed; therefore, no dissipation of excess pore water pressures is possible [16].

1.7 REFERENCES

[1] ISO 14688-1:2002, Geotechnical investigation and testing -- Identification and classification of soil -- Part 1: Identification and description, International Organization for Standardization, 2002

[2] ISO 14688-2:2004, Geotechnical investigation and testing -- Identification and classification of soil -- Part 2: Principles for a classification, International Organization for Standardization, 2004

[3] EN 1997-1:2004, Euro code 7: Geotechnical design - Part 1: General rules, European Committee for Standardization, 2004

[4] EN 1997-2:2007, Euro code 7: Geotechnical design - Part 2: Ground investigation and testing, European Committee for Standardization, 2007

[5] Atkinson J.: The Mechanics of Soils and Foundations. 2nd Ed. Routledge. London, 2007

[6] Aysen A.: Soil Mechanics: Basics Concepts and Engineering Applications. A.A Balkema Publishers, 2002

[7] Bond A., Harris, A.: Decoding Eurocode 7, Taylor & Francis Group, 2008

[8] Cytowicz N. A.: Mechanika gruntów. Wydawnictwa Geologiczne, Warszawa, 1958

[9] Craig R. F.: Soil Mechanics. 7th Ed. Spon Press, London 2004

[10] Das B. M.: Geotechnical Engineering Handbook, J. Ross Publishing, 2011

[11] Das B. M.: Advanced Soil Mechanics. 3rd Ed. Taylor&Francis, London, 2008

[12] Fang H. Y.: Foundation Engineering handbook, Van Nostrand Reinhold, New York, 1991

[13] Head K. H.: Manual of Soil Laboratory Testing 3rd edition, Vol. 1: Soil Classification and Compaction Tests, CRC Press, 2006

[14] Head K. H. Epps R.J.: Manual of Soil Laboratory Testing 3rd edition, Vol. 2: Permeability, Shear Strength and Compressibility Tests, CRC Press, 2011

[15] Head K. H. Epps R.J.: Manual of Soil Laboratory Testing 3rd edition, Vol. 3: Effective Stress Tests, CRC Press, 2014

[16] Helwany S.: Applied Soil Mechanics with ABAQUS Applications, John Wiley & Sons, 2007
[17] Jeske T., Przedecki T., Rossiński B.: Mechanika gruntów. PWN, Warszawa, 1966
[18] Pisarczyk S.: Mechanika gruntów, Wydawnictwa Politechniki Warszawskiej, Warszawa 1992
[19] Pisarczyk S.: Gruntoznawstwo inżynierskie, PWN, Warszawa, 2012
[20] Pisarczyk S., Rymsza B.: Badania laboratoryjne i polowe gruntów, Oficyna Wydawnicza Politechniki Warszawskiej, Warszawa, 1993
[21] Obrycki M., Pisarczyk S.: Zbiór zadań z mechaniki gruntów. Oficyna Wydawnicza Politechniki Warszawskiej, Warszawa, 1995
[22] Sawicki A.: Zarys mechaniki gruntów sypkich. Wydawnictwo IBW PAN, Gdańsk, 2012
[23] Wei Dong Guo: Theory and Practice of Pile Foundations, CRC Press, New York, 2013
[24] Wiłun Z.: Zarys geotechniki. Wyd. 4. Wydawnictwa Komunikacji i Łączności, Warszawa 2008
[25] Wiłun Z.: Mechanika gruntów i gruntoznawstwo drogowe. Wyd. 2. Wydawnictwa Komunikacji i Łączności, Warszawa, 1967
[26] Wiłun Z., Starzewski R.: Soil Mechanics in Foundation Engineering. Vol. 1: Properties of Soils. Intertext Books, London, 1973

CHAPTER 2
INTRODUCTION TO STRUCTURAL MECHANICS (M.KRUK)

2.1 INTERNAL FORCES IN BASIC PLANAR, LINEAR STRUCTURAL ELEMENTS

2.1.1 Types of planar linear structural elements, load and support idealization

There are many different types of structures with variety of shapes and materials used, which makes them complex for analyze and design. It is common to use simplifications by grouping elements with the same patterns or carrying similar type of loads. Then any complex structure can be split into simple structural elements.

It is important for an engineer to recognize the various types of elements composing a structure and to be able to classify them as to the form and function. This process is called "structure idealization" and is necessary for the engineer to perform a practical force analysis of the whole structure and its members. The main idea of this idealization is to make a mathematical model of the real construction that is convenient for analysis and calculation.

Structural elements can be classified based on its geometry:

- a rod is a structural member which is long and slender and is capable of carrying load along its axis via elongation, e.g. beam, column.
- surface structure is a three-dimensional solid whose thickness is very small when compared with other dimensions. e.g. wall (load applied over the thickness of the element), plate (load applied perpendicular to the surface), shell,
- volumetric structures, solids with similar dimensions in every direction.

System composed of many slender rods connected together is called a bar structural system. If the axes of the bars are in one plane and if the load is also acting

in that plane, then the system is called a planar bar system. The structures used in civil engineering are spatial bar systems, but most often they can be divided into a series of flat sub-elements. This greatly simplifies the static calculations for any structure.

Some of the most common structural elements are as follows:

- **beams -** single-span and multi-span beams

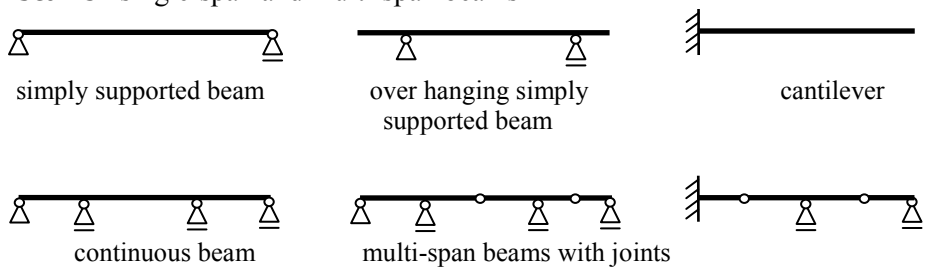

Figure 2.1. Examples of beams

- **frames and arches**

  Composed of beams and columns that are connected together. Members connection can be rigid or hinged.

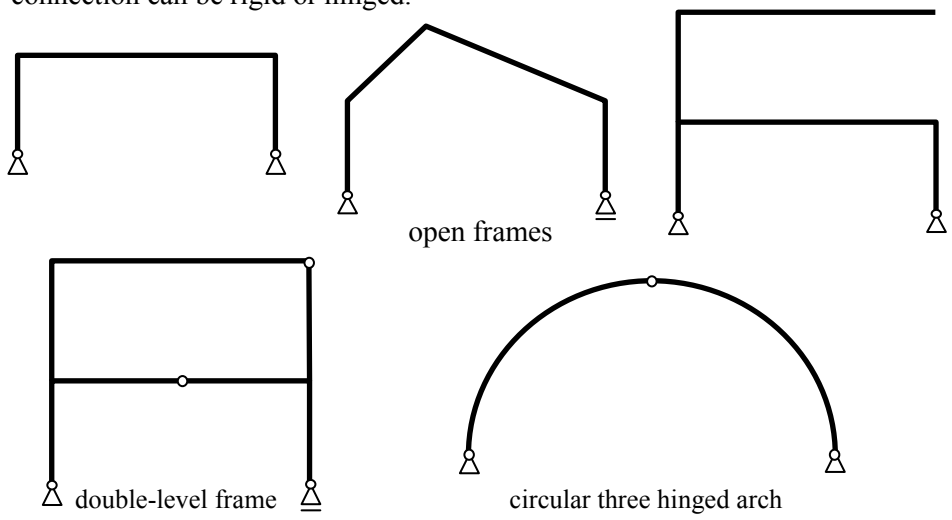

Figure 2.2. Examples of frames and arches

- **trusses**

  Truss composed of straight members connected by means of pin joints.

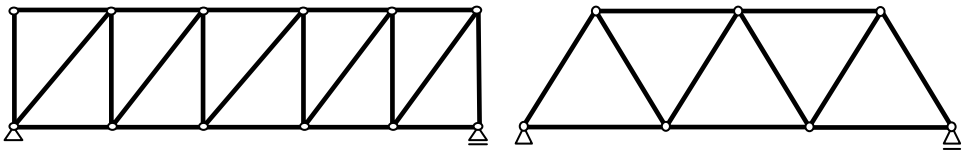

Figure 2.3. Examples of trusses

All bar structural systems have to be placed on the ground or attached to another structure by fixing points called supports. Support will react against the tendency of the applied loads to cause the structural member to move. The forces generated in the supports are called reactions.

The following types of planar supports are used:

- **roller support (hinge)**
  reaction R_A applied in point A
  with the direction perpendicular to the movement,

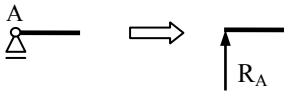

- **pinned support (hinge)**
  reaction R_A applied in point A
  with unknown direction, we decompose it
  into vertical V_A and horizontal H_A components,

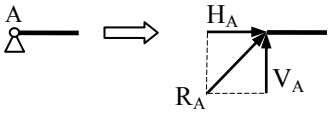

- **built-in suport (fixed)**
  horizontal H_A and vertical V_A components of
  the reaction force, moment M_A,

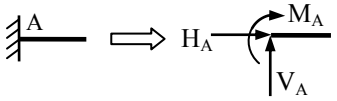

- **fixed support with sliding movement (guide)**
  Only vertical reaction force V_A and
  moment M_A (H_A=0 because sliding in
  horizontal direction is possible),

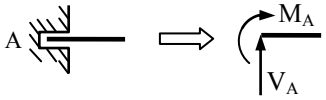

- **fixed support with transversal movement**
  Only horizontal reaction force H_A and
  moment M_A (V_A=0 because sliding in
  vertical direction is possible).

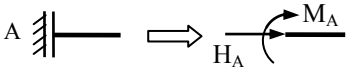

Figure 2.4. Supports types

Reaction forces in supports are passive external forces occurring as a result of active external forces (loadings) acting on the structure.

Loadings acting on planar bar structural systems:
- concentrated force P_z, P_y, P_x [kN],
- moment applied to a point M_y, M_z, M_x [kNm],
- evenly distributed load q_z, q_y (acting perpendicular to the rod axis) and q_x (acting along the rod axis) [kN/m],
- unevenly distributed load p_z, p_y i p_x [kN/m],
- evenly distribute moments m_x, m_y i m_z [kNm/m].

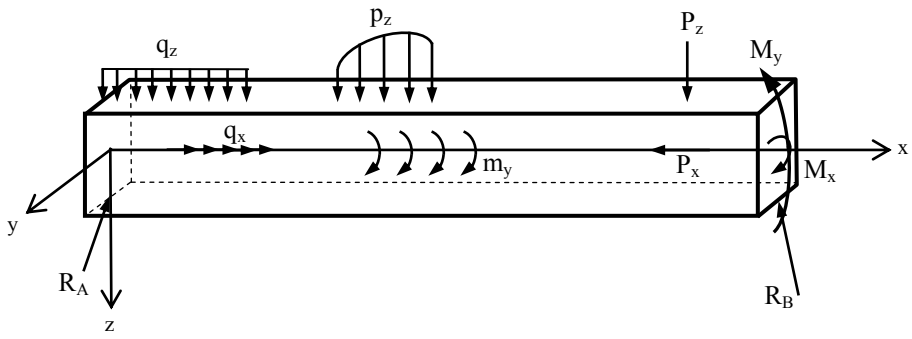

Figure 2.5. Example of loads

Loads acting along the main longitudinal rod axis x, shown in Fig. 2.5 (P_x, p_x, q_x) create **tension** (compression). Moments M_y (m_y) and M_z (m_z) cause **bending** of the rod. Moments M_x (m_x), sometimes called torques, cause **torsion** of the rod. Forces P_z i P_y (p_z, q_z p_y, q_y) induce **shear**.

All structural elements deform under applied loading. Sections of the rod under compression become shorten (cross sections of the rod, the ones perpendicular to the main x axis, approach each other and the displacement along x axis $du<0$). Sections of the rod under tension become longer (cross sections of the rod are moving apart and the displacement along x axis $du<0$).

Planar cross-sections are perpendicular to the axis of the undeformed beam and they remain planar and perpendicular to the deflection curve of the deformed beam. An angle between the neutral plane and the cross-section rotation is denoted as $d\varphi$.

In case of torsion, end cross-sections rotate through and angle $d\theta$ around the main longitudinal x axis. $d\theta$ is called the angle of mutual twist of the cross-sections.

In shearing deformation parallel cross-sections planes slide past one another along z-axis (displacement dw) or along y-axis (displacement dv).

In real engineering structures mentioned deformation types exists simultaneously and, for example, we can analyze the following combinations: bending with

shearing, bending with compression or tension, bending with shearing and compression, twisting with compression.
The more general case is when the longitudinal force acts parallel to x-axis, but not along the axis of the rod. Then, we are dealing with eccentric compression or eccentric stretching, and we can replace original loading by the statically equivalent axial force and bending moment (bending with compression or tension).
For structural analysis of any bar system, which is the determination of internal forces in the structure, it is convenient to use superposition principle. It states that the total displacement or internal forces at a point in a structure subjected to several external loadings can be determinate by adding together the displacements or internal forces caused by each of the external loads acting separately.

2.1.2 Cross-sectional forces in planar bar structures

Consider a straight bar with constant cross-sectional area, subjected to loading and satisfying the equilibrium conditions. The external load causes internal forces. The internal forces can be visualized by an imaginary cut of the rod. In order to determine those forces we first choose an imaginary cut perpendicular to the axis of the bar. Interaction between divided parts is replaced by resultant force vector $\overrightarrow{W}$ and moment vector $\overrightarrow{M_w}$. The forces are shown in the free-body diagram (see Fig 2.6).
The resultant force vector $\overrightarrow{W}$ has to be decomposed into components: perpendicular to the cross-section $\overrightarrow{N_x}$ and acting in the plane of the cross-section $\overrightarrow{T}$. Then we continue decomposition of the vector $\overrightarrow{T}$ by introducing $\overrightarrow{T_y}$ and $\overrightarrow{T_z}$ components acting along y and z axis (we assume right-handed coordinate system). Similarly, we decompose the resultant moment vector $\overrightarrow{M_w}$ into torsional moment acting along the x axis $\overrightarrow{M_x}$ (perpendicular to the cross-section) and a bending moment $\overrightarrow{M}$ acting in cross-section plane. Finally, we introduce $\overrightarrow{M_y}$ i $\overrightarrow{M_z}$ as the components of the $\overrightarrow{M}$, acting along y and z axis.

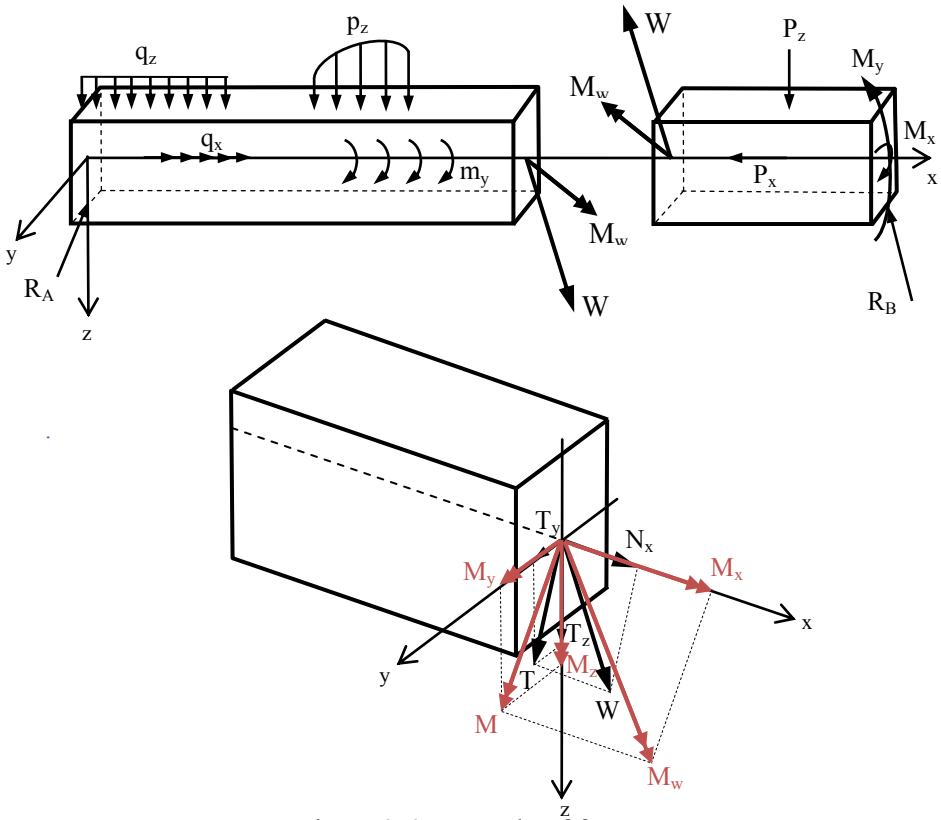

Figure 2.6. Example of forces

The procedure can be written using vector notation as a formula:

$$\overrightarrow{W} = \overrightarrow{N_x} + \vec{T} = \overrightarrow{N_x} + \overrightarrow{T_y} + \overrightarrow{T_z}$$

$$\overrightarrow{M_w} = \overrightarrow{M_x} + \overrightarrow{M} = \overrightarrow{M_x} + \overrightarrow{M_y} + \overrightarrow{M_z}$$

Six components have been introduced: three for resultant force vector and three resultant moment vector. Together, these quantities are constituting internal forces, are called **cross-sectional forces** and denoted:

N_x – axial force causing tension or compression,
T – shear force, parallel to a cut across the section, causing shearing,
T_y – shear force acting in xy plane,
T_z – shear force acting in xz plane,

M_x – torque, moment causing torsion,
M – bending moment,
M_y – bending moment in xz plane,
M_z – bending moment in xy plane.

Thus, in the cross-section of an arbitrarily loaded rod there are six components of the internal force: N_x, T_y, T_z, M_x, M_y i M_z. These forces are determined by considering steady state of structure in equilibrium.

Value of the axial force N_x in considered rod cross-section is equal to the algebraic sum of all external loadings, acting on either side of the cross-section, projected on the longitudinal axis (x).

Value of the shear force T_y (T_z) in considered rod cross-section is equal to the algebraic sum of all external loadings, acting on either side of the cross-section, projected on the perpendicular axis (y or z).

Value of the bending moment M_y (M_z) in considered rod cross-section is equal to the algebraic sum of all moments acting on either side of the cross-section. Moment is taken as a perpendicular force (vertical for M_y and horizontal for M_z) acting about a specific, chosen point.

Value of the torque (twisting moment) M_x in considered rod cross-section is equal to the algebraic sum of all external twisting moments, acting on either side of the cross-section, projected on the longitudinal axis (x).
Sign convention for cross-sectional forces is specified with respect to the default coordinate system of a bar. In section with normal pointing to the positive x-axis direction (n+) directions of all positive resultant vectors are pointing towards a positive directions of the corresponding axes. In section with normal pointing to the negative x-axis direction (n-) directions of all positive resultant vectors are pointing towards a negative directions of the corresponding axes.

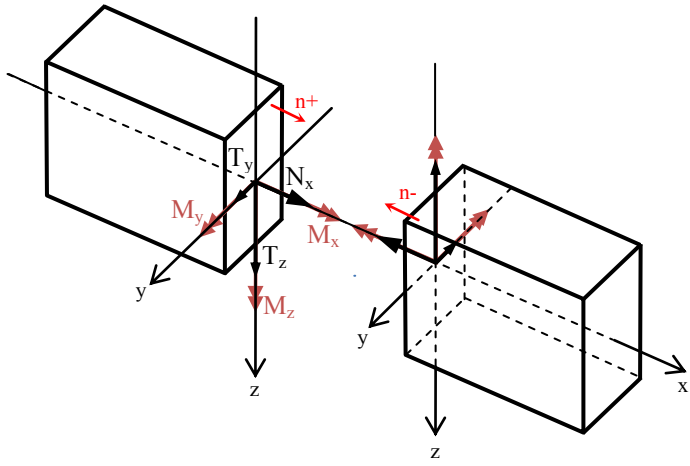

In xz plane:

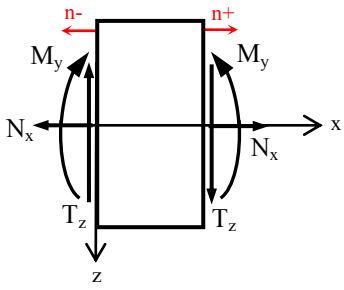

in xy plane:

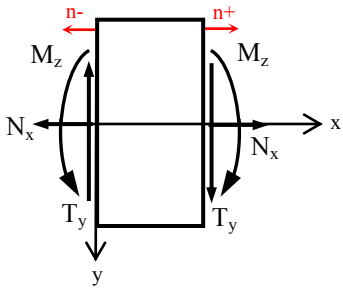

Figure 2.7. Example of forces and moments

Determining the internal forces in rods under axial loading causing tension or compression.

We consider a rod under tension or compression, which is subjected to a concentrated load or loads equally distributed along the x-axis. Only the normal force N_x is taken into consideration, all other cross-sectional forces are equal to zero.

Truss structures constitute a special class of structures in which individual straight members are connected at joints. The members are assumed to be connected to the joints in a manner that permits rotation, and thereby it follows from equilibrium considerations, to be detailed in the following, that the individual structural members act as bars, i.e. structural members that can only carry an axial force in either tension or compression.

Example 1.
A vertical bar with arbitrary cross-section area is fixed at one end and subjected to: a) axial load P, b) axial loads P i 2P shown in Fig. 2.8. Determine and plot the normal force along the bar.

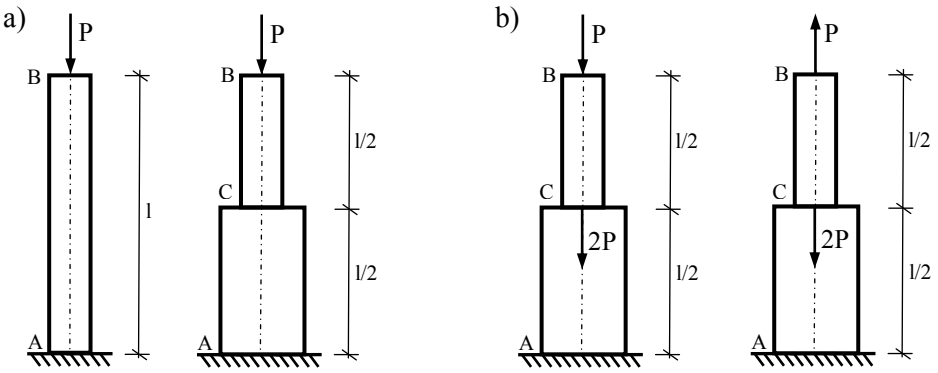

Figure 2.8. Rods under axial loading, example 1

Solution:
The bars shown in Fig. 2.8 are subjected only to the external loads acting longitudinal to the main axis (x). The only internal forces in the example are the normal forces.

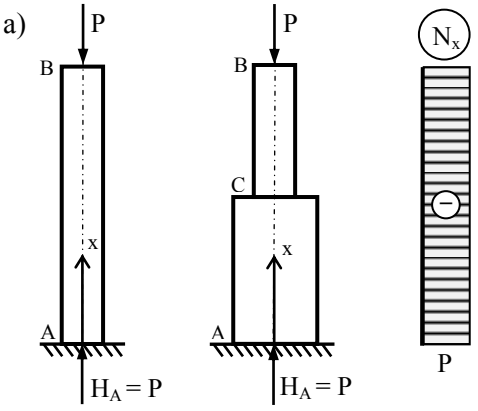

We introduce the coordinate x, starting in point A and with direction parallel to the bar. Then we calculate a reaction force H_A in support A by writing force equilibrium equation $\Sigma X=0$. That equation furnishes $H_A=P$ (assumed direction of reaction vector H_A is correct). Other reaction forces are equal: $M_A=0$ and $V_A=0$.

Figure 2.9. Example 1 - calculations

The next step is to write an algebraic sum of the components in the direction parallel to the axis of the bar of all external loads and support reactions acting on either side of the section of AB bar being considered. In every cross section we get axial load equal $N_x=-P$. Subsequently, we can create a plot of axial force

N_x along the line parallel to the main axis of the bar. We mark the ordinate P and the sign of calculated force. In this example we found force –P so the bar is under compression with magnitude equal to P.
It is worth noting that internal force plot is constant for both bars and does not depend on the change in the cross-section of the bar.

b)

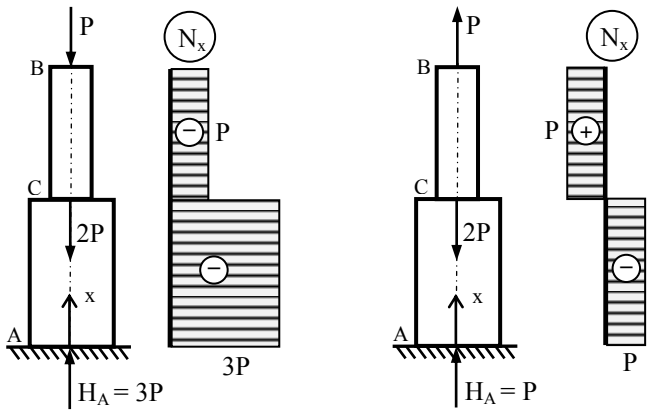

Figure 2.10. Example 1 - solution

Similar to case a) we introduce the coordinate x, starting in point A and write the equation of equilibrium $\Sigma X=0$, calculate support A reaction force H_A. In the bar on the left we get $H_A=3P$, for the bar on the right we get $H_A=P$.
Next, considering arbitrary point in section AC of the bar we can write an algebraic sum of the components in the direction parallel to the axis of the bar of all external loads acting on either side of the section being considered. This way we get result $N_x^{AC}=-3P$ for the first rod, and $N_x^{AC}=-P$ for the second. Subsequently, we consider arbitrary point in section CB of the bar. We write an algebraic sum of the components in the direction parallel to the axis of the bar of all external loads acting on either side of the section being considered. We get result $N_x^{CB}=-P$ for the first rod, and $N_x^{CB}=+P$ for the second. Having the results for both bars we create a plot of axial force N_x along the line parallel to the main axis.

Example 2.
A concrete column with variable cross-sectional area A_1 i A_2 is fixed at one end (see Fig. 2.11). It is subjected to a vertical axial load P=10kN at point C.
Determine and plot the normal force along the column taking into account its own weight.
Given: l=1,5m; A_1=225cm^2; A_2=400cm^2;
unit weight per concrete volume γ_b=24kN/m^3.

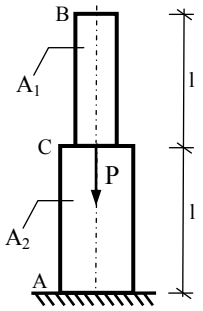

Figure 2.11. Example 2 - axial loading

Solution:
We introduce the coordinate x, starting in point B and with direction parallel to the column. Normal force depends on the location as volume force is acting along the main axis (function of x). Before we start to calculate the longitudinal forces in the cross-sections of the column, the units for all given quantities must be consistent.

$P = 10kN$, $A_1 = 225cm^2$, $A_2 = 400cm^2$,
$l = 1,5m = 150cm$, $\gamma_b = 24kN/m^3 = 0,000024kN/cm^3$.

Normal force on the BC segment:
$N_x^{BC}(x) = -\gamma_b \cdot A_1 \cdot x = -0,000024 \cdot 225 \cdot x = -0,0054 \cdot x$ where $x \in \langle 0,150cm \rangle$
czyli $N_x^B = 0$ i $N_x^C = -0,0054 \cdot 150 = -0,81kN$.

Normal force on the CA segment:
$N_x^{CA}(x) = -0,0054 \cdot 150 - P - \gamma_b \cdot A_2 \cdot (x - 150)$ where $x \in \langle 150cm,300cm \rangle$
czyli $N_x^C = -0,0054 \cdot 150 - 10 = -10,81kN$
$N_x^A = -0,0054 \cdot 150 - 10 - 0,000024 \cdot 400 \cdot 150 = -12,25kN$.

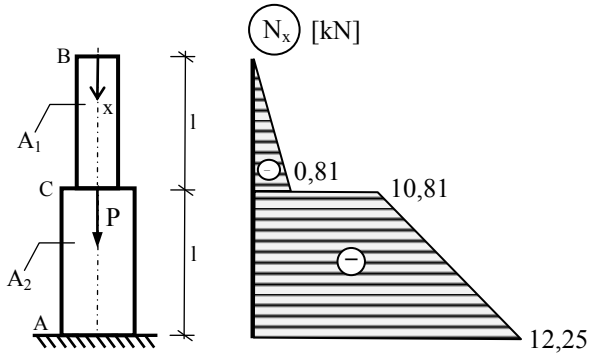

We can create a diagram for axial force N_x in each segment.

Figure 2.12. Example 2 - solution

Example 3.
Determine the force in each member of the truss.

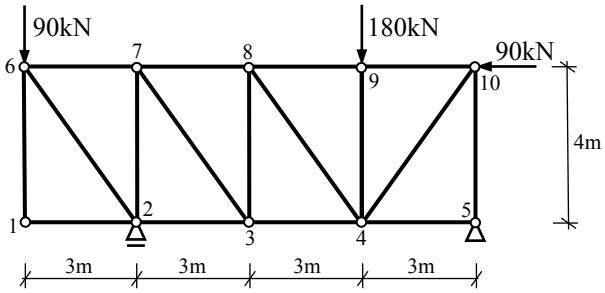

Figure 2.13. Example 3 - truss

Solution:
We introduce Cartesian coordinate xz. Reaction forces at the supports can be calculated using three equations of equilibrium: $\Sigma x=0$, $\Sigma M_2=0$ i $\Sigma M_5=0$.

$\Sigma x = 0 \quad H_5 - 90 = 0$

$H_5 = 90kN$

$\Sigma M_2 = 0$

$180 \cdot 6 - 90 \cdot 3 - 90 \cdot 4 + -V_5 \cdot 9 = 0$

$V_5 = 50kN$

$\Sigma M_5 = 0$

$V_1 \cdot 9 - 90 \cdot 4 - 180 \cdot 3 + - \ 90 \cdot 12 = 0$

$V_1 = 220kN$

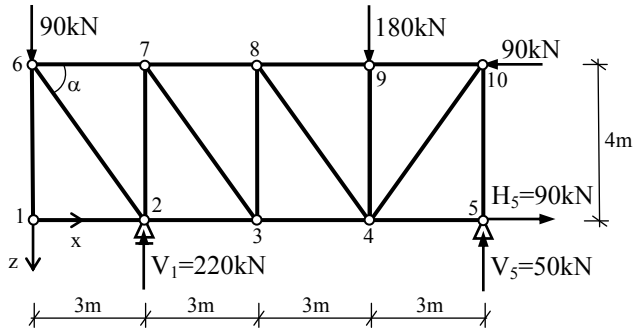

Figure 2.14. Example 3 - solution

The most common way to determine forces inside a truss is method of joints. The basic concept of the method is that, since the truss is in equilibrium, each joint of the truss will also be in equilibrium. The procedure for method of joints is as follows: we cut each node successively, starting with the one where there are not more than 2 members, in which forces are unknown. We introduce the forces by which the bars act on the joint. Equilibrium of the joint requires that two force projection equations are satisfied: $\Sigma x=0$ i $\Sigma z=0$ ($\sin\alpha = 0{,}8$; $\cos\alpha = 0{,}6$).

Node 1: $\Sigma x = 0$ $N_{1\text{-}2} = 0$
$\Sigma z = 0$ $N_{1\text{-}6} = 0$.

Node 6: $\Sigma z = 0$ $90 + N_{6\text{-}2} \cdot \sin\alpha = 0$
$N_{6\text{-}2} = -112{,}5\text{kN}$
$\Sigma x = 0$ $N_{6\text{-}7} + N_{6\text{-}2} \cdot \cos\alpha = 0$
$N_{6\text{-}7} = 67{,}5\text{kN}$.

Node 2: $\Sigma x = 0$ $N_{2\text{-}3} + 112{,}5 \cdot \cos\alpha = 0$
$N_{2\text{-}3} = -67{,}5\text{kN}$
$\Sigma z = 0$ $-220 - N_{2\text{-}7} + 112{,}5 \cdot \sin\alpha = 0$
$N_{2\text{-}7} = -130\text{kN}$.

Node 7: $\Sigma z = 0$ $N_{7\text{-}3} \cdot \sin\alpha - 130 = 0$
$N_{7\text{-}3} = 162{,}5\text{kN}$
$\Sigma x = 0$ $N_{7\text{-}8} + N_{7\text{-}3} \cdot \cos\alpha - 67{,}5 = 0$
$N_{7\text{-}8} = -30\text{kN}$

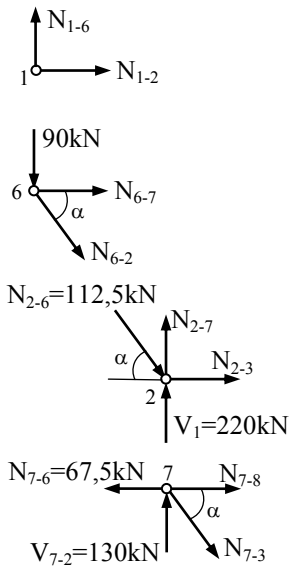

Figure 2.15. Steps of the calculations

The calculation of the bar forces proceeds by considering the individual joints sequentially until we solve all the unknown forces in truss.

Determined forces in the planar truss has been presented below:

$N_{1-2} = N_{2-1} = 0$,	$N_{1-6} = N_{6-1} = 0$,	$N_{2-6} = N_{6-2} = -112{,}5\text{kN}$,
$N_{2-7} = N_{7-2} = -130\text{kN}$,	$N_{2-3} = N_{3-2} = -67{,}5\text{kN}$,	$N_{3-7} = N_{7-3} = 162{,}5\text{kN}$,
$N_{3-8} = N_{8-3} = -130\text{kN}$,	$N_{3-4} = N_{4-3} = 30\text{kN}$,	$N_{4-8} = N_{8-4} = 162{,}5\text{kN}$,
$N_{4-9} = N_{9-4} = -180\text{kN}$,	$N_{4-10} = N_{10-4} = 62{,}5\text{kN}$,	$N_{4-5} = N_{5-4} = 90\text{kN}$,
$N_{5-10} = N_{10-5} = -50\text{kN}$,	$N_{6-7} = N_{7-6} = 67{,}5\text{kN}$,	$N_{7-8} = N_{8-7} = -30\text{kN}$,
$N_{8-9} = N_{9-8} = -127{,}5\text{kN}$,	$N_{9-10} = N_{10-9} = -127{,}5\text{kN}$.	

For given loads two bars in a truss structure have zero force (N=0), thus being essentially inactive in this load case. There are 9 bars under compression (N<0), and 6 bars under tension (N>0).

Determining the internal forces in rods under torsion.

We consider a straight, prismatic structural member of constant cross section subjected to applied torque M_x about its long axis. This kind of member, designed primarily to transmit torque, is called a shaft. This chapter covers torsion of straight rods with the circular cross-sections.

Example 4.
Consider the shaft attached to a wall and subjected to a torques (see Fig. 2.16). Determine the end reactions and plot the torque diagram for the shaft.

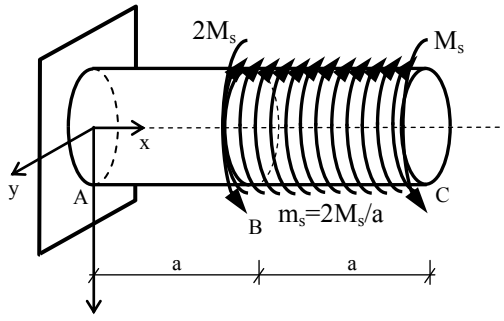

Figure 2.16. Example 4 - the shaft

Solution:
Force equilibrium is used for analysis. The loading is written in a vector form (Fig.2.17) and the reaction M_x^A can be found using the equilibrium equation $\Sigma x=0$.

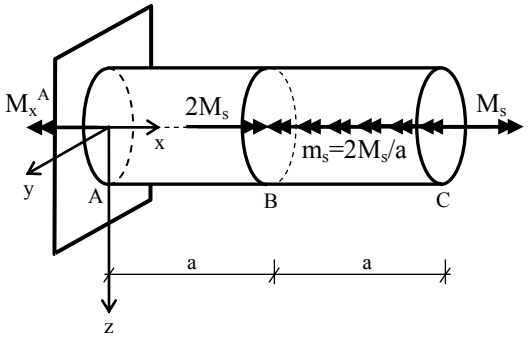

$$\Sigma x = 0$$
$$-M_x^A + 2M_s - \frac{2M_s}{a} \cdot a + M_s = 0$$
$$M_x^A = M_s$$

We write equilibrium equations for torque on the rod segments.

Segment AB:
$M_x^{AB}(x) = M_x^A = M_s$

Figure 2.17. Example 4 - calculations

Segment BC:
$$M_x^{AB}(x) = M_x^A - 2M_s + \frac{2M_s}{a} \cdot (x - a) \qquad \text{where } x \in \langle a,2a \rangle$$
and $M_x^B = M_s - 2M_s = -M_s$ i $M_x^C = M_s - 2M_s + \frac{2M_s}{a} \cdot a = M_s$

The torque M_x diagram for the shaft is shown in the Fig. 2.18.

Figure 2.18. Example 4 - solutions.

Determining the internal forces in beams

We consider straight beam in equilibrium, subjected to load in xz plane: evenly distributed loads $q_x(x)$, $q_z(x)$ and evenly distribute bending moments $m_y(x)$. Subsequently, we pass two planes, perpendicular to the beam, creating two infinitely close transverse cross-sections α_1-α_1 and α_2-α_2. We have obtained small beam element of length dx, carrying any resultant internal forces. The beam is loaded in xz plane, so in every cross-section there are 3 out of 6 possible internal forces: normal force N_x, shear force T_z and bending moment M_y.

The element separated by cross-sections α_1-α_1 and α_2-α_2 remains in equilibrium under the action of the external loads and internal forces applied by the adjacent parts of the beam (Fig.2.19).

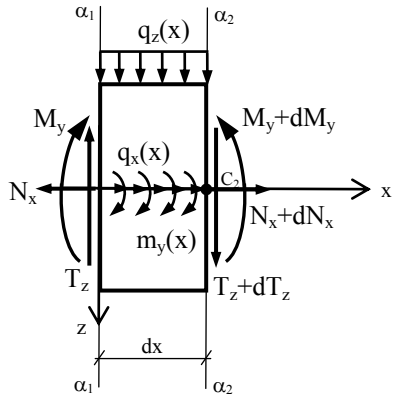

Figure 2.19. Beams internal forces

The element remains in equilibrium if the following equations are satisfied:

1) $\Sigma x = 0$ gives $-N_x + q_x(x)dx + (N_x + dN_x) = 0$

$$\frac{dN_x}{dx} = -q_x(x)$$

First derivative of the normal force N_x with respect to the x-coordinate is equal to negative value of the intensity of evenly distribute loads q_x acting along the beam axis.

2) $\Sigma z = 0$ gives $-T_z + q_z(x)dx + (T_z + dT_z) = 0$

$$\frac{dT_z}{dx} = -q_z(x)$$

First derivative of the shear force T_z with respect to the x-coordinate is equal to negative value of the intensity of evenly distribute loads q_z acting perpendicularly to the beam.

3) $\Sigma M_{(C_2)} = 0$ gives $M_y + T_z dx + m_y(x)dx - q_z(x)dx\frac{dx}{2} - (M_y + dM_y) = 0$

$$\frac{dM_y}{dx} = T_z + m_y(x)$$

(Note: terms of the second order has been omitted, on account of the restriction to infinitely small strain).
First derivative of the bending moment M_y with respect to the x-coordinate is equal to the value of shear force T_z increased by the intensity of evenly distribute bending moments acting on the beam.

Analogous differential relations between cross-sectional forces and loads are true for bending in the xy plane:

$$\frac{dT_y}{dx} = -q_y(x)$$

$$\frac{dM_z}{dx} = -T_y + m_z(x).$$

In cases of the external loads perpendicular to the beam axis, the internal forces are as follows: bending in the xz plane is accompanied by shear force T_z and bending moment M_y, while bending in the xy plane is accompanied by shear force T_y and bending moment M_z.
The diagrams for shear forces and bending moments in case of single-span, simple supported beam, carrying a concentrated load P (Fig.2.20) or uniformly distributed load (Fig.2.21), has been presented below.

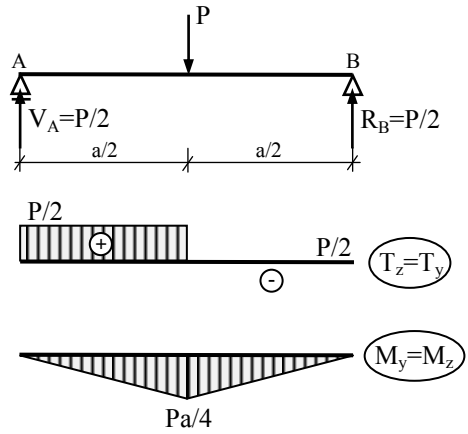

Figure 2.20. Example of concentrated load

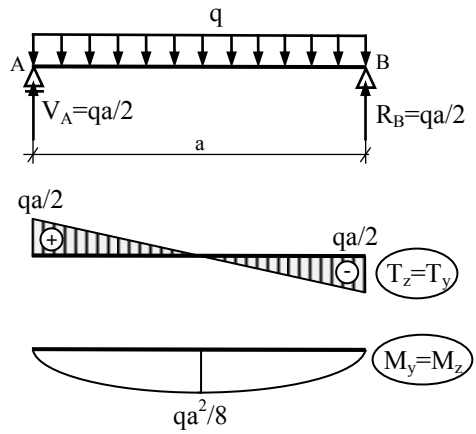

Figure 2.21. Example of the distributed load

In case of a two-span, simply supported beam, the solutions can be found in Winkler's table. The results (shear forces and bending moments diagrams) for selected beams carrying concentrated loads in the middle of the span or a uniformly distributed load at the span, has been presented in the table below.

Type of load and diagrams for T, M	Reactions at supports and shear forces					Support moments and moments on the span				
	$R_A=T_A$	R_B	$R_C=-T_C$	T_B^l	T_B^p	M_B	M_1	x_1	M_2	x_2
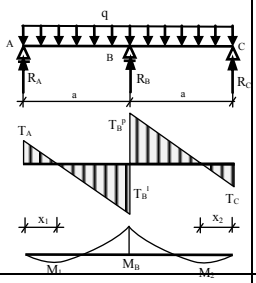	0,375 qa	1,25 qa	0,375 qa	-0,625 qa	0,625 qa	-0,125 qa^2	0,0703 qa^2	0,375 a	0,0703 qa^2	0,375 a
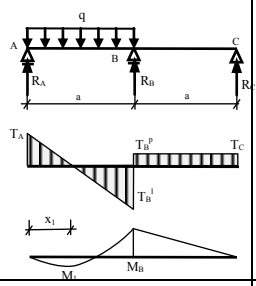	0,4375 qa	0,625 qa	-0,0625 qa	-0,5625 qa	0,0625 qa	-0,0625 qa^2	0,0957 qa^2	0,4375 a	---	---
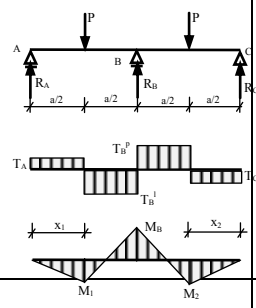	0,3125 P	1,375 P	0,3125 P	-0,6875 P	0,6875 P	-0,1875 Pa	0,15625 Pa	0,5 a	0,15625 Pa	0,5 a
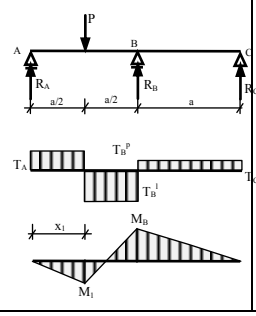	0,40625 P	0,6875 P	-0,09375 P	-0,59375 P	0,09375 P	-0,09375 Pa	0,203125 Pa	0,5 a	---	---

2.2 STRESS, STRAIN AND DISPLACEMENT IN STRAIGHT ROD

The internal force resultants, exposed by an imaginary cutting plane containing the point through the member, are usually resolved into stress components, normal and tangent to the cross-section.

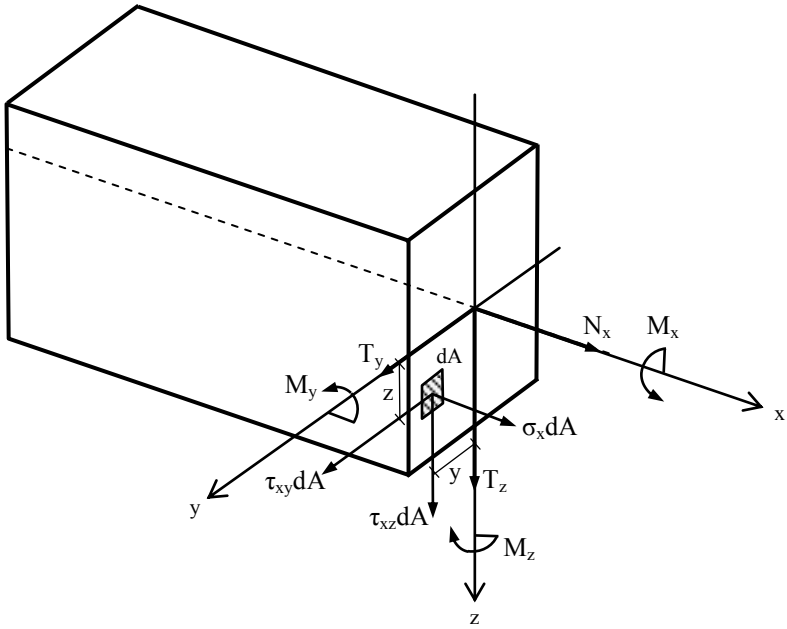

Figure 2.22. Example of cross sectional forces

Relations between normal stress σ_x and shear stresses τ_{xy}, τ_{xz} acting over the cross-section, and the internal forces and moments in a beam, can be established by considering a typical infinitesimal area dA of the cross-section, shown in Fig. 2.22. The stress components on the cross-section cause the following resultants: a force $\sigma_x dA$ parallel to the x-axis, a force $\tau_{xy} dA$ parallel to the y-axis and a force $\tau_{xz} dA$ parallel to the z-axis. In other words, cross-sectional forces N_x, T_y, T_z and moments M_x, M_y i M_z are the resultants of the elementary forces $\sigma_x dA$, $\tau_{xy} dA$ and $\tau_{xz} dA$ according to the equations presented below:

$$N_x = \int_A \sigma_x dA \qquad T_y = \int_A \tau_{xy}\, dA \qquad T_z = \int_A \tau_{xz}\, dA$$

$$M_x = \int_A (\tau_{xz} y - \tau_{xy} z)\, dA \qquad M_y = \int_A \sigma_x z dA \qquad M_z = -\int_A \sigma_x y dA$$

Any structural member subjected to a set of forces and moments undergo linear and angular deformations. Subsequently, particular points and cross-sections undergo linear translations and angular rotations.
Methods to calculate stress, strain and displacement in straight rods has been presented in the next section.

2.2.1 Stress, strain and displacement in rods under axial loading

We consider a prismatic rod, subjected to axial loading. Internal axial forces N_x produce a uniform tension ($N_x>0$) or compression ($N_x<0$). The perpendicular force distributed over the cross-section is called **normal stress σ_x,** and can be calculated using a formula:

$$\sigma_x = \frac{N_x}{A} \qquad \text{where:} \qquad A - \text{cross-sectional area.}$$

When a rod with constant cross-sectional area, equal to A, is stretched with force P, then the uniformly distributed stress $\sigma_x = \frac{P}{A}$ will be generated in any cross-section of the rod (see Fig.2.23).

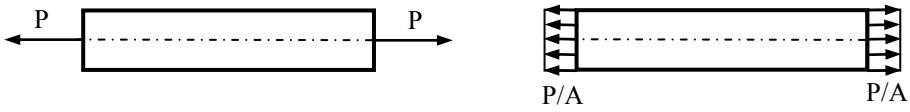

Figure 2.23. Example of the rod under axial loading

Under the action of axial forces the elastic rod will change its length. The change is denoted du (du>0 for elongation in tension and du<0 for compression).
Consider a rod with an undeformed length l and a constant normal force (N_x=const.). The elongation (or shortening) of the rod will be uniform, i.e. for any arbitrary selected section dx of the rod, one can write a formula:

$$\frac{\Delta du}{dx} = \frac{\Delta l}{l} = \varepsilon_x = \text{const.} \qquad \text{where:} \qquad \Delta du - \text{elongation of dx.}$$

The dimensionless quantity $\boldsymbol{\varepsilon_x}$ is called **strain** and describes the ratio between the elongation and the original (undeformed) length.

The physical relation that connects strain ε_x and normal stress σ_x is called constitutive law. For the elastic deformation the law is called Hooke's law:

$$\sigma_x = E\,\varepsilon_x \qquad \text{where:} \qquad E - \text{Young's modulus.}$$

The proportionality factor: Young's modulus E, called modulus of elasticity, is a constant which depends on the material and which can be determined with the aid of a tension test.

To determine the elongation of the rod with undeformed length l, constant cross-sectional area A, made of the material characterized by modulus of elasticity E and stretched with force P we can use a formula:

$$\Delta l = \varepsilon_x l = \frac{\sigma_x}{E} l = \frac{\frac{P}{A}}{E} l = \frac{P\,l}{EA}\,.$$

2.2.2 Stress, strain and displacement in circular rods under torsion

We consider a rod subjected to torsional moment (torque) M_x which generates tangent shear stress τ. For the special case of an elastic rod with circular (or ring) cross-section under torsion the shear stress is described by a formula:

$$\tau_\rho = \frac{M_x\,\rho}{J_0} \qquad \text{where} \qquad \rho \text{ - radial distance from the center,}$$

J_0 – polar moment of inertia.

It can be seen from the stress formula, that shear stress in the rod cross-section is directly proportional to the distance to its x-axis, i.e. it varies linearly with the radial distance ρ.

Diagrams for shear stress distribution in the plane of cross-section has been presented in Fig. 2.24. On the left, a diagram for a circular rod with radius r subjected to torque $M_s>0$ is shown. On the right, a diagram for a hollow shaft with external radius R and internal r, subjected to torque $M_s>0$ is shown.

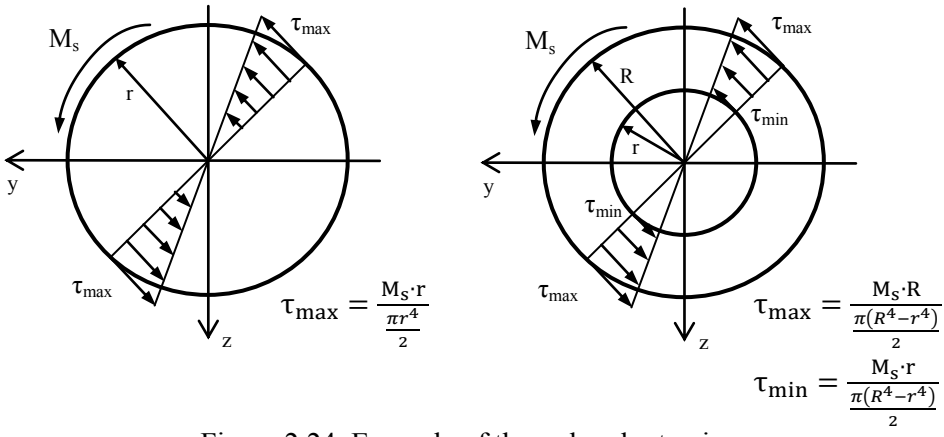

Figure 2.24. Example of the rod under torsion

Distribution of the shear stress in an axial planes is also linear, what follows the condition of equality of perpendicular tangential stress.

A torqued rod produces a relative rotation of one end respect to the other and this relative rotation is called the twist angle θ. The twist angle per unit of x-length is called the twist rate dθ and can be calculated for elementary section dx based on a formula:

$$d\theta = \frac{M_x dx}{GJ_0} \qquad \text{where:} \quad G \text{ –Kirchoff's modulus.}$$

Kirchoff's modulus G, also called the shear modulus of elasticity, is a constant, which depends on the material properties and describes the material's response to shear stress. The relation between the Young's modulus and the Kirchoff's modulus is given by the equation: $G = \frac{E}{2(1+\nu)}$.

Limiting values for the Poisson's ration are $\nu \in \langle 0;0{,}5 \rangle$ while $G \in \langle \frac{E}{3}; \frac{E}{2} \rangle$.

Twist angle θ, for a given section with length x, subjected to a constant torque $M_x=M_s$ can be calculated using a formula:

$$\theta = \int_0^x d\theta = \int_0^x \frac{M_s\, dx}{G J_0} = \frac{M_s\, x}{G J_0}\,.$$

We can simplify the above formula for constant torque M_s through a segment with length l and constant properties GJ_0, getting:

$$\theta = \frac{M_s\, l}{G J_0}\,.$$

2.2.3 Stress, strain and displacement at pure bending and bending with shear

Pure bending refers to flexure of a beam under constant bending moment, which means that the shear force is zero. In contrast, non-uniform bending refers to flexure in the presence of shear forces, which means that the bending moment changes as we move along the beam main axis. Most structures will be experiencing a combination of both forces at once.

We consider first the **pure bending** e.g. the case when both bending vectors M_y and M_z are directed along the principal centroidal axes of the cross-section: vector M_y lies along the y-axis and vector M_z lies along the z-axis.

In the next part we will consider unsymmetrical bending, when resultant bending moment M and resultant shear force vector T are not directed along any principal centroidal axis, and the neutral axis does not coincide with the axis of the moment.

For symmetrical bending in xz plane all the external forces, e.i. loads and reaction forces, and deformed axis of the beam lie in xz plane. Bending moment M_y and shear force T_z acts along the axis perpendicular to xz plane.

For symmetrical bending in xy plane all the external forces, e.i. loads and reaction forces, and deformed axis of the beam lie in xy plane. Bending moment M_z and shear force T_y acts along the axis perpendicular to xy plane.

The **normal stresses σ_x** caused by the bending moment are known as bending stress, or flexure stresses. The relationship between these stresses and the bending moment is called the flexure formula:

in xz plane $$\sigma_x = \frac{M_y\ z}{J_y},$$

in xy plane $$\sigma_x = -\frac{M_z\ y}{J_z},$$

where J_y and J_z are the moments of inertia for a given cross-section, while y and z are any distance from the neutral axis along y and z.

In the elastic range, the normal stress σ_x varies linearly with the distance from the neutral surface (see Fig. 2.25).

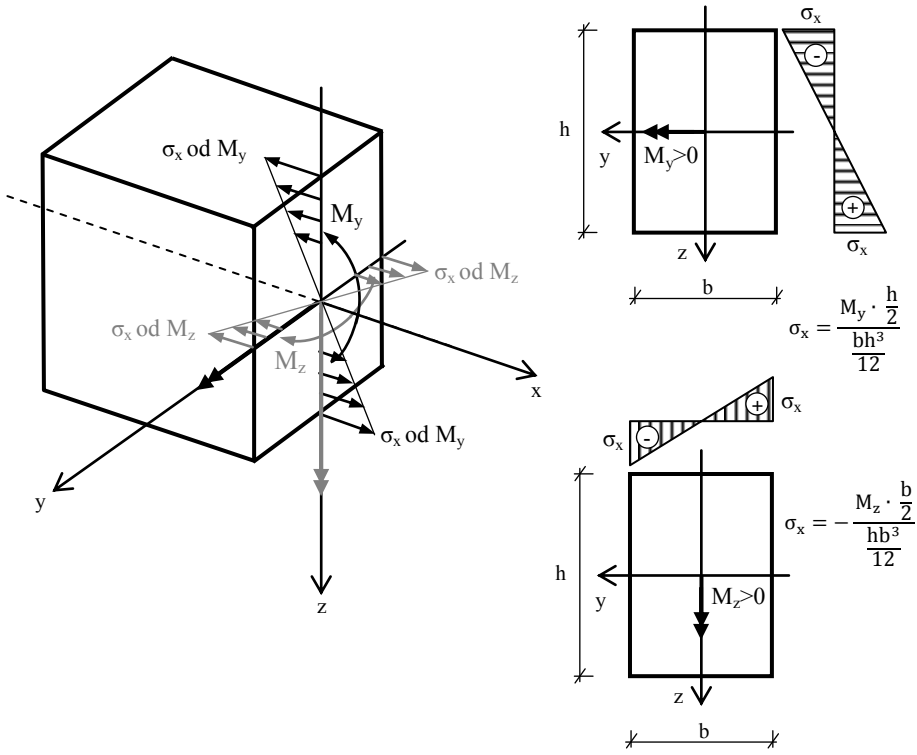

Figure 2.25. Example of the normal stress

Transversal shear force T_z (when bending in xz plane) and shear force T_y (when bending in xy plane) are responsible for shear stress acting on the cross-section.
Shear stress in a beam of arbitrary cross-section can be estimated using formulas:

in xz plane $\tau_{xz} = \frac{T_z\,|\overline{S_y}|}{J_y\,b}$ (and $\tau_{xy} = \frac{T_z\,|\overline{S_y}|}{J_y\,\hat{b}}$),

in xy plane $\tau_{xy} = \frac{T_y\,|\overline{S_z}|}{J_z\,b}$ (and $\tau_{xz} = \frac{T_y\,|\overline{S_z}|}{J_z\,\hat{b}}$),

where J_y and J_z are the moments of inertia for a given cross-section, $|\overline{S_y}|$ is an absolute value of the first moment with respect to the neutral axis of the portion A of the cross section of the beam, that is located above the line parallel to y axis in the point of interest, while b ($\hat{b}$) is the width of the element at the cut. Respectively, $|\overline{S_z}|$ is an absolute value of the first moment with respect to the neutral axis of the portion A of the cross section of the beam, that is located

above the line parallel to z axis in the point of interest, while b ($\hat{b}$) is the width of the element at the cut in that direction.
Distribution of the shear stress is represented by shear flow (the name commonly used to refer to the shear per unit length). Shear stress distribution has been shown in Fig. 2.26, Fig. 2.27 and Fig. 2.28 (bending in xz plane) and Fig. 2.29 (bending in xy plane).

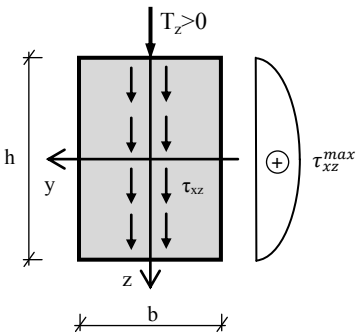

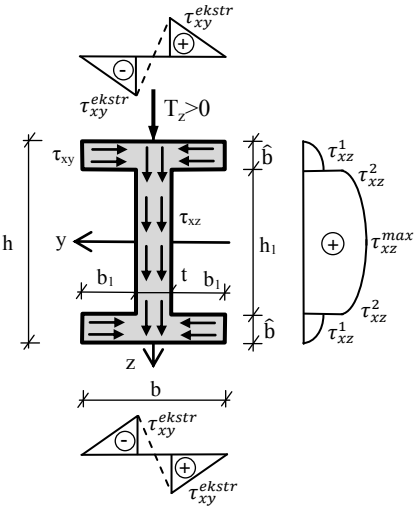

Figure 2.26. Bending xz plane example Figure 2.27. Bending xy plane example

Maximum value of shear stress has been shown in Fig. 2.26 and can be calculated using formula:

$$\tau_{xz}^{max} = \frac{T_z \cdot \left(b \cdot \frac{h}{2} \cdot \frac{h}{4}\right)}{J_y \cdot b} \qquad \text{where} \qquad J_y = \frac{bh^3}{12}.$$

Values of shear stress shown in Fig. 2.27 can be calculated using formulas:

$$\tau_{xz}^{1} = \frac{T_z \cdot \left[b \cdot \hat{b} \cdot \left(\frac{h_1}{2} + \frac{\hat{b}}{2}\right)\right]}{J_y \cdot b} \qquad \tau_{xz}^{2} = \frac{T_z \cdot \left[b \cdot \hat{b} \cdot \left(\frac{h_1}{2} + \frac{\hat{b}}{2}\right)\right]}{J_y \cdot t}$$

$$\tau_{xz}^{max} = \frac{T_z \cdot \left[b \cdot \hat{b} \cdot \left(\frac{h_1}{2} + \frac{\hat{b}}{2}\right) + t \cdot \frac{h_1}{2} \cdot \frac{h_1}{4}\right]}{J_y \cdot t}$$

$$\tau_{xy}^{ekstr} = \frac{T_z \cdot \left[b_1 \cdot \hat{b} \cdot \left(\frac{h_1}{2} + \frac{\hat{b}}{2}\right)\right]}{J_y \cdot \hat{b}} \qquad \text{and} \qquad J_y = \frac{bh^3}{12} - \frac{2b_1 h_1^3}{12}.$$

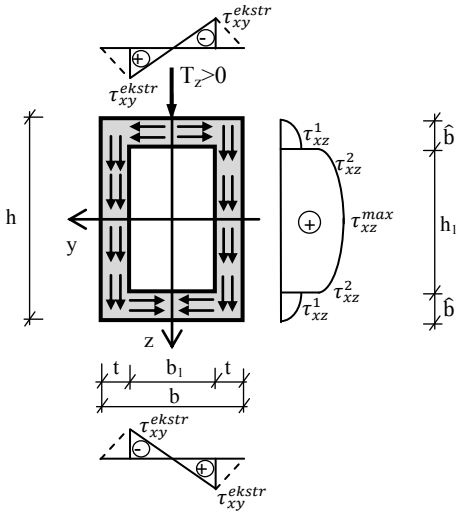

Figure 2.28. Bending xz plane example

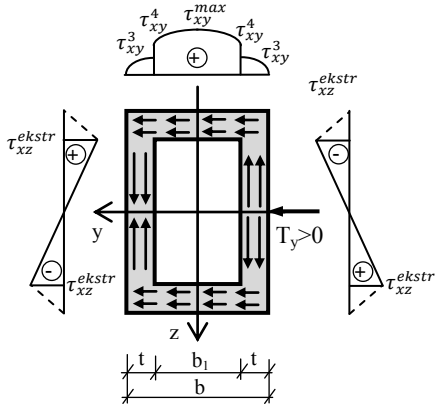

Figure 2.29. Bending xy plane example

Moments of inertia calculated for box cross-section shown in Fig. 2.28 and Fig. 2.29 are equal $J_y = \frac{bh^3}{12} - \frac{b_1 h_1^3}{12}$ and $J_z = \frac{hb^3}{12} - \frac{h_1 b_1^3}{12}$.

Values of shear stress shown in Fig. 2.28 can be calculated using formulas:

$$\tau_{xz}^{1} = \frac{T_z \cdot \left[b \cdot \hat{b} \cdot \left(\frac{h_1}{2} + \frac{\hat{b}}{2} \right) \right]}{J_y \cdot b} \qquad \tau_{xz}^{2} = \frac{T_z \cdot \left[b \cdot \hat{b} \cdot \left(\frac{h_1}{2} + \frac{\hat{b}}{2} \right) \right]}{J_y \cdot 2t}$$

$$\tau_{xz}^{max} = \frac{T_z \cdot \left[b \cdot \hat{b} \cdot \left(\frac{h_1}{2} + \frac{\hat{b}}{2} \right) + 2t \cdot \frac{h_1}{2} \cdot \frac{h_1}{4} \right]}{J_y \cdot 2t} \qquad \tau_{xy}^{ekstr} = \frac{T_z \cdot \left[\frac{b_1}{2} \cdot \hat{b} \cdot \left(\frac{h_1}{2} + \frac{\hat{b}}{2} \right) \right]}{J_y \cdot \hat{b}}.$$

Values of shear stress shown in Fig. 2.29 can be calculated using formulas:

$$\tau_{xy}^{3} = \frac{T_y \cdot \left[h \cdot t \cdot \left(\frac{b_1}{2} + \frac{t}{2} \right) \right]}{J_z \cdot h} \qquad \tau_{xy}^{4} = \frac{T_y \cdot \left[h \cdot t \cdot \left(\frac{b_1}{2} + \frac{t}{2} \right) \right]}{J_z \cdot 2\hat{b}}$$

$$\tau_{xy}^{max} = \frac{T_y \cdot \left[h \cdot t \cdot \left(\frac{b_1}{2} + \frac{t}{2} \right) + 2\hat{b} \cdot \frac{b_1}{2} \cdot \frac{b_1}{4} \right]}{J_z \cdot 2\hat{b}} \qquad \tau_{xz}^{ekstr} = \frac{T_y \cdot \left[\frac{h_1}{2} \cdot t \cdot \left(\frac{b_1}{2} + \frac{t}{2} \right) \right]}{J_z \cdot t}.$$

The **neutral axis** is an axis in the cross section of a beam along which there are no longitudinal stresses or strains.

The equation for neutral axis in case of bending in xz plane: $\frac{M_y\ z}{J_y} = 0$, while for bending in xy plane: $\frac{M_z\ y}{J_z} = 0$.

When a beam with a straight longitudinal axis is loaded by lateral forces and undergo symmetrical bending, the axis is deformed into a curve. **Linear displacements** of the cross-sections occur:

- „w" displacements parallel to the z-axis in case of xz plane bending,
- „v" displacements parallel to the y-axis in case of xy plane bending,

and **rotations** φ ($\varphi = \frac{dw}{dx}$ or $\varphi = \frac{dv}{dx}$) also known as angle of inclination and angle of slope (Fig.2.30 and 2.31).

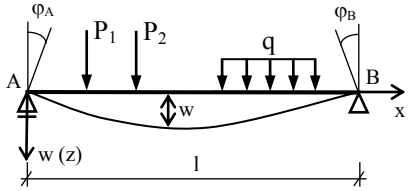

Figure 2.30. Angle of inclination

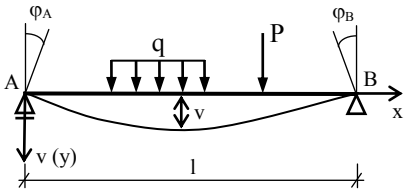

Figure 2.31. Angle of slope

A curve in plane, described by the equation w = w(x) or v = v(x) is called the deflection curve of the beam (in xz or xy plane respectively).

Differential equation of the deflection curve, if we assume coordinate system as shown in Fig 2.30 and 2.31, can be written:

- bending in xz plane $EJ_y \frac{d^2w(x)}{dx^2} = -M_y(x)$,
- bending in xy plane $EJ_z \frac{d^2v(x)}{dx^2} = M_z(x)$.

The equation of the deflection curve w(x) or v(x) is obtained by integrating twice in x the governing differential equation for the elastic curve (assumed EJ_y=const., EJ_z=const.):

$$EJ_y \frac{d^2w(x)}{dx^2} = -M_y(x) \quad \text{and} \quad EJ_z \frac{d^2v(x)}{dx^2} = M_z(x),$$

$$EJ_y \frac{dw(x)}{dx} = -\int M_y(x)dx + C \quad \text{and} \quad EJ_z \frac{dv(x)}{dx} = \int M_z(x)dx + \overline{C},$$

$$EJ_y\, w(x) = -\int\left[\int M_y(x)dx\right]dx + Cx + D,$$

$$\text{and} \quad EJ_z\, v(x) = \int\left[\int M_z(x)dx\right]dx + \overline{C}x + \overline{D}.$$

The constants of integration C, D and $\overline{C}, \overline{D}$ are determined from the boundary conditions (more precisely, from the conditions imposed on the beam by its supports) and continuity conditions for displacement and rotation.

In case of unsymmetrical bending external load acts in more than one plane. Resultant bending moment M is directed along the axis perpendicular to the trace of the load plane. We can resolve M into components M_y and M_z along the principal axes and superposed the stresses due to the component moments (T_z and T_y similarly).
Normal stress can be computed using an expression:

$$\sigma_x = \frac{M_y z}{J_y} - \frac{M_z y}{J_z}.$$

Shear stress due to unsymmetrical bending can be determined, based on superposition principle, separately for T_z (shear τ_{xz} and τ_{xy}) and T_y (shear τ_{xy} and τ_{xz}). Subsequently, for any given point of the cross-section we can superpose the shear stress caused by T_z and T_y forces.
We determine the orientation of the neutral axis in unsymmetrical bending by writing:

$$\frac{M_y z}{J_y} - \frac{M_z y}{J_z} = 0.$$

The neutral axis of the cross section is a straight line passes through the center of the yz local coordinate. Additionally, it passes through the same quarters of the coordinate as an axis determined by the direction of the resultant bending moment M. The neutral axis of the cross-section is perpendicular to the trace of the bending plane.
Calculating the displacement due to the unsymmetrical bending we separately consider bending in xz and xy plane. We calculate the displacements w and v in these planes and then the resulting displacement from a formula:

$$\delta = \sqrt{w^2 + v^2}.$$

The direction of this displacement is different in every cross-section, which means that the deflection curve due to unsymmetrical bending is a spatial curve in general. If the external loads and the reaction forces acts in the same plane for all the cross-sections, then the deflection curve is a curve in plane. The deflection curve lies in the bending plane.

2.2.4 Stress due to eccentric tension or compression

Consider a straight rod subjected to an eccentric axial force N_x, and let e_y and e_z denote the distances from the line of action of the force to the principal centroidal axes of the cross section of the member. This type of loading is called

eccentric tension if the force $N_x > 0$ or eccentric compression if the force $N_x < 0$ (see Fig.2.32).

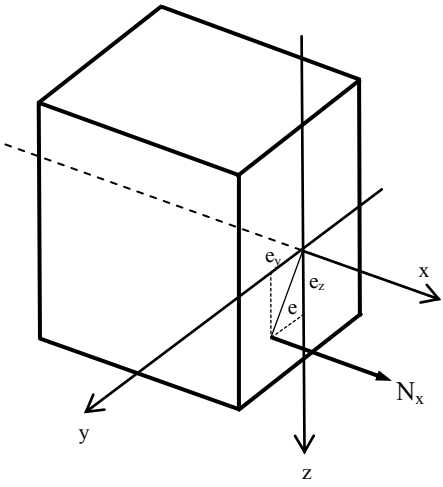

Figure 2.32. Eccentric tension

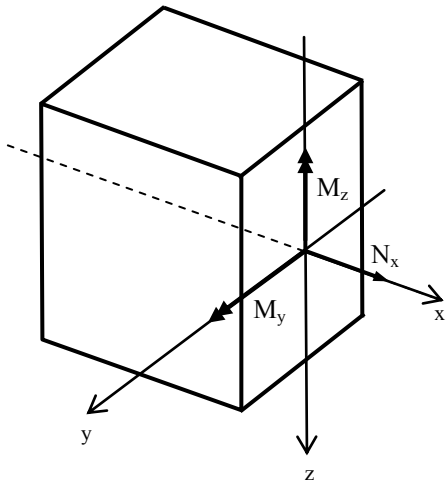

Figure 2.33. Eccentric compression

Eccentric tension (compression) can be replaced by superposition of unsymmetrical bending and centric axial force (Fig.2.33).
We write, therefore: $M_z = -N_x e_y$ and $M_y = N_x e_z$.

Normal stress due to unsymmetrical bending with centric axial force can be calculated from a formula:

$$\sigma_x = \frac{M_y z}{J_y} - \frac{M_z y}{J_z} + \frac{N_x}{A}.$$

Substituting $M_z = -N_x \cdot e_y$ and $M_y = N_x \cdot e_z$ we get:

$$\sigma_x = \frac{N_x e_z z}{J_y} + \frac{N_x e_y y}{J_z} + \frac{N_x}{A}$$

$$\sigma_x = \frac{N_x}{A}\left(\frac{e_z z}{i_y^2} + \frac{e_y y}{i_z^2} + 1\right) \text{ where: } i_y = \sqrt{\frac{J_y}{A}} \text{ and } i_z = \sqrt{\frac{J_z}{A}}.$$

where i_y and i_z denote the radius of gyration of the cross section with respect to the z axis and the x axis, respectively.
Normal stresses can be expressed only by the axial force, the coordinates e_y, e_z of the point where the force is applied and cross-section geometry characteristics A, i_y, i_z.

The equation defining the neutral axis for eccentric loading can be written as:

$$\frac{e_z z}{i_y^2} + \frac{e_y y}{i_z^2} + 1 = 0$$

or in the two intercept form:

$$\frac{y}{-\frac{i_z^2}{e_y}} + \frac{z}{-\frac{i_y^2}{e_z}} = 1 .$$

The neutral axis is a straight line that does not pass through the origin of the yz coordinate system in the given cross section of the bar in subjected to eccentric tension (compression). The neutral axis location with respect to the cross-section depends on the e_y and e_z values, so on the location of the axial load N_x with respect to yz.

Three possibilities of the neutral axis location with respect to the cross-section in case of axial tension (N_x>0) has been presented in Fig. 2.34.

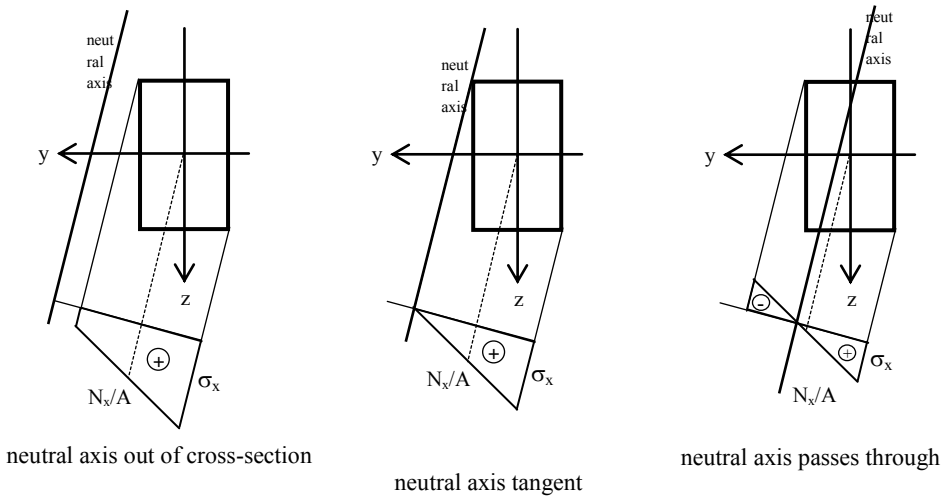

neutral axis out of cross-section

neutral axis tangent

neutral axis passes through

Figure 2.34. Neutral axis location – example

If the material of the rod is characterized by high permissible compression stresses but low permissible tensile stresses (e.g. concrete), it is important to know the location of the compression load (eccentricity e_y and e_z) so that tensile stresses never develop in the cross-section.

A **cross-section kern** is the convex region in which a compressive axial load N_x may be applied without producing any tensile stress on the cross section. In this case the neutral axis doesn't intersect the cross-section.

To determine the location of cross-section kern the algorithm is as follows:

1. find the principal centroidal axes and the principal moments of inertia J_y and J_z associated with these principal axes, then calculate moments of gyration i_y^2, i_z^2,

2. next, we assume that the axial force Nx is applied consecutively at each vertex of the cross-section. If the cross-section is concave polygon, then we apply Nx at each vertex of the smallest convex region that includes cross-section. For all selected point we derive the neutral axis equation. All the lines determined this way define boundary of the kern.

The kern of the cross-section is always limited by a convex polygon.
Examples of the kern shapes for rectangular, triangular and circular cross-sections has been presented in Fig 2.35.

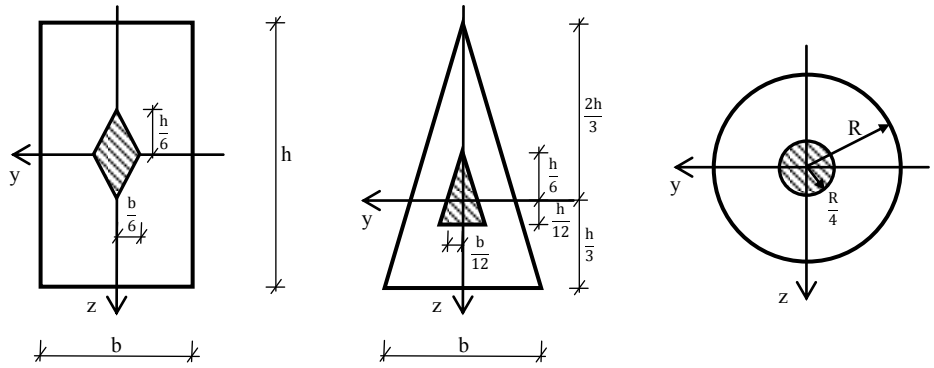

Figure 2.35. Kern shapes examples

For a wide flange symmetrical cross-section the kern shape is a diamond. Determining a shape of the cross-section kern for T-beam we start with finding the principal centroidal axes and the principal moments of inertia J_y and J_z associated with these principal axes. Subsequently, we draw the smallest hexagonal polygon containing concave T-shape, and calculate boundary of the kern. The cross-section of the rod and the kern of the cross-section are mutual polygons, i.e. each vertex of the kern corresponds to one side of the cross-section, and each side of the kern corresponds to one vertex of the cross-section. So if the axial force N_x acts at the vertex of the kern, then the neutral axis passes through the corresponding side of the cross section. If the force N_x acts at the point on the side of the kern, then the neutral axis passes through the corresponding vertex of the cross-section.

2.3 STABILITY OF COLUMNS

Any structure, and its elements, has to meet stability condition (besides the other conditions e.g. its ability to support a specified load without experiencing excessive stress or undergoing unacceptable deformations).

The buckling phenomenon (also called instability or loss of stability) of the axially compressed rod consists in the loss of ability to support a given load without experiencing a sudden change in its configuration.
The critical load (critical force) is the maximum load (force) which a column can bear while staying straight (longitudinal axis of the rod becomes sharply curved). A well designed structure shall be stable under all conceivable conditions. To fulfill this condition, a structure has to be geometrically stable (rigidity condition) and the applied load should not exceed a certain value (critical load).
Design process consists of determining the magnitude of the critical load for the structure and checking if the value of the applied load (multiplied by a safety factor) is lower than the critical load.
The value of the stress corresponding to the critical load P_{kr} is called the critical stress:

$$R_{kr} = \frac{P_{kr}}{A}$$ where: A – area of the cross-section.

If the critical stress remains below the proportional limit (R_H)
e.i. $R_{kr} \leq R_H$ elastic buckling behavior,
otherwise $R_{kr} > R_H$ inelastic buckling behavior.

For **elastic buckling** of columns with various boundary conditions and subjected to compression, the critical load can be calculated using Euler's formula:

$$P_{kr} = \frac{\pi^2 E J_{min}}{(\mu l)^2},$$

where: μ - effective length factor, depends on type of supports.
J_{min}=min (J_y, J_z), J_y i J_z calculated for principal axes of the cross-section,
l – length of the column.

Effective length factors for various support conditions have been presented in Fig 2.36.

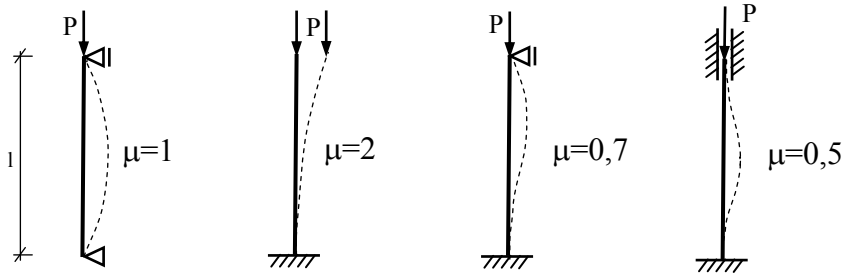

Figure 2.36. Effective length factors for various support conditions

The value of the stress corresponding to the critical load:

$$R_{kr} = \frac{P_{kr}}{A} = \frac{\pi^2 E J_{min}}{(\mu l)^2 A} = \frac{\pi^2 E}{(\mu l)^2} \frac{J_{min}}{A} = \frac{\pi^2 E}{(\mu l)^2} i_{min}^2 = \pi^2 E \frac{i_{min}^2}{(\mu l)^2} = \frac{\pi^2 E}{\lambda_{max}^2}$$

where: $\lambda_{max} = \frac{\mu l}{i_{min}}$ is an effective slenderness ratio.

The effective slenderness ratio depends on the length of the column and its radius of gyration (geometrical properties of the cross-section).
Euler's formula can be applied only if $R_{kr} \leq R_H$

therefore, $\frac{\pi^2 E}{\lambda_{max}^2} \leq R_H \quad \Rightarrow \quad \lambda_{max}^2 \geq \frac{\pi^2 E}{R_H}$

$$\lambda_{max} \geq \sqrt{\frac{\pi^2 E}{R_H}}$$

$$\lambda_{max} \geq \lambda_{gr} \quad \text{where} \quad \lambda_{gr} = \pi \sqrt{\frac{E}{R_H}}$$

λ_{gr} is a slenderness limit and depends only on the mechanical properties of the material the column is made of. Therefore, if $\lambda_{max} \geq \lambda_{gr}$, then the column will experience elastic buckling and Euler's formula can be used. Whereas for $\lambda_{max} < \lambda_{gr}$ Euler's formula is not valid anymore, since the buckling is inelastic (material of the column will diverge from a linear stress-strain behaviour).
For the case of **inelastic buckling** the critical force (critical stress) can be determined by the use of the tangent modulus of elasticity or empirical formulas based on laboratory tests:

$$P_{kr} = A \left(R_{pl} - \frac{R_{pl} - R_H}{\lambda_{gr}^2} \lambda^2 \right).$$

where: R_{pl} is the yield strength of the material.

2.4 REFERENCES

1. Jastrzębski P., Mutermilch J, Orłowski W.: Wytrzymałość Materiałów, część 1 i 2. Arkady, Warszawa 1986.
2. Grabowski J. Iwanczewska A.: Zbiór zadań z wytrzymałości materiałów. Wydawnictwo PW, Warszawa 2008.
3. Bijak-Żochowski M. - red.: Mechanika Materiałów i Konstrukcji. Wydawnictwo PW, Warszawa 2006.
4. Garstecki A. Dębiński J.: Wytrzymałość Materiałów. Wydanie internetowe Alma Mater Politechniki Poznańskiej.

CHAPTER 3
PRACTICAL APPLICATIONS

3.1 SHALLOW FOUNDATIONS (K. JÓZEFIAK, A. ZBICIAK)

3.1.1 Introduction

A foundation is a structural element that is expected to transfer a load from a structure to the ground safely. The two major classes of foundations are shallow foundations and deep foundations. A shallow foundation transfers the entire load at a relatively shallow depth. A common understanding is that the depth of a shallow foundation (D_f) must be less than the breadth (B). Breadth is the shorter of the two plan dimensions. Shallow foundations include pad footings, strip (or wall) footings, combined footings, and mat foundations. Deep foundations have a greater depth than breadth and include piles, pile groups, and piers. A typical building can apply 10–15 kPa per floor, depending on the column spacing, type of structure, and number of floors [10].

Shallow foundations generally are designed to satisfy two criteria: bearing capacity and settlement. The bearing capacity criterion ensures that there is adequate safety against possible bearing capacity failure within the underlying soil. This is done through provision of an adequate factor of safety of about 3. In other words, shallow foundations are designed to carry a working load of one-third of the failure load. The settlement criterion ensures that settlement is within acceptable limits. For example, pad and strip footings in granular soils generally are designed to settle less than 25 mm [10].

3.1.2 Base pressure under foundation

During geotechnical calculations of shallow foundation we are mainly interested in vertical stresses at any point in a soil-mass under foundation base due to external vertical loadings. To calculate these stresses we assume constant distribution of pressure under foundation base, and we treat this as the loading.

However, the distribution of pressure under shallow foundation base depends on how the loads form the build are applied to the foundation. As shown in Figure 3.1a the base pressure is constant only when the load *P* from the structure is applied in the centre of the footing. When the loading is eccentric but applied inside the core of the footing cross-section (Figure 3.1b) the distribution changes linear. In this case, for calculations of stresses in soil we usually assume an average value of the minimum and maximum pressures.

When designing shallow foundations the load *P,* generally in most cases, has to be applied within the core of the cross-section. Otherwise some of the foundation would separate from the ground as soil has no tensile strength. When such a problem occurs the planar dimensions of the footing (B and L) have to be changed so that the force is inside the cross-section's core.

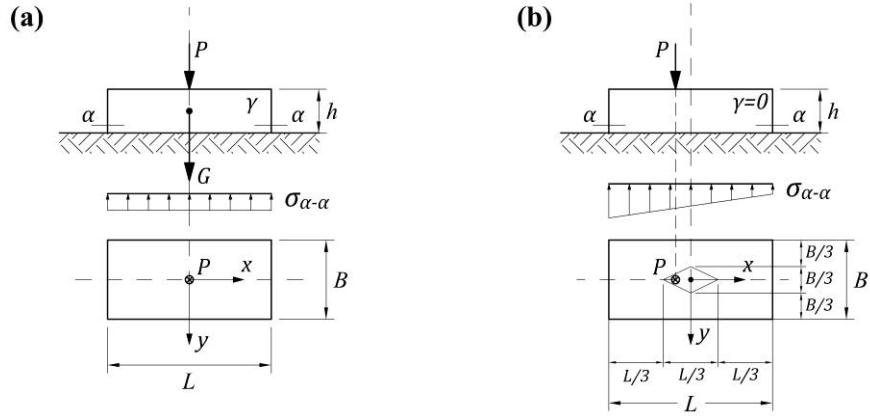

Fig. 3.1. Base pressure distribution under footing base

3.1.3 Stress distribution in soil mass due to surface loading

Estimation of vertical stresses at any point in a soil-mass due to external vertical loadings are of great significance in the prediction of settlements of buildings, bridges, embankments and many other structures [9].

According to elastic theory, constant ratios exist between stresses and strains. For the theory to be applicable, the real requirement is not that the material necessarily be elastic, but there must be constant ratios between stresses and the corresponding strains. Therefore, in non-elastic soil masses, the elastic theory may be assumed to hold so long as the stresses induced in the soil mass are relatively small [9]. Since the stresses in the subsoil of a structure having adequate

factor of safety against shear failure are relatively small in comparison with the ultimate strength of the material, the soil may be assumed to behave elastically under such stresses [9].

Many formulas based on the theory of elasticity have been used to compute stresses in soils. They are all similar and differ only in the assumptions made to represent the elastic conditions of the soil mass. The formulas that are most widely used are the Boussinesq and Westergaard formulas. These formulas were first developed for point loads acting at the surface. These formulas have been integrated to give stresses below uniform strip loads and rectangular loads [9].

Point load

The problem of point load applied to infinite half-space was solved by Boussinesq in 1885 on the following assumptions:

1. the soil mass is elastic, isotropic, homogeneous and semi-infinite,
2. the soil is weightless,
3. the load is a point load acting on the surface.

Stress components in the cylindrical coordinate system shown in Figure 3.2 are as follows:

$$\sigma_z = \frac{3Q}{2\pi z^2}\left\{\frac{1}{1+\left(\frac{r}{z}\right)^2}\right\}^{5/2} \tag{3.1}$$

$$\sigma_r = \frac{3Q}{2\pi}\left\{\frac{3r^2 z}{(r^2+z^2)^{5/2}} - \frac{1-2\nu}{r^2+z^2+z(r^2+z^2)^{1/2}}\right\} \tag{3.2}$$

$$\sigma_\theta = -\frac{Q}{2\pi}(1-2\nu)\left\{\frac{z}{(r^2+z^2)^{3/2}} - \frac{1}{r^2+z^2+z(r^2+z^2)^{1/2}}\right\} \tag{3.3}$$

$$\sigma_{rz} = \frac{3Q}{2\pi}\left\{\frac{rz^2}{(r^2+z^2)^{5/2}}\right\} \tag{3.4}$$

For geotechnical calculations one mainly needs the vertical stress component $\sigma_z \equiv \sigma_v$. According to Equation (3.1) vertical stress diminishes with depth and with the distance from the point load as shown in Figure 3.3.

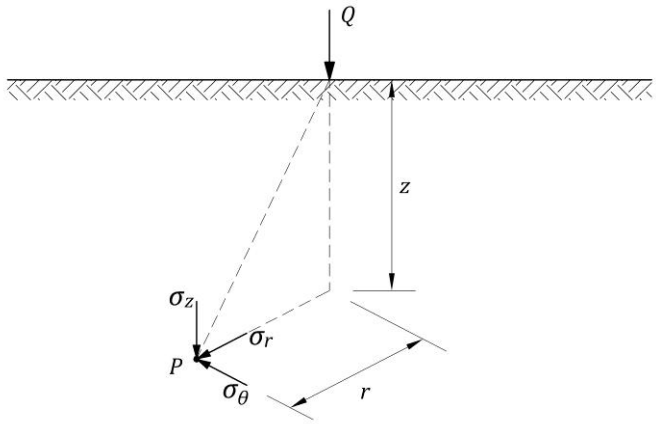

Fig. 3.2. Stress components and coordinate system used in the Boussinesq solution[9]

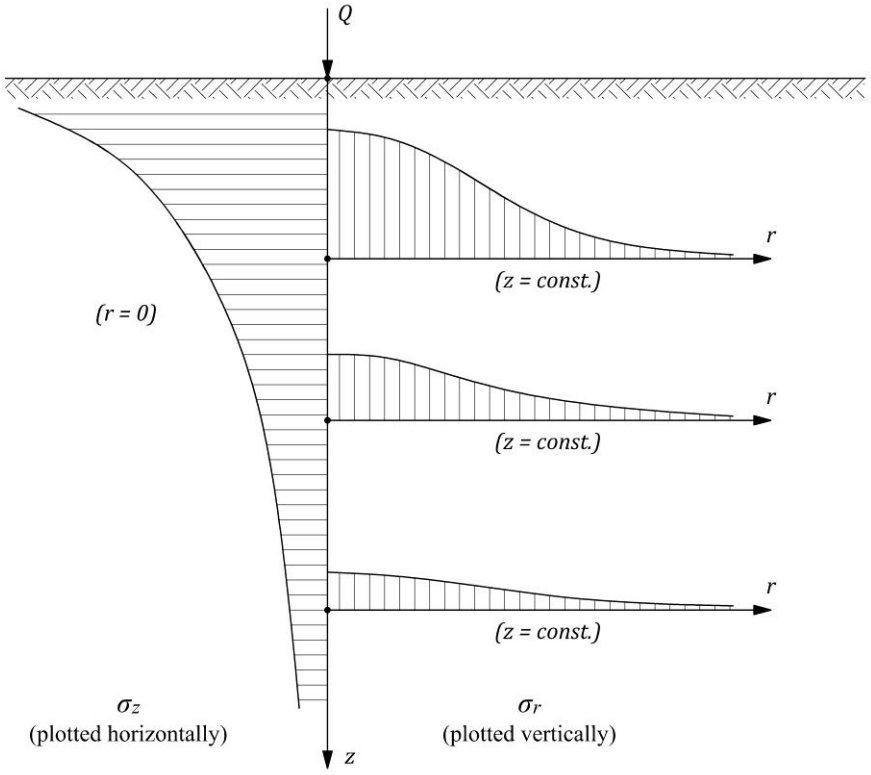

Fig. 3.3. Stress distribution under point load [9]

The solution of point load can be used to estimate the stress caused by a distant footing foundation.

Stresses beneath the corner of a rectangular flexible foundation

The solution for stresses beneath the corner of a rectangular flexible foundation was obtained by Steinbrenner in 1934:

$$\sigma_z = q \cdot \eta_n \tag{3.5}$$

where

$$\eta_n = \frac{1}{2\pi}\left\{\frac{L\,B\,z\left(L^2+B^2+2\,z^2\right)}{(L^2+z^2)(B^2+z^2)(L^2+B^2+z^2)^{1/2}} + \arctan\left[\frac{L\,B}{z\,(L^2+B^2+z^2)^{1/2}}\right]\right\} \tag{3.6}$$

Where L is the longer dimension of the footing, B is the shorter dimension of the footing and z is the vertical coordinate (see Figure 3.1).

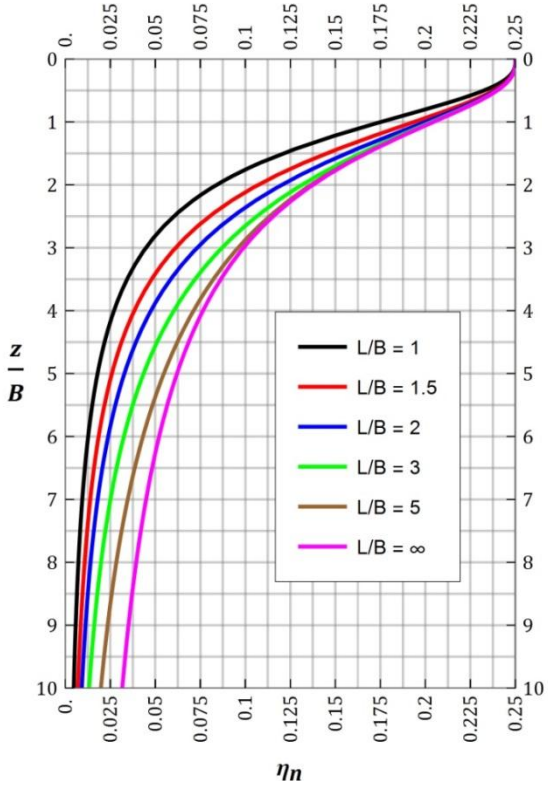

Fig. 3.4. Coefficient of vertical stress beneath the corner of a rectangular flexible foundation according to equation (3.6)

Instead of Equation (3.6), in practice, nomograms are commonly used to obtain values of η_n as shown in Figure 3.4.

Using solution (3.6) stress distribution under any other point can by calculated using the superposition principle. For example to calculate stress under point O in Figure 3.5a we need to add solutions for the four small squares

$$\sigma_z^{(O)} = q \cdot (\eta_{n1} + \eta_{n2} + \eta_{n3} + \eta_{n4}) \tag{3.7}$$

and for a point outside the area of the foundation (Figure 3.5b)

$$\sigma_z^{(O)} = q \cdot (\eta_n^{OB_1CD_1} - \eta_n^{OA_1DD_1} - \eta_n^{OB_1BD_2} + \eta_n^{OA_1AD_2}) \tag{3.8}$$

The method of stresses calculation based on Equation (3.6) is called the corners point method.

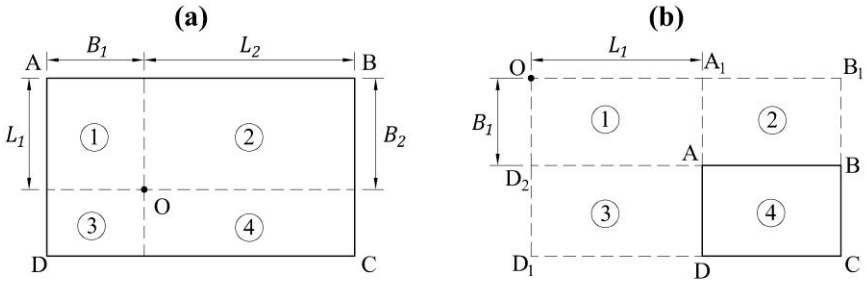

Fig. 3.5. Estimating stress under any point using the solution for stresses beneath the corner of a rectangular flexible load [11]

3.1.4 Limit state calculations of shallow foundations

The mechanism of failure under a strip or square foundation is shown in Figure 3.6. Terzaghi presented his bearing capacity equation for shallow foundations in 1943. The equation was derived for a strip (continuous) foundation with general shear failure. A strip foundation is a foundation with a finite width B and a very long length L (thus $B/L \approx 0$).

$$R_{Terzaghi}^{strip} = A\left(c'N_c + q'N_q + \frac{1}{2}\gamma' B N_\gamma \right) \tag{3.9}$$

where

$$N_q = \mathrm{e}^{\pi \tan \phi'} \tan^2\left(45° + \frac{\phi'}{2}\right) \tag{3.10}$$

$$N_c = \left(N_q - 1\right) \cot \phi' \tag{3.11}$$

$$N_\gamma = \left(N_q - 1\right) \tan(1.4\phi') \tag{3.12}$$

Equation (3.9) can be modified to estimate bearing capacity for a square foundation

$$R_{Terzaghi}^{square} = A\left(1.3\, c' N_c + q' N_q + 0.4\, \gamma' B N_\gamma\right) \tag{3.13}$$

Generalized bearing capacity equation that includes correction factors for foundation depth, foundation shape and for inclined load was developed by Meyerhof in 1963. A slightly modified version of the Meyerhof's equation is proposed by the Eurocode 7 [12], in which for drained condition

$$R_{EC7} = A'\left(c' N_c b_c s_c i_c + q' N_q b_q s_q i_q + \frac{1}{2}\gamma' B' N_\gamma b_\gamma s_\gamma i_\gamma\right) \tag{3.14}$$

where γ' – effective unit weight of soil (weight of soil taking buoyancy into account), $q' = \gamma' D_{min}$ – effective overburden pressure at foundation depth, $A' = B'L'$ – effective foundation cross-sectional area (see Fig. 3.7b):

$$B' = B - 2e_B \tag{3.14}$$

$$L' = L - 2e_L \tag{3.15}$$

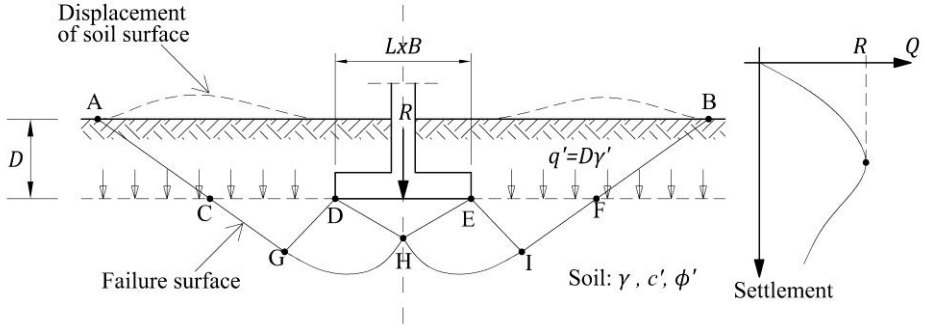

Fig. 3.6. Shear failure of a strip or square foundation [9]

Bearing capacity factors are:

$$N_q = \mathrm{e}^{\pi \tan \phi'} \tan^2\left(45° + \frac{\phi'}{2}\right) \tag{3.16}$$

$$N_c = \left(N_q - 1\right)\cot\phi' \tag{3.17}$$

$$N_\gamma = 2\left(N_q - 1\right)\tan\phi' \tag{3.18}$$

Factors taking into account the inclination of foundation's base with respect to horizontal (see Figure 3.7a for the angle α) are:

$$b_c = b_q - \frac{1-b_q}{N_c \tan\phi'} \tag{3.19}$$

$$b_q = b_\gamma = (1 - \alpha\tan\phi')^2 \tag{3.20}$$

Shape factors are

$$s_q = 1 + \left(\frac{B'}{L'}\right)\sin\phi' \tag{3.21}$$

$$s_\gamma = 1 - 0.3\left(\frac{B'}{L'}\right) \tag{3.22}$$

$$s_c = \frac{s_q N_q - 1}{N_q - 1} \tag{3.23}$$

Factors taking into account the inclination of the load with respect to the vertical caused by a horizontal load H

$$i_c = i_q - \frac{1-i_q}{N_c \tan\phi'} \tag{3.24}$$

$$i_q = \left[1 - \frac{H}{V + A'c'\cot\phi'}\right]^m \tag{3.25}$$

$$i_\gamma = \left[1 - \frac{H}{V + A'c'\cot\phi'}\right]^{m+1} \tag{3.26}$$

where

$$m = m_B = \frac{2 + (B'/L')}{1 + (B'/L')} \tag{3.27}$$

if the load H is applied in the direction of B' and

$$m = m_L = \frac{2 + (L'/B')}{1 + (L'/B')} \tag{3.28}$$

if the load H is applied in the direction of L'.

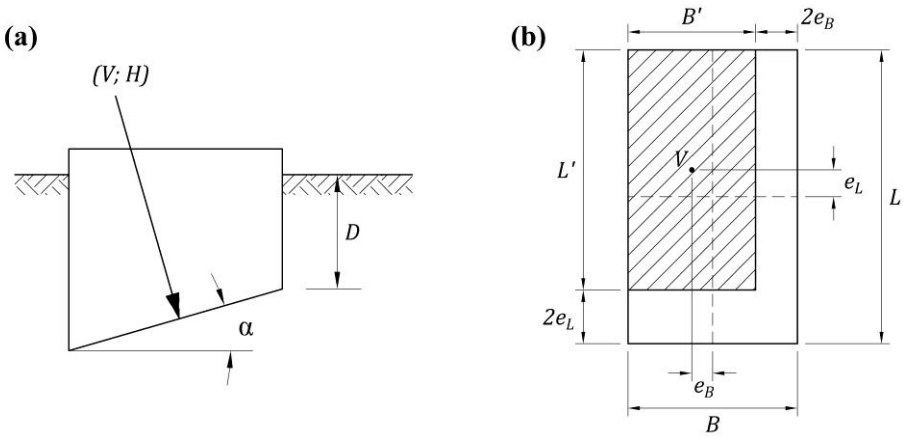

Fig. 3.7. a) Inclination of foundation base,
b) Effective area of foundation base [12]

Equation (3.7) applies for drained conditions that is for the state in which pore pressure induced by external loading (excess pressure) has dissipated and is close to zero. This state appears fast or slowly depending on soil conditions. For clays it takes years for pore pressure to dissipate and we can assume that drained conditions will be present at the end for the building usage period. For sands pore pressure dissipates rapidly as sands have got high coefficients of permeability. Drained conditions have to be considered always as buildings are designed to last for many decades.

Sometimes, however, it is safe to check also bearing capacity in undrained conditions. Such state, when pore water pressure is high due to external loading, can occur when loading is applied relatively fast. For example undrained conditions can be considered in clays just after building construction has been finished or due to any unpredicted short-lasting loading (building repairs, special loading cases).

Undrained bearing capacity formula is as follows:

$$R_{EC7}^{ud} = A'[(\pi + 2)c_u b_c s_c i_c + q] \tag{3.29}$$

where c_u – soil's undrained shear strength determined in a triaxial compression unconsolidated undrained test (TXUU), q – total overburden pressure at foundation depth and

$$b_c = 1 - \frac{2\alpha}{\pi+2} \tag{3.30}$$

$$s_c = 1 + 0.2\frac{B'}{L'} \tag{3.31}$$

$$i_c = \frac{1}{2}\left(1 + \sqrt{1 - \frac{H}{A'c_u}}\right) \quad ; \qquad H \le A'c_u \tag{3.32}$$

In the above calculations partial and correlation factors should be also taken into account according to [12]. These factors differ between European countries and weren't discussed in this chapter. Recommended values of these factors are included in Annex A of the Euro code 1997 [12].

3.1.5 Settlement calculations of shallow foundations

Settlement of shallow foundations can be calculated based on the results on oedometer (one-dimentional) consolidation test described earlier in this chapter. For engineering purposes the ultimate settlement is important that is the settlement at the end of consolidation which takes place in the soil layers under foundation.

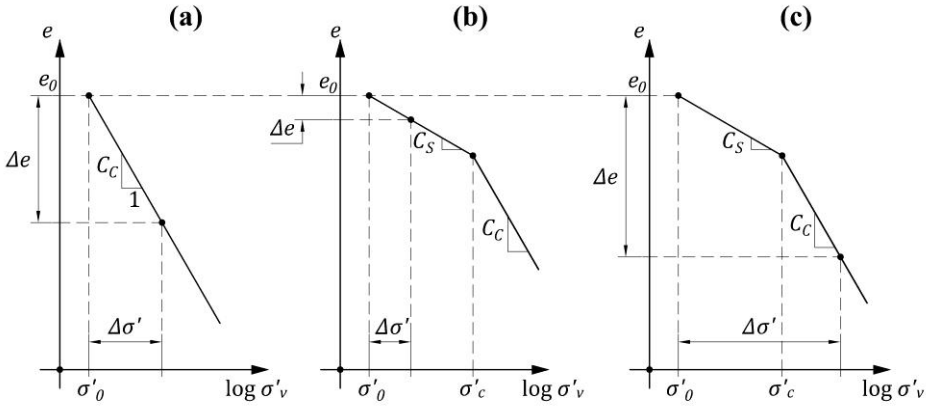

Fig. 3.8. Calculation of settlement. a) Normally consolidated soil, b) Over-consolidated soil (case 1), c) Over-consolidated soil (case 2).

To calculate ultimate settlement of soil under foundation first we have to divide the soil layers into sub-layers and calculate the rise of effective stress caused by external loading in the middle of every sub-layer. The height of a sub-layer has to be small enough to achieve sufficient accuracy. Generally $H_i \le B/2$ is sufficient.

The ultimate settlement of a number, *N*, of soil sub-layers is related to the change in every layer void ratio

$$S_c = \sum_{i=1}^{N} \frac{\Delta e_i}{1+e_{0,i}} H_i \tag{3.33}$$

where: Δe_i – change in void ratio of an i-th sub-layer, e_0 – initial void ratio of an i-th sub-layer, H_i – height of an i-th sub-layer.

The changes in void ratio for every soil layer Δe_i are caused by the rise of effective stress in the middle of every layer and depend on relation between soil overconsolidation pressure and stress caused by external loading.

For a normally consolidated soil (see Figure 3.8a)

$$\Delta e = C_c \log \frac{\sigma'_0 + \Delta\sigma'}{\sigma'_0} \tag{3.34}$$

For an over-consolidated soil (see Figure 3.8b)

$$\Delta e = C_s \log \frac{\sigma'_0 + \Delta\sigma'}{\sigma'_0} \tag{3.35}$$

or (see Figure 3.4)

$$\Delta e = C_s \log \frac{\sigma'_c}{\sigma'_{0,}} + C_c \log \frac{\sigma'_0 + \Delta\sigma'}{\sigma'_c} \tag{3.36}$$

3.2 DEEP FOUNDATIONS (K. JÓZEFIAK, A. ZBICIAK)

3.2.1 Introduction

Piles are long, slender structural members that transmit superstructure loads to greater depths within the underlying soil. Piles are generally used when soil conditions are not suited for the use of shallow foundations. Piles resist applied loads through shaft friction (skin friction) and end bearing as indicated in Figure 3.9. Friction piles resist a significant portion of their loads by the interface friction developed between their surface and the surrounding soils. On the other hand, end-bearing piles rely on the bearing capacity of the soil underlying their bases. Usually, end-bearing piles are used to transfer most of their loads to a stronger stratum that exists at a reasonable depth [9].

Piles can be either driven or cast in place (bored piles). Pile driving is achieved by impact dynamic forces from hydraulic and diesel hammers, vibration, or jacking. Concrete and steel piles are most common. Timber piles are less common. Driven piles with solid sections (e.g., concrete piles with square cross section) tend to displace a large amount of soil due to the driving process. These are full-displacement piles. Hollow piles such as open-ended pipe piles tend to displace a minimal amount of soil during the driving process. These are called partial displacement piles. Cast-in-place (or bored) piles do not cause any soil displacement since no pile driving is involved; therefore, they are non-displacement piles [9].

3.2.2 Bearing capacity of a single pile

There are two routinely used methods of piles' bearing capacity calculation: total stress approach (α-method) and effective stress approach (β-method). A detailed outline of these methods and problems related to them can be found e.g. in [13, 14].

Total capacity of a single pile is estimated as follows:

$$P_u = Q_b + Q_s = q_b A_b + \tau_s A_s \tag{3.37}$$

where P_u – total ultimate capacity, q_b – pressure on pile base, τ_s – friction along pile shaft, A_b – section area of the pile base, A_s – area of the pile shaft.

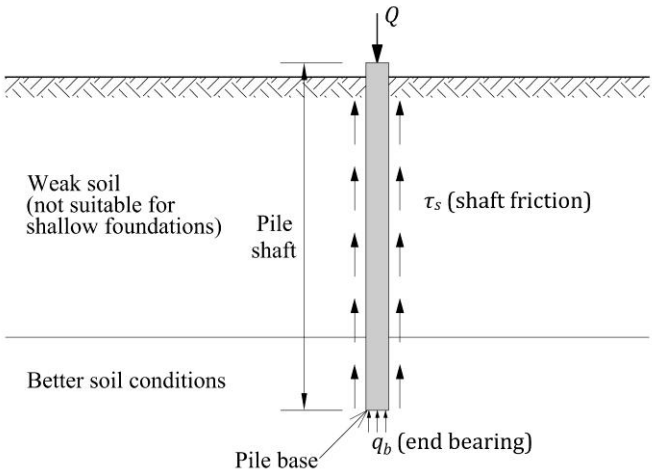

Fig. 3.9. Pile's shaft friction and end bearing.

Total stress approach (α-method)

The α-method is used to calculate the load capacity of piles in cohesive soils. This method is based on the undrained shear strength of cohesive soils; thus, it is well suited for short-term pile load capacity calculations. The ultimate load capacity of a pile is the sum of its friction capacity, Q_s , and end-bearing capacity, Q_b [9].

The interface shear stress, τ_s , between the pile surface and the surrounding soil determines the value of skin friction, Q_s (or shaft friction.) In this method the interface shear stress is assumed to be proportional to the undrained shear strength, c_u, of the cohesive soil as follows [9]:

$$\tau_s = \alpha c_u \tag{3.38}$$

where α is a factor that can be obtained from one of several semi-empirical equations available in the literature. For example the equation by API (1984) values for α as a function of c_u as follows:

$$\alpha = \begin{cases} 1 - \frac{c_u - 25}{90} & \text{for } 25\text{kPa} < \mathrm{c}_u < 70kPa \\ 1.0 & \text{for } c_u \leq 25kPa \\ 0.5 & \text{for } c_u \geq 70kPa \end{cases} \tag{3.39}$$

For a pile with variable diameter that is embedded in a layered system containing *N* layers the friction force between pile surface and soil [9]

$$Q_s = \sum_{i=1}^{N} [\alpha_i (c_u)_i \cdot perimeter_i \cdot lenght_i] \quad (3.40)$$

The end bearing capacity, for cohesive soils, can be estimated, using Terzaghi's bearing capacity equation

$$q_b = (c_u)_b N_C \quad (3.41)$$

where $(c_u)_b$ – the undrained shear strength of the cohesive soil under the base of the pile, N_c – bearing capacity coefficient that can be assumed equal to 9.0 (Skempton, 1959). The corresponding load capacity is

$$Q_b = (c_u)_b N_C A_b \quad (3.42)$$

where A_b – cross-sectional area of the tip of the pile.

Effective stress approach (β-method)

This method can be used for both cohesive and cohesionless soils. The method is based on effective stress analysis and is suited for short- and long-term analyses of pile load capacity [9].

The unit shaft resistance is calculated as

$$\tau_s = \beta \sigma'_{vz} \quad (3.43)$$

where σ'_{vz} denotes effective overburden pressure and

$$\beta = K \tan \delta \quad (3.44)$$

where δ is interface frictional angle and K is lateral earth pressure coefficient related to the lateral earth pressure coefficient at rest, $K_0 = (1 - \sin \phi')OCR^{0.5}$. Values of K are recommended by various researchers, taking into account pile displacement and construction methods. For example, for drilled shaft cast-in-place K/K_0 ranges between 2/3 and 1.0. When not enough data is available $K = K_0$ should be assumed.

The interface frictional angle between the pile shaft and the soil, δ, depends on construction method as well, being a function of pile surface roughness, and can be related to effective friction angle of the soil, ϕ'. For clays it is usually assumed that $\delta = \frac{2}{3}\phi'$ and for sands $\delta = \phi'$.

For a pile with variable diameter that is embedded in a layered system containing N layers the shaft friction force

$$Q_s = \sum_{i=1}^{N} [\beta_i (\sigma_{vz})_i \cdot perimeter_i \cdot lenght_i] \quad (3.45)$$

Using Terzaghi's bearing capacity equation, the bearing capacity at the base of the pile can be calculated [9]:

$$q_b = (\sigma'_v)_b N_q + c'_b N_c \tag{3.46}$$

where: $(\sigma'_v)_b$ – vertical effective stress at the base of the pile, c'_b – cohesion of the soil under the base of the pile, N_q, N_c – bearing capacity coefficients.

Janbu (1976) presented equations to estimate N_q and N_c for various soils:

$$N_q = \left(\tan\phi' + \sqrt{1 + \tan^2\phi'}\right)^2 \exp(2\eta \tan\phi') \tag{3.47}$$

$$N_c = \left(N_q - 1\right)\cot\phi' \tag{3.48}$$

where η – angle defining the shape of the shear surface around the tip of a pile. The angle η ranges from $\pi/3$ for soft clays to 0.58π for dense sands.

The load capacity, Q_b, is

$$Q_b = q_b A_b = [(\sigma'_v)_b N_q + c'_b N_c] A_b \tag{3.49}$$

where A_b – cross-sectional area of the base of the pile.

3.3 FORMWORK AND FALSEWORK (C. MOTZKO)

3.3.1 Introduction

For the management of construction projects, the area of formwork and falsework is a relevant element, since they are temporary works equipment for the support and/or assembly of structural building parts until these structures have reached a sufficient load bearing capacity. Furthermore, certain types of falsework and scaffolds serve to design and to secure workplaces from which, for example, assembly works can be carried out. They are relevant to the work progress and therefore to the economy, safety and adherence to time schedule of the construction project. This type of work accompanies a building in the whole life cycle, in the phase of construction, during the operation in the case of possible repair or modernization works as well as in case of demolition. Temporary works equipment additionally include working and façade scaffolds, protection fans for scaffolds as well as specific construction techniques in bridge and civil engineering construction. Examples include climbing systems and the slipform

method for the erection of vertical components, incremental launching and launching truss systems for the production of horizontal bridge superstructures as well as tunnel formworks for the construction of underground buildings. A possible systematic approach of the temporary works equipment as discussed above is shown in Figure 3.10.

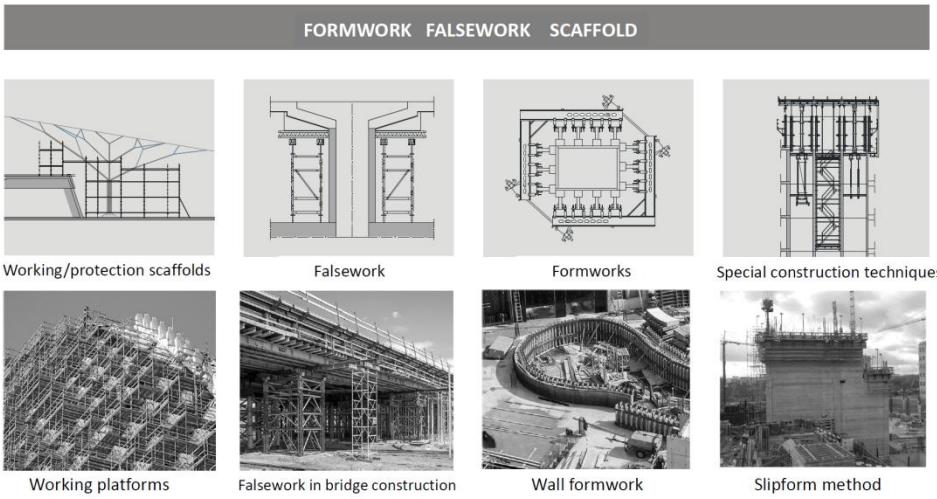

Fig. 3.10. Formwork, falsework, scaffolds – application cases (ref. to [1])

Within this chapter, only selected aspects of the scope of formworks and falsework can be discussed in a coherent overview, since these are complex engineering systems, which require special care and the use of experts and specialists in their design and application. In particular, reference is made to the cooperation between the management of the construction site and the falsework/formwork engineers. In the focus of the following discussion, formworks and falsework on the basis of German and European Standards and Directives are treated. The national standards and directives are to be applied.

3.3.2 Normative bases and definitions

Standards for formworks, falsework and scaffolds

The rules for the design and dimensioning of falsework are normatively defined in Germany according to DIN EN 12812: 2008-12 [R1] (the equivalent is, for example, BS EN 12812: 2008). Of relevance to the management of construction sites is Annex A (informative), which specifies the coordination of the works in

the area of falsework, thus regulating the aspect of safety. The following standards are also to be specified in connection with falsework:

- DIN EN 12813:2004-09 Temporary works equipment - Load bearing towers of prefabricated components - Particular methods of structural design [R2],
- DIN EN 1065:1998-12 Adjustable telescopic steel props - Product specifications, design and assessment by calculation and tests [R3],
- DIN EN 16031:2012-09 Adjustable telescopic aluminum props - Product specifications, design and assessment by calculation and tests [R4],
- DIN EN 13377:2002-11 Prefabricated timber formwork beams - Requirements, classification and assessment [R5],
- DIN 20000-2:2013-12 Application of construction products in structures - Part 2: Prefabricated timber formwork beams [R6],
- DIN 18216:1986-12 Formwork ties; requirements, testing, use [R7],
- DIN 18218:2010-01 Pressure of fresh concrete on vertical formwork [R8]. This standard is dealt with in chapter 3.4.4, since it is of particular relevance for the daily use of vertical formwork in terms of quality and work safety.

The following standards are to be specified for the working and protective scaffoldings:

- DIN EN 12811-1:2004-03 Temporary works equipment - Part 1: Scaffolds - Performance requirements and general design [R9],
- DIN EN 12811-2:2004-04 Temporary works equipment - Part 2: Information on materials [R10],
- DIN EN 12811-3:2003-02 Temporary works equipment - Part 3: Load testing [R11],
- DIN EN 12811-4:2014-03 Temporary works equipment - Part 4: Protection fans for scaffolds - Performance requirements and product design [R12],
- DIN EN 12810-1:2004-03 Facade scaffolds made of prefabricated components - Part 1: Products specifications [R13],
- DIN EN 12810-2:2004-03 Facade scaffolds made of prefabricated components - Part 2: Particular methods of structural design [R14],
- DIN EN 13374:2013-07 Temporary edge protection systems - Product specification - Test methods [R15].

It should be pointed out, that the requirements of DIN EN 12812: 2008-12 must be taken into account in case of special design and foundation engineering requirements for working and protective scaffolds. The requirements of DIN EN 12811-1: 2004-03 are to be used with regard to occupational health and safety

requirements for falsework [2]. In this context, the application of adequately supervised and certified systems is required.

Differentiation between Formwork and Falsework

DIN EN 12812:2008-12 [R1] can be used to define the differentiation criterion of the terms of formwork and falsework:
Quote:
3.3
falsework
temporary support for a part of a structure while it is not self-supporting and for associated service loads
3.4
formwork
part of temporary works used to give the required shape and support to in-situ concrete
Quote End

Figure 3.11 shows the differentiation between formwork and falsework using the example of the superstructure of a bridge. The formwork forms the concrete body of the bridge superstructure, and the falsework supports this form until the time of proper and appropriate stripping of formwork.

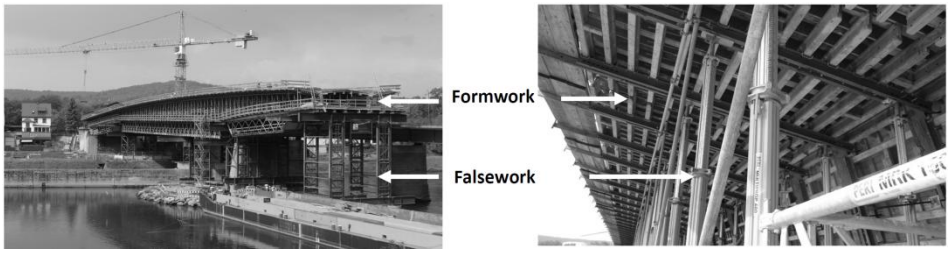

Fig. 3.11. Differentiation Formwork – Falsework in case of a bridge superstructure (Source: Motzko)

According to DIN EN 12812:2008-12[R1], the design classes A and B are defined for falsework, which should be selected by the falsework design engineer. The design class A defines falsework, which comply with established good practice and covers in situ erected simple slabs and beams with limited geometric dimensions concerning their cross-sections, span widths and heights (see

DIN EN 21812:2008-12, No. 4.2). The design class B contains falsework, which has to be completely calculated on the basis of the corresponding Eurocodes and according to the additional boundary conditions and specifications of the subclasses B1 and B2 (see DIN EN 21812: 2008-12, No. 4.3). The management of a construction site should be aware of the four relevant load cases for the design of the falsework to be applied according to individual circumstances as per DIN EN 21812: 2008-12, No. 8.5:

- Load case 1: Unloaded falsework e.g. bevor concreting phase,
- Load case 2: Falsework during loading, e.g. concreting phase,
- Load case 3: Loaded falsework, e.g. the phase after concreting,
- Load case 4: Loaded falsework subjected to seismic effects, for the case of the area of significant earthquake risk.

Table 3.1 shows the combination factors ψ, which shall be applied under regard of the No. 8.1 to 8.3 of DIN EN 21812: 2008-12 as well as the individual conditions of the project.

Tab. 3.1. Load combination factors ψ [DIN EN 12812: 2008-12]

Action	Type of action	Combination factors ψ			
		Load case 1	Load case 2	Load case 3	Load case 4 [a]
	Direct actions				
Q_1	Permanent actions	1,0	1,0	1,0	1,0
Q_2	Variable persistent vertical imposed actions	0	1,0	1,0	1,0
Q_3	Variable persistent horizontal imposed actions	0	1,0	1.0	0
Q_4	Variable transient imposed actions	0	1,0	0	0
Q_5	Maximum Wind	1.0	0	1,0	0
	Working Wind	0	1,0	0	0
Q_6	Flowing water actions	0,7	0,7	0,7	0,7
Q_7	Seismic effects	0	0	0	1,0
	Indirect actions				
$Q_{8,i}$	Temperature	0	1,0	1,0	1,0
	Settlements		0	1,0	1,0
	Prestressing		0	1,0	1,0
Q_9	Other loading conditions	0	1,0	1,0	1,0
[a] This load case is a non-collapse requirement in accordance with EN 1998-1-1.					

It is important to note, that in the case of creation of the specification for the tendering of works in the area of falsework, the definition of the design class is not always appropriate since, as already stated, the classification is carried out by the falsework design engineer and is not fundamentally the subject of an agreement between the owner/investor and the contractor (s. [2], p. 9/19).

3.3.3 Constructive and use-specific boundary conditions

With regard to the structural as well as to the use-specific boundary conditions, the temporary works equipment such as falsework is differently conceptualized in comparison to the permanent structures. For the management of construction sites, a number of differentiation elements based on [1] and [2] is listed below. Referring to the fact, that the falsework and formwork areas have a high degree of engineering-technical complexity, the participation of experts and falsework design engineers in the planning and construction phase is highly recommended.

- Temporary works equipment is not subject to the scope of the Regulation (EU) No. 305/2011, which lays down the harmonised conditions for the marketing of construction products, because it does not remain permanently in the structure of the building.
- Temporary works equipment has a more unfavorable frequency distribution of the resistance and effects of actions than in case of permanent structures. Figure 3.12 shows the difference between permanent structure components of bridges and buildings (light, thin line) and falsework in new condition (dark, bold line) as well as falsework in used condition (dotted line). We observe a relatively wide distribution of effects of actions (S) of bridge and building components (permanent buildings) in combination with a small number of extreme loads opposite to relatively narrow distribution of load effects (S) of falsework components (temporary works equipment) in combination with extreme loads, which partly overshoot the design limits. On the resistance side, the significantly wider as well as for new and used components differentiated frequency distribution of falsework (dark, bold line and dashed line) shows a markedly increased overlapping range of the load effects (S) and resistance (R) areas, which indicates a greater damage frequency in comparison to the permanent buildings.

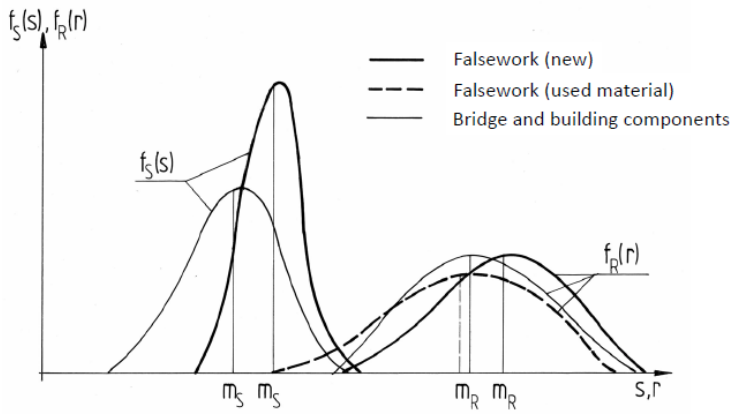

Fig. 3.12. Frequency distribution of effects of actions S and resistance R in comparison between permanent buildings and falsework ([3])

- Formworks and falsework are designed under the premises of a multiple and efficient assembly and disassembly processes at different construction sites and under varying operating conditions as well as to fulfil changing tasks. This is paired with the principle of material minimization and stationary production processes (robot application). Permanent structures usually follow the principles of (local) optimization of construction costs, construction time and quality as well as increasingly the life cycle consideration in a one-time manufacturing process and refer to a one-off structure, which can be standardized under specific conditions (Systems Construction).
- Especially for the load bearing capacity of falsework and scaffolds, the dimensional and form deviations of the components as well as the product of tolerance related cross-sectional values and scattering resistance of the material must be taken into account. Due to the requirement of easy assembly and disassembly processes on construction sites in case of formworks, falsework and scaffolds, clearance fits are often required at the connection points of the components. Depending on these fits with the parallelism and coaxiality tolerances, the system geometries of a lattice tower are shown in Figure 3.13. The considerations of the dimensional deviations are of relevance and should be kept within narrow limits for both, the technical concepts and the static calculations. Particularly in the case of falsework with high normal loads the correct imperfection assumptions for the static calculation depend on the system tolerances.

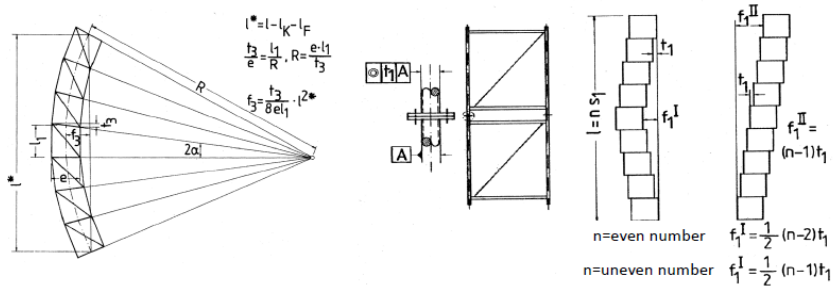

Fig. 3.13. Parallelism tolerances (left) and coaxiality tolerances (right, [1])

- The foundation of falsework and scaffolds is another important element, which has to be subjected to intensive monitoring during the works on construction site. DIN EN 12812: 2008-12 [R1] defines various possible types of foundations within the validity of Eurocodes, such as a specific substructure provided for the purpose, direct foundation on the surface of the existing ground, e.g. rock, a partly excavated and prepared surface, e.g. in soil, foundation on a structure which already exists and foundation according to No. 7.5.2. - support without any embedment in the ground. It should be borne in mind that the foundation of temporary works equipment is not as complexly designed as the case of permanent constructions (example see Figure 3.14). In order to ensure sufficient stability, extensive static calculations must be done, which not only consider the force transmission into the ground, but also takes into account the interaction with the falsework, for example the differential settlement.

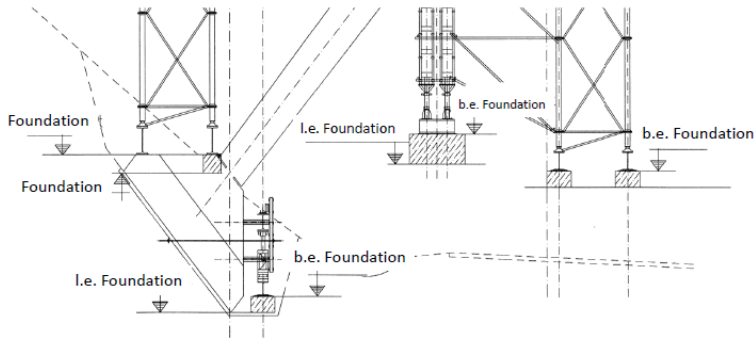

Fig. 3.14. Examples of foundations of falsework ([1])

- The temporary works equipment (formworks, scaffolds, falsework) is constantly and repeatedly used under design values of actions (loads). In opposite to this, permanent structures in the majority of the cases do not achieve the design values of actions (loads). That leads to significant differences in the design approaches, for example the structure of node points.
- Formwork and falsework have a high degree of panelization as well as standardization and are developed partly as modular systems, thus also in compatibility of different product groups (s. Figure 3.15), while permanent structures are designed as prototypes.
- Temporary works equipment can be complemented by mechanical or hydraulic moving aids in the case of specific tasks (e.g. self climbing forworks), in contrast to the definitive design of permanent constructions.
- In addition to complying with the constructive rules, the requirements for occupational health and safety are of relevance for the management of a construction project.

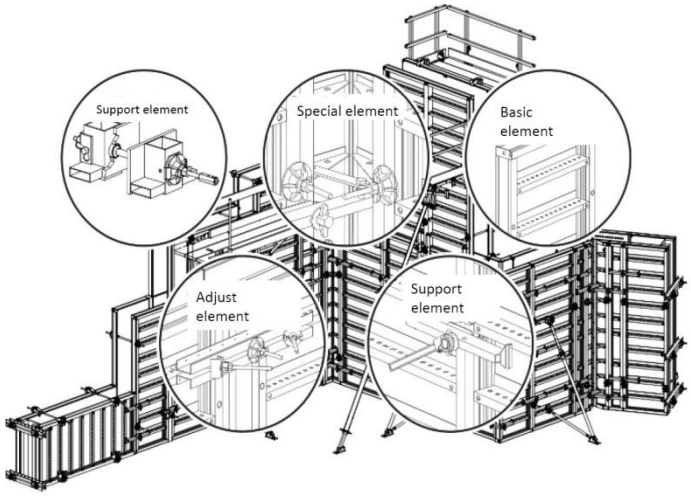

Fig. 3.15. Modular panel wall formwork Baukastensystematik (System Hünnebeck Manto, [4])

- The instructions for erection and use and additional documents are required for the use of falsework on construction sites, which indicates the validation parameters or design classes for the present case. Furthermore, the provi-

sions of No. 5 DIN EN 13670:2011-03 [R16] have to be considered. The same applies to formworks, where appropriate, the type of support, assembly, anchorage, disassembly, including possible emergency support, must be indicated precisely.

3.3.4 Fresh concrete pressure

Pressure of fresh concrete on vertical formwork

Relevant actions on falsework and formwork include the weight of the fresh concrete as well as the fresh concrete pressure. Especially in the case of vertical construction elements of the concrete structures, it is observed on construction sites, that the rise in level of the fresh concrete during the concreting phase is not subject to any control, which generates high values of fresh concrete pressure. The formwork has to be dimensioned for this values, which is not always the case. This leads to excessive deformations resulting in severe unevenness of the concrete surfaces up to the complete failure of the formwork construction. Particularly when using flowable or high flowable concretes, adequate care is required in planning and monitoring during the execution of the production processes. As an example, two methods for the calculation of fresh concrete pressure in the case of vertical formwork are presented below.

Great Britain: CIRIA-Report 108

The Construction Industry Research and Information Association (CIRIA) defines in Report 108 [5] the fresh concrete pressures on formwork on basis of 350 measurements and gives the following formula:

$$p_{max1} = \gamma_c * (C_1 * \sqrt{v} + C_2 * K_T * \sqrt{h - C1 * \sqrt{v}} \quad \text{for -5°C < T < 30°C}$$

or

$$p_{max2} = \gamma_c * h$$

whichever is the smaller,

where

$p_{,max}$ maximum fresh concrete pressure [kN/m^2]

Υ_c weight density of concrete [kN/m^3]

v rate at which the concrete rises vertically in the form [m/h]

h vertical pouring height [m]

C_1 coefficient dependent on the size and shape of formwork (1,0 for walls; 1,5 for columns (b < 2,00 m))

C_2 coefficient dependent on the composition of the concrete (0,30 – 0,60)

K_T temperature coefficient taken as $K_T = (36/T+16)^2$

Maximum values according to the experience:

$p_{b,max} = 90$ kN/m^2 for walls

$p_{b,max} = 166$ kN/m^2 for columns

Germany: DIN 18218:2010-01

In 2010 the German Standard DIN 18218:2010-01 [R8] was amended and applies to vertical formworks with a maximum deviation of ± 5 ° from the vertical. It builds up the area of fresh concrete of the consistency classes F1 to F4 on the basis of the previous version of this standard from 1981 and completes this with flowable concretes of the consistency classes F5, F6 and SCC. From the construction-practical point of view, it is important to note, that the new generation of F4 concretes may produce higher fresh concrete pressures than specified in the standard. It is possible to calculate the lateral fresh concrete pressure as a characteristic value of the action σ_{hk}. For the dimensioning of the formwork constructions and their supports as well as for the formwork anchors, it is necessary to apply the design value of the fresh concrete pressure $\sigma_{hd} = \gamma_F \cdot \sigma_{hk}$. The partial safety factor γ_F should be chosen according to the specifications of DIN EN 12812:2008-12 ($\gamma_F = 1,5$ in case of not favorable effects of actions; $\gamma_F = 1.0$ in case of favorable effects of the actions).

Figure 3.16 shows the distribution of the fresh concrete as action over the height of the formwork $h_E = v * t_E$ for the ultimate limit state, assuming the most unvourable load position. In case of height H, the formwork shall be designed by a moving load that changes upwards over the height of the formwork.

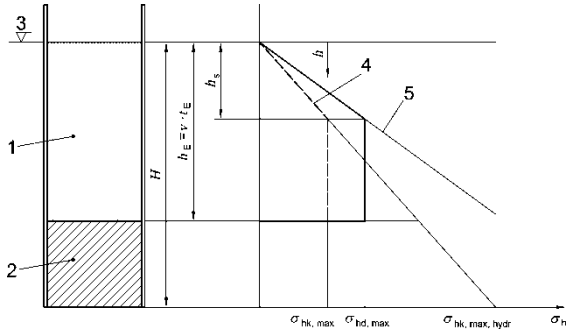

Key

1 fresh concrete
2 set (hardened) concrete
3 upper level of concrete
4 hydrostatic fresh concrete pressure
5 γ_F-times hydrostatic fresh concrete pressure
h_E height of concrete at final setting time t_E
h_s hydrostatic pressure head
H overall height to be concreted
v placing rate [m/h]
t_E final setting time

Fig. 3.16. Distribution of the fresh concrete pressure over the height of a formwork according to DIN 18218:2010-01 [R8]

Under the conditions, that the density of the fresh concrete amounts to γ_c = 25 kN/m³, the actual setting time of the fresh concrete built into the formwork does not exceed the value of the final setting time $t_{E,}$ the fresh concrete is compacted using an internal vibrator, the formwork is dense, the average placing rate v for the concretes of the consistency classes F1, F2, F3 and F4 lies below the maximum value of 7.0 m / h at each point, and the concrete is placed into the formwork form above, the value of the fresh concrete pressure $\sigma_{hk\ max}$ can be calculated according to the formulas in Table 3.2 (the factors *K1* are recorded in Table 3.3).

Tab. 3.2. Characteristic values of maximum lateral fresh concrete pressure (where concrete is placed form above) according to DIN 18218:2010-01 [R8]

1	Consistency class	Maximum lateral fresh concrete pressure when placed in opposite direction to the rise in level (i.e. from above) $\sigma_{hk,max}$ [kN/m²]
2	F1	$(5 \cdot v + 21) \cdot K1 \geq 25$
3	F2	$(10 \cdot v + 19) \cdot K1 \geq 25$
4	F3	$(14 \cdot v + 18) \cdot K1 \geq 25$
5	F4	$(17 \cdot v + 17) \cdot K1 \geq 25$
6	F5	$25 + 30 \cdot v \cdot K1 \geq 30$
7	F6	$25 + 38 \cdot v \cdot K1 \geq 30$
8	SVB	$25 + 33 \cdot v \cdot K1 \geq 30$
In the above *v* is the placing rate (pouring rate) in m/h. *K1* is the factor taking into account the setting behaviour according to table 2.		

Tab. 3.3. Factors *K1* for setting behaviour according to DIN 18218:2010-01 [R8]

	1	2	3	4	5
1	Consistency class	Factors *K1*			
2		Final setting time t_E = 5 h	Final setting time t_E = 10 h	Final setting time t_E = 20 h	General [b]
3	F1 [a]	1,0	1,15	1,45	$1 + 0{,}03 \cdot (t_E - 5)$
4	F2 [a]	1,0	1,25	1,80	$1 + 0{,}053 \cdot (t_E - 5)$
5	F3 [a]	1,0	1,40	2,15	$1 + 0{,}077 \cdot (t_E - 5)$
6	F4 [a]	1,0	1,70	3,10	$1 + 0{,}14 \cdot (t_E - 5)$
7	F5, F6, SVB	1,0	2,00	4,00	$t_E / 5$
	[a] Applies for concreting sections of a height *H* up to 10 m. [b] Applies for $5h \leq t_E \leq 20h$; t_E in h.				

The maximum characteristic value of the fresh concrete pressure when installed from above amounts to the hydrostatic value $\sigma_{hk,\,max,\,hydr} = \gamma_c \cdot H$.

It should be noted, that different factors can increase or decrease the fresh concrete pressure to be applied, such as the cooling of concrete, the type of compaction, the concrete mix design, the degree of reinforcement, any shocks during the setting process, relation of the fresh concrete placing temperature $T_{c,Einbau}$ to the reference temperature $T_{c,Ref}$ or the outside temperature, when the fresh concrete temperature T_c drops below the placing temperature $T_{c,Einbau}$ during the concrete setting. When filling the formwork with SCC from below, the maximum height amounts to 3,5 m and the hydrostatic fresh concrete pressure is to be used for the dimensioning of the formwork construction. The details of the verification must be taken from the standard and should be applied accordingly.

Finally, it should be pointed out, that tie systems are very important and take over the actions of the fresh concrete pressure transferred from the formwork construction. Figure 3.17 shows the load distribution model of fresh concrete pressure for single-sided and double-sided wall formworks. The dimensioning of the tie system must therefore be performed with the same care as the design of the formwork and falsework itself.

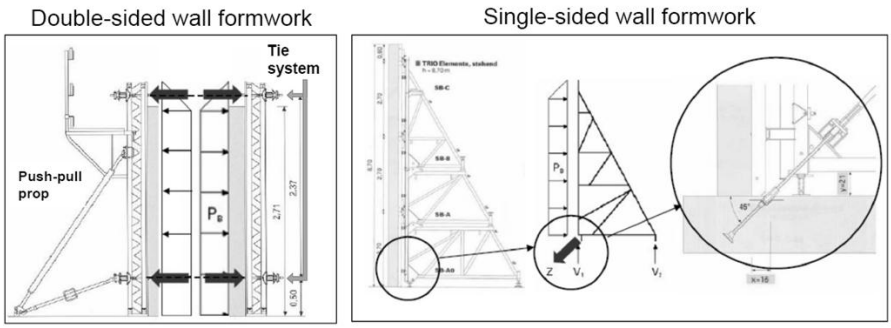

Fig 3.17. Load distribution model of fresh concrete pressure for single-sided and double-sided wall formworks (acc. Motzko/Peri)

Lifting forces due to fresh concrete pressure

When designing formwork constructions, in particular for inclined formwork as well as for built-in components, additional lifting forces must be considered. Figure 3.18 shows the principle of the action on a box-out element for a door opening.

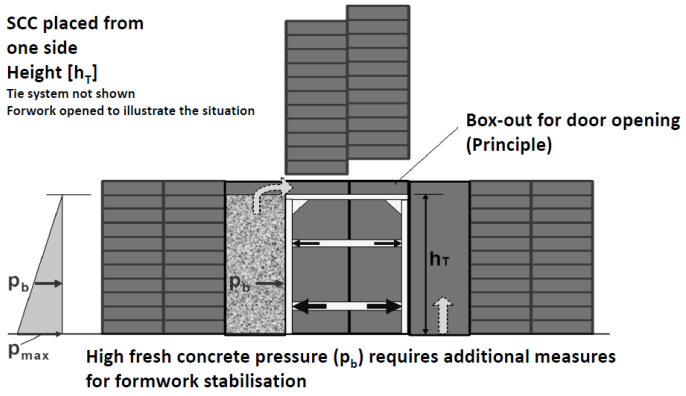

Fig. 3.18. Fresh concrete pressure on a box-out for a door opening ([6])

Furthermore, the friction force between formwork sheets and fresh concrete has to be considered. In addition to the individual parts, the buoyancy safety of the entire formwork must also be checked. If the weight of the relevant effective

formwork area is not sufficient for buoyancy protection, additional measures, such as anchoring of the formwork with unit´s base (e.g. concrete slab) or ballasting, are necessary. The forces that occur must be precisely calculated. Particularly when using SCC, it must be borne in mind that, in cases where the formwork is slightly raised, the fresh concrete can flow out at the leaking point.

Pressure of fresh concrete on inclined formwork

Concerning the fresh concrete pressure in the case of inclined formworks, reference is made to the information in [7].

3.3.5 Stripping timelines of formwork

The determination of the stripping time of formwork and falsework is of high relevance both from the technological as well as from the construction-economic point of view. In case, if the designers do not give any advice, the falsework, the formwork and the auxiliary supports may only be stripped, when the concrete has attained sufficient strength to support itself and the applied loads.

When stripping, one has to take into account, among other things, that no damage to the concrete surfaces, no impermissible deflections and no adverse weather influences arise. Details can be found in DIN EN 13670:2001-03 [R16].

The construction-economic relevance is revealed by the efficient use of the equipment. Figure 3.19 shows, that the formwork costs are the dominant part in the sector of structural works costs. The choice of the appropriate formwork and falsework system as well as the clock production modelling of the processes on the construction site influences the concrete structures construction progress significantly.

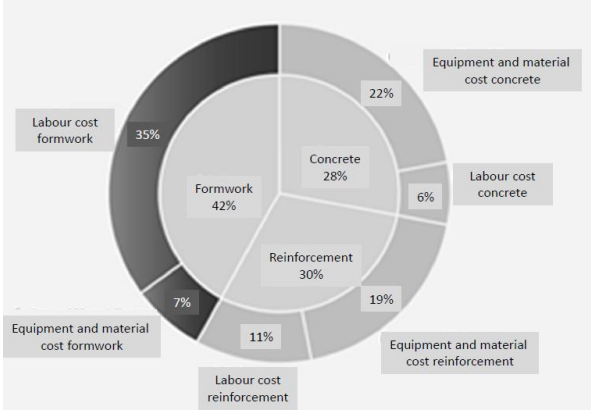

Fig. 3.19. Cost structure of concrete structural works

The site management determines the time of stripping of formworks and false-work, which underlines the responsibility for the occupational safety of the processes at the construction site, the load-bearing capacities and usability of the elements of the construction, as well as the importance for the economic and temporal success of the construction project.

For the determination of the stripping times for in situ concrete construction components under bending stress, the DBV-Instruction *Formwork and stripping timelines* (*Betonschalungen und Ausschalfristen)* [8] provides three methods:

- Determination of the stripping time according to experience,
- Tabular indications of the stripping time for typical building construction,
- Determination of the stripping time based on concrete performance.

Determination of stripping time according to experience

The determination of the stripping time according to experience is dependent on the qualification of the site management or company´s experience in total. Not less than State of the Art, general acknowledged Rules of Technique as well as the valid standards are to be applied.

Tabular reference values of the stripping time for typical building construction

For concrete and reinforced concrete components in typical building constructions and without special requirements for the serviceability (for example deflection limitation), restricted to beams and slabs up to 6 m span as well as for

lintels and ring beams, the stripping timelines are defined in [8] (s. Table 3.4). It is assumed, that the effects of actions at the stripping time point t_0 only consist of dead loads and effective vertical loads, which results in an effect of actions of approximately 70% of the final state with $E_{do} = 0{,}70 * Ed_{28}$ ($\alpha_0 = 0{,}70$).

Tab. 3.4. Reference values of the stripping time t_0 for typical building construction and $\alpha_0 = 0{,}70$ ([8])

	1	2	3	4
	Component temperature[2]	Strength development of concrete r= f_{cm2}/f_{cm28}[1]		
		Fast	Intermediate	Slow
	ϑ in °C	$r \geq 0{,}50$	$r \geq 0{,}30$	$r \geq 0{,}15$
1	$\vartheta \geq 15$	4	8	14
2	$15 > \vartheta \geq 5$ [3]	6	12	20

[1] The strength development of the concrete is determined by the ratio of the mean values of the concrete compressive strengths after 2 days and after 28 days. The strength development must be declared by the concrete supplier or can be taken from the concrete delivery ticket.

[2] The actual temperature of the component ϑ during the discharge of the hydration heat and in the formwork is generally higher than the air temperature. Instead of the temperature of the component ϑ, the mean air temperature ϑ_m can be applied. The mean air temperature ϑ_m is the mean value of the highest and lowest day air temperature close to the structure.

[3] In the case of air temperatures $\vartheta_m < 5$°C, it is necessary to extend the time required for stripping by the days, on which the component temperature $\vartheta < 5$° C was.

The reference values in Table 3.4 also apply to auxiliary supports (Back propping), for example when using panelized slab formwork with drophead systems. Figure 3.20 shows an example of such a slab formwork with the arrangement of the auxiliary support props.

Fig. 3.20. Example of the use of a panelized slab formwork with drophead including auxiliary support props (Source: Motzko)

Determination of stripping time based on the fresh concrete performance monitoring

If the above mentioned methods are not applicable, the stripping time point t_0 must be defined by the required compressive strength of concrete f_{cm0} or the minimum concrete strength class in the planning process (participation of structural engineers, work preparation and site management). The strength f_{cm0} at stripping time point is to be demonstrated on the basis of hardening tests, maturity tests or other concrete performance monitoring methods.

3.4 REFERENCES

[1] Hertle, R.; Motzko, C.: Gerüstbau. Beton Kalender 2007, Ernst & Sohn, Berlin, 2007
[2] Hertle, R.: Gerüstbau – Vereinheitlichte Europäische Regeln und deren Anwendung. Stahlbau Kalender, Ernst & Sohn, Berlin, 2015
[3] Nather, F.; Lindner, J.; Hertle, R.: Handbuch des Gerüstbaus. Ernst & Sohn , Berlin, 2005
[4] Motzko, C.: Systemschalungen - Ergebnis komplexer Aufgabenstellung. BD-Baumaschinendienst 7-8/2000, Krafthand Verlag Walter Schulz GmbH, 2000
[5] Clear, C. A.; Harison, T. A.: The pressure of concrete in formwork – CIRIA Research Report Nr. 108, Construction Industry Research and Information Association, London, 1985
[6] Güteschutzverband Betonschalungen Europa e.V.: GSV-Publikation Schalungstechnische Empfehlungen beim Einsatz von F5- und F6-Betonen sowie Selbstverdichtendem Beton (SVB), Ratingen, 2007
[7] Freund, B.; Proske, T.; Graubner, C.-A.: Experimentelle Untersuchungen und numerische Verifizierung zum Frischbetondruck bei geneigten Schalungssystemen. In: Beton- und Stahlbetonbau 109, Heft 11 (2014), Verlag Ernst & Sohn, Berlin, 2014, 803-811
[8] Deutscher Beton- und Bautechnik-Verein E.V.: DBV-Merkblatt Betonschalungen und Ausschalfristen, Berlin, 2006
[9] Helwany S.: Applied Soil Mechanics with ABAQUS Applications, John Wiley & Sons, 2007
[10] Das B. M.: Geotechnical Engineering Handbook, J. Ross Publishing, 2011
[11] Pisarczyk S.: Gruntoznawstwo inżynierskie, PWN, Warszawa, 2012
[12] EN 1997-1:2004, Euro code 7: Geotechnical design - Part 1: General rules, European Committee for Standardization, 2004

[13] Fang H. Y.: Foundation Engineering handbook, Van Nostrand Reinhold, New York, 1991
[14] Wei Dong Guo: Theory and Practice of Pile Foundations, CRC Press, New York, 2013

[R1] DIN EN 12812:2008-12 Falsework - Performance requirements and general design. Berlin, 2012.
[R2] DIN EN 12813:2004-09 Temporary works equipment - Load bearing towers of prefabricated components - Particular methods of structural design. Berlin, 2004.
[R3] DIN EN 1065:1998-12 Adjustable telescopic steel props - Product specifications, design and assessment by calculation and tests. Berlin, 1998.
[R4] DIN EN 16031:2012-09 Adjustable telescopic aluminum props - Product specifications, design and assessment by calculation and tests. Berlin, 2012.
[R5] DIN EN 13377:2002-11 Prefabricated timber formwork beams - Requirements, classification and assessment. Berlin, 2002.
[R6] DIN 20000-2:2013-12 Application of construction products in structures - Part 2: Prefabricated timber formwork beams. Berlin, 2013.
[R7] DIN 18216:1986-12 Formwork ties; requirements, testing, use. Berlin, 1986.
[R8] DIN 18218:2010-01 Pressure of fresh concrete on vertical formwork. Berlin, 2010.
[R9] DIN EN 12811-1:2004-03 Temporary works equipment - Part 1: Scaffolds - Performance requirements and general design. Berlin, 2004.
[R10] DIN EN 12811-2:2004-04 Temporary works equipment - Part 2: Information on materials. Berlin, 2004.
[R11] DIN EN 12811-3:2003-02 Temporary works equipment - Part 3: Load testing. Berlin, 2003.
[R12] DIN EN 12811-4:2014-03 Temporary works equipment - Part 4: Protection fans for scaffolds - Performance requirements and product design. Berlin, 2014.
[R13] DIN EN 12810-1:2004-03 Facade scaffolds made of prefabricated components - Part 1: Products specifications. Berlin, 2004.
[R14] DIN EN 12810-2:2004-03 Facade scaffolds made of prefabricated components - Part 2: Particular methods of structural design. Berlin, 2004.
[R15] DIN EN 13374:2013-07 Temporary edge protection systems - Product specification - Test methods. Berlin, 2013.
[R16] DIN EN 13670:2011-03 Ausführung von Tragwerken aus Beton. Berlin, 2011.

CHAPTER 4
CASE STUDIES

4.1 CALCULATION OF FRESH CONCRETE PRESSURE ON VERTICAL FORMWORK ACCORDING TO DIN 18218:2010-01 (C. MOTZKO)

In the following the fresh concrete pressure is calculated according to DIN 18218:2010-01 for the production of a reinforced concrete wall [R1].

Boundary conditions:

- height of the reinforced concrete wall — H = 3,00 m
- consistency class — F3
- final setting time — t_E = 10 h
- fresh concrete placing rate — v = 3 m/h
- fresh concrete density — $\gamma_c = 25 \frac{kN}{m^3}$

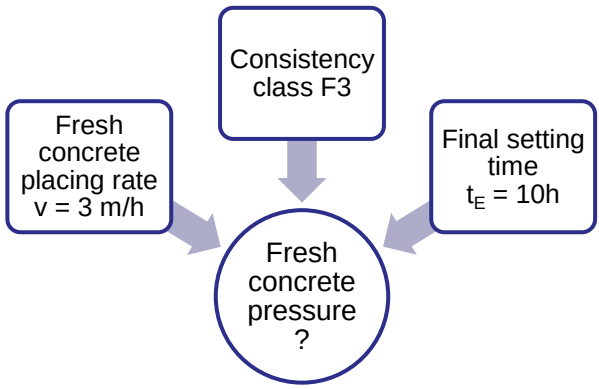

1) Selection of the formula for calculating the characteristic value of the maximum lateral concrete pressure on the basis of consistency class of the concrete in table 1 of DIN 18218:2010-01 [R1]:

1	Consistency class	Maximum lateral fresh concrete pressure when placed in opposite direction to the rise in level (i.e. from above) $\sigma_{hk,max}$ [kN/m²]
2	F1	$(5 \cdot v + 21) \cdot K1 \geq 25$
3	F2	$(10 \cdot v + 19) \cdot K1 \geq 25$
4	F3	$(14 \cdot v + 18) \cdot K1 \geq 25$
5	F4	$(17 \cdot v + 17) \cdot K1 \geq 25$
6	F5	$25 + 30 \cdot v \cdot K1 \geq 30$
7	F6	$25 + 38 \cdot v \cdot K1 \geq 30$
8	SVB	$25 + 33 \cdot v \cdot K1 \geq 30$
In the above v is the placing rate (pouring rate) in m/h. $K1$ is the factor taking into account the setting behaviour according to table 2.		

$$\sigma_{hk,max} = (14 \cdot v + 18) \cdot K1$$

2) Selection of the factor *K1* to take account of the setting behaviour on the basis of consistency class and the final setting time of the concrete in table 2 of DIN 18218:2010-01 [R1]:

	1	2	3	4	5
1	Consistency class	Factors *K1*			
2		Final setting time $t_E = 5$ h	Final setting time $t_E = 10$ h	Final setting time $t_E = 20$ h	General [b]
3	F1 [a]	1,0	1,15	1,45	$1 + 0{,}03 \cdot (t_E - 5)$
4	F2 [a]	1,0	1,25	1,80	$1 + 0{,}053 \cdot (t_E - 5)$
5	F3 [a]	1,0	1,40	2,15	$1 + 0{,}077 \cdot (t_E - 5)$
6	F4 [a]	1,0	1,70	3,10	$1 + 0{,}14 \cdot (t_E - 5)$
7	F5, F6, SVB	1,0	2,00	4,00	$t_E / 5$
[a] Applies for concreting sections of a height H up to 10 m. [b] Applies for $5h \leq t_E \leq 20h$; t_E in h.					

$$K1 = 1{,}40$$

Alternatively, the factor *K1* can also be exactly calculated:

$$K1 = 1 + 0{,}077 \cdot (t_E - 5) = 1 + 0{,}077 \cdot (10 - 5) = 1{,}385$$

3) Inserting the boundary conditions and the factor *K1* in the formula for calculating the characteristic value of the maximum lateral concrete pressure:

$$\sigma_{hk,max} = (14 \cdot v + 18) \cdot K1 = (14 \cdot 3 + 18) \cdot 1{,}40 = 84 \frac{kN}{m^2}$$

4) Graphical solution for calculating the characteristic value of the maximum lateral concrete pressure [R1]:

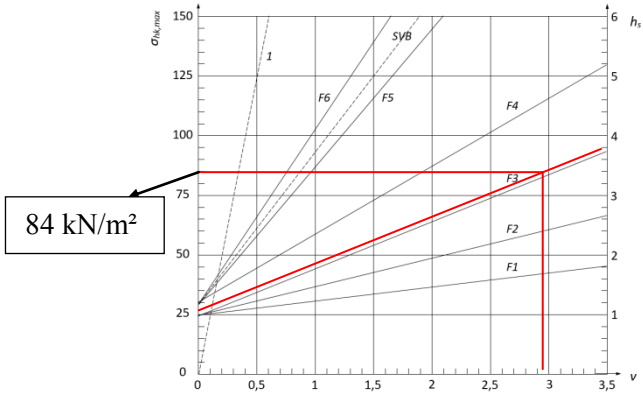

Key

1 hydrostatic up to t_E

t_E = 10 h
γ_c = 25 kN/m³
maximum value of fresh concrete pressure $\sigma_{hk,max}$ in kN/m²
placing rate v in m/h
hydrostatic pressure head h_s in m
Only applies up to a height of concrete section of 10 m for consistency classes F1 and F4.

5) Check whether the hydrostatic concrete pressure is decisive:

$$\sigma_{hk,max,hydr} = \gamma_c \cdot H = 25\ \frac{kN}{m^3} \cdot 3{,}00\ m = 75\ \frac{kN}{m^2}$$

$$\sigma_{hk,max,hydr} = 75\ \frac{kN}{m^2} < 84\ \frac{kN}{m^2} = \sigma_{hk,max}$$

The hydrostatic concrete pressure is less than the calculated maximum lateral occurring fresh concrete pressure. Thus, the hydrostatic concrete pressure in this example is relevant since this is the maximum characteristic value of fresh concrete pressure that can occur during installation of the concrete in opposite direction to the rise in level (from above).

4.2 CALCULATION OF THE MAXIMUM FRESH CONCRETE PLACING RATE (C. MOTZKO)

In the following the maximum fresh concrete placing rate is calculated for the production of a reinforced concrete wall. The maximum acceptable characteristic fresh concrete pressure of the formwork is 70 kN/m².

Boundary conditions:

- height of the reinforced concrete wall H = 3,00 m
- consistency class F3
- final setting time t_E = 5 h
- fresh concrete density $\gamma_c = 25\ \frac{kN}{m^3}$

1) Selection of the formula for the characteristic value of the maximum lateral concrete pressure on the basis of consistency class of the concrete in table 1 of DIN 18218:2010-01 [R1]:

1	Consistency class	Maximum lateral fresh concrete pressure when placed in opposite direction to the rise in level (i.e. from above) $\sigma_{hk,max}$ [kN/m²]
2	F1	$(5 \cdot v + 21) \cdot K1 \geq 25$
3	F2	$(10 \cdot v + 19) \cdot K1 \geq 25$
4	F3	$(14 \cdot v + 18) \cdot K1 \geq 25$
5	F4	$(17 \cdot v + 17) \cdot K1 \geq 25$
6	F5	$25 + 30 \cdot v \cdot K1 \geq 30$
7	F6	$25 + 38 \cdot v \cdot K1 \geq 30$
8	SVB	$25 + 33 \cdot v \cdot K1 \geq 30$
In the above v is the placing rate (pouring rate) in m/h. $K1$ is the factor taking into account the setting behaviour according to table 2.		

$$\sigma_{hk,max} = (14 \cdot v + 18) \cdot K1$$

2) Conversion of the formula after the placing rate:

$$\sigma_{hk,max} = (14 \cdot v + 18) \cdot K1 \rightarrow v = \frac{\sigma_{hk,max} - 18 \cdot K1}{14 \cdot K1}$$

3) Selection of the factor $K1$ to take account of the setting behaviour on the basis of consistency class and the final setting time of the concrete in table 2 of DIN 18218:2010-01 [R1]:

	1	2	3	4	5
1	Consistency class	Factors $K1$			
2		Final setting time t_E = 5 h	Final setting time t_E = 10 h	Final setting time t_E = 20 h	General [b]
3	F1 [a]	1,0	1,15	1,45	$1 + 0{,}03 \cdot (t_E - 5)$
4	F2 [a]	1,0	1,25	1,80	$1 + 0{,}053 \cdot (t_E - 5)$
5	F3 [a]	1,0	1,40	2,15	$1 + 0{,}077 \cdot (t_E - 5)$
6	F4 [a]	1,0	1,70	3,10	$1 + 0{,}14 \cdot (t_E - 5)$
7	F5, F6, SVB	1,0	2,00	4,00	$t_E / 5$
[a] Applies for concreting sections of a height H up to 10 m. [b] Applies for 5h ≤ t_E ≤ 20h; t_E in h.					

$$K1 = 1{,}0$$

4) Inserting the boundary conditions and the factor *K1* in the formula for determining the maximum placing rate:

$$v = \frac{\sigma_{hk,max} - 18 \cdot K1}{14 \cdot K1} = \frac{70\ \frac{kN}{m^2} - 18 \cdot 1{,}0}{14 \cdot 1{,}0} = 3{,}7\ m/h$$

4.3 GENERAL CLASSIFICATION OF SOIL - CASE STUDY (K. JÓZEFIAK, A. ZBICIAK)

Problem: Determine the names of soils according to [1] corresponding to curve no. 3 and no. 4 in Figure 1.5.

Solution. First we have to determine percentages of individual fractions. For example the content of clayey fraction is indicated by the intersection point of the red curve with the horizontal grid line of 0.002 mm which is the boundary particle size between clayey and silty fractions. So:

- for particle size distribution curve no. 3 we obtain: $f_{Cl} = 23\%$, $f_{Si} = 94\% - 23\% = 71\%$, $f_{Sa} = 100\% - 71\% - 23\% = 6\%$,
- for particle size distribution curve no. 4 we obtain: $f_{FSa} = 10\%$, $f_{MSa} = 88\%$, $f_{CSa} = 12\%$.

We can see that soil no. 3 is a cohesive soil and soil no. 4 is a granular soil (a kind of sand). To obtain the name of the soil no. 3 we need to use the procedure shown in Figure 1.6. Determined fraction percentages of this soil indicate that in the triangle we are in the area denoted "Si clSi siCl Cl". Hence, our soil name is one of these four. The square below the triangle is used to clarify the name. As the soil no. 3 has 23% of clayey fraction we are in the area denoted "siCl" in the square. Hence, the name of soil no. 3 is siCl.

For soil no. 4 the sandy soil name is determined by the fraction with the highest content. In our case it's the content of medium sand which is 88%. Hence, the soil no. 4 name is MSa.

4.4 PHYSICAL AND MECHANICAL PARAMETERS OF SOIL - CASE PROBLEMS (K. JÓZEFIAK, A. ZBICIAK)

Problem 1. Derive the relationship between dry unit weight and water content

$$\gamma_d = \frac{100\,\gamma}{100+\omega} \tag{4.4.1}$$

in which water content, ω, should be substituted in percent.

Solution. Let us denote $m = m_s + m_w$ to be mass of a wet soil sample. Then from the definition of soil dry density we obtain

$$\rho_d = \frac{m_s}{V} = \frac{m-m_w}{V} = \frac{m}{V} - \frac{m_w}{V} = \rho - \frac{m_w}{V} \tag{4.4.2}$$

Mass of water, from the definition of water content

$$m_w = 100\ \omega\ m_s \tag{4.4.3}$$

so we obtain

$$\rho_d = \rho - \frac{100\ \omega\ m_s}{V} = \rho - 100\ \omega\ \rho_d \tag{4.4.4}$$

Multiplying both sides by gravitational acceleration we obtain the equation

$$\gamma_d = \gamma - 100\ \omega\ \gamma_d \tag{4.4.5}$$

that we can solve for γ_d which gives

$$\gamma_d = \frac{100\,\gamma}{100+\omega} \tag{4.4.6}$$

Problem 2. Derive the well-known relationship which relates unit weight of soil to particle unit weight, porosity and degree of saturation

$$\gamma = (1 - \mathrm{n})\gamma_s + S_r n\ \gamma_w \tag{4.4.7}$$

and the same formula for unit weight of a saturated soil sample

$$\gamma_{sat} = (1 - \mathrm{n})\gamma_s + n\ \gamma_w \tag{4.4.8}$$

Solution. From definition of void ratio we have

$$V_v = eV_s \tag{4.4.9}$$

From the definition of degree of saturation we obtain volume of water

$$V_w = S_r V_p = S_r\, eV_s \tag{4.4.10}$$

As mass of water $m_w = V_w \rho_w$ we get

$$m_w = S_r\, eV_s\, \rho_w \tag{4.4.11}$$

As mass of a whole sample $m = m_w + m_s$, substituting Eq. (4.4.11) and the definition of particle density, we obtain

$$m = S_r\, e\, V_s\, \rho_w + V_s \rho_s = V_s(S_r e \rho_w + \rho_s) \tag{4.4.12}$$

From the definition of bulk density

$$\rho = \frac{m}{V} = \frac{V_s(S_r e \rho_w + \rho_s)}{V} \tag{4.4.13}$$

Volume a soil sample is equal to (see Figure 1.1)

$$V = V_v + V_s = eV_s + V_s = V_s(1 + e) \tag{4.4.14}$$

Substituting Eq. (4.4.13) to Eq. (4.4.14) we obtain

$$\rho = \frac{m}{V} = \frac{V_s(S_r e \rho_w + \rho_s)}{V_s(1+e)} = \frac{1}{1+e}\rho_s + \frac{e}{1+e} S_r \rho_w \tag{4.4.15}$$

Multiplying both sides by gravitational acceleration

$$\gamma = \frac{1}{1+e}\gamma_s + \frac{e}{1+e} S_r \gamma_w \tag{4.4.16}$$

To obtain relationship (4.4.7) we need to use formula (1.14) which relates void ratio to porosity. Substituting this formula $e = \frac{n}{1-n}$

$$\gamma = (1 - n)\gamma_s + S_r n\, \gamma_w \tag{4.4.17}$$

For a saturated soil there are only voids filled with water and $S_r = 1.0$ so

$$\gamma_{sat} = (1 - n)\gamma_s + n\, \gamma_w \tag{4.4.18}$$

Problem 3. A soil sample in its natural state has, when fully saturated, a water content of 30%. Determine the void ratio, dry and total unit weights. Calculate the total weight of water required to saturate a soil mass of volume 10 m^3. Assume $\rho_s = 2.62\ kg/m^3$, $\rho_w = 1.0\ kg/m^3$ and $g = 9.81 \frac{m}{s^2}$.

Solution. Given parameters are as follows: $S_r = 1.0$, $\omega = 30\%$, $V = 10m^3$, $\rho_s = 2.62\ kg/m^3$. We need to find: e, $\gamma = \gamma_{sat}$, γ_d, W_w.

From the definition of degree of saturation assuming $V_v = e\,V_s$ we obtain

$$S_r = \frac{V_w}{V_v} = \frac{V_w}{eV_s} \tag{4.4.19}$$

We also know that the volume of water:

$$V_w = \frac{m_w}{\rho_w} = \frac{\frac{\omega m_s}{100}}{\rho_w} = \frac{\omega\, m_s}{100\,\rho_w} = \frac{\omega\, V_s \rho_s}{100\rho_w} \tag{4.4.20}$$

In the above Eq. (4.4.20) we used the definition of water content from which $m_w = \frac{\omega\, m_s}{100}$. Substituting Eq. (4.4.20) into (4.4.19) we get

$$S_r = \frac{V_w}{eV_s} = \frac{\omega\, V_s\, \rho_s}{100\rho_w\, e\, V_s} = \frac{\omega\, \rho_s}{100\,\rho_w\, e} \tag{4.4.21}$$

Using Eq. (4.4.21) we can calculate void ratio:

$$e = \frac{\omega\, \rho_s}{100\, S_r\, \rho_w} = \frac{30{\cdot}2.62 kg/m^3}{100{\cdot}1.0{\cdot}1.0\ kg/m^3} = \mathbf{0.786} \tag{4.4.22}$$

and then calculate weights (substituting $\gamma_s = \rho_s g = 25.70\ kN/m^3$ and $\gamma_w = 9.81\ kN/m^3$):

$$\gamma = \gamma_{sat} = \frac{1}{1+e}\gamma_s + \frac{e}{1+e} S_r \gamma_w = \frac{25.70\,\frac{kN}{m^3}}{1+0.786} + \frac{0.786{\cdot}1.0{\cdot}9.81\frac{kN}{m^3}}{1+0.786} = \mathbf{18.71}\,\frac{\boldsymbol{kN}}{\boldsymbol{m^3}} \tag{4.4.23}$$

From Eq. (4.4.6) we can calculate the dry unit weight

$$\gamma_d = \frac{100\,\gamma}{100+\omega} = \frac{100{\cdot}18.71}{100+30} = \mathbf{14.39}\,\frac{\boldsymbol{kN}}{\boldsymbol{m^3}} \tag{4.4.24}$$

The total weight of water required to saturate a soil mass of volume V=10 m^3

$$W_w = W_{tot} - W_s = \gamma\, V - \gamma_d\, V \tag{4.4.25}$$

Substituting numerical values we obtain

$$W_w = 18.71\,\frac{kN}{m^3} \cdot 10m^3 - 14.39\,\frac{kN}{m^3} \cdot 10m^3 = \mathbf{43.2\ kN} \tag{4.4.26}$$

4.5 IN-SITU STRESS STATE IN SOIL - CASE PROBLEM (K. JÓZEFIAK, A. ZBICIAK)

Problem: A 3.5-m-thick silt layer underlain by a 3-m-thick clay layer is shown in Figure 4.5.1a. Calculate the total stress, pore pressure, and effective stress at points A, B, C, D and E. The water table is located 2.5 m below the ground

surface. The capillary rise in the silt layer is 1.5 m. Assume that the silt layer has a degree of saturation $S_r = 60\%$ in the zone of capillary rise.

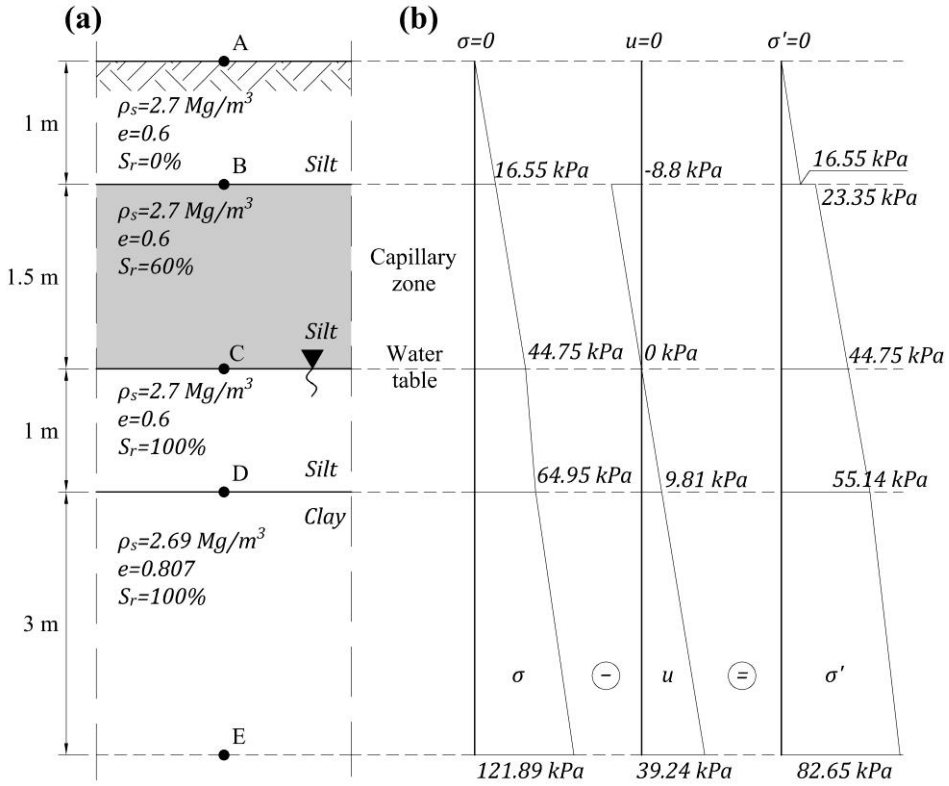

Fig. 4.5.1a. Case problem no. 1: (a) data given, (b) solution.

First we have to calculate densities of individual soil layers. For layer AB (see Equation (4.4.16)):

$$\gamma^{AB} = \gamma_d = \frac{\rho_s g + e\, S_r \gamma_w}{1+e} = \frac{2.7 \cdot 9.81}{1+0.6} = 16.55 \frac{kN}{m^3} \tag{4.5.1}$$

For layers BC, CD and DE respectively:

$$\gamma^{BC} = \frac{\rho_s g + e\, S_r \gamma_w}{1+e} = \frac{2.7 \cdot 9.81 + 0.6 \cdot 0.6 \cdot 9.81}{1+0.6} = 18.8 \frac{kN}{m^3} \tag{4.5.2}$$

$$\gamma^{CD} = \gamma_{sat} = \frac{\rho_s g + e\, S_r \gamma_w}{1+e} = \frac{2.7 \cdot 9.81 + 0.6 \cdot 1.0 \cdot 9.81}{1+0.6} = 20.2 \frac{kN}{m^3} \tag{4.5.3}$$

$$\gamma^{BC} = \gamma_{sat} = \frac{\rho_s g + e\, S_r \gamma_w}{1+e} = \frac{2.69 \cdot 9.81 + 0.807 \cdot 1.0 \cdot 9.81}{1+0.807} = 18.98 \frac{kN}{m^3} \tag{4.5.4}$$

Then we calculate total stress in every point

$$\sigma_{B,above} = \sigma_{B,below} = 16.55 \cdot 1.0 = 16.55kPa \quad (4.5.5)$$

$$\sigma_C = 16.55 + 18.8 \cdot 1.5 = 44.75\ kPa \quad (4.5.6)$$

$$\sigma_D = 44.75 + 20.2 \cdot 1.0 = 64.95\ kPa \quad (4.5.7)$$

$$\sigma_E = 64.95 + 18.98 \cdot 3.0 = 121.89\ kPa \quad (4.5.8)$$

and pore pressure

$$u_{B,below} = -\frac{60\%}{100\%} \cdot 9.81 \cdot 1.5 = -8.8kPa \quad (4.5.9)$$

$$u_C = 0 \quad (4.5.10)$$

$$u_D = 9.81 \cdot 1.0 = 9.81kPa \quad (4.5.11)$$

$$u_E = 9.81 + 9.81 \cdot 3.0 = 39.24\ kPa \quad (4.5.12)$$

By subtracting pore pressure from total stress we obtain effective stress

$$\sigma'_{B,above} = \sigma_B = 16.55kPa \quad (4.5.13)$$

$$\sigma'_{B,below} = \sigma_B - u_{B,below} = 16.55 - (-8.8) = 25.38\ kPa \quad (4.5.14)$$

$$\sigma'_C = \sigma_C = 44.75kPa \quad (4.5.15)$$

$$\sigma'_D = \sigma_D - u_D = 64.95 - 9.81 = 55.14kPa \quad (4.5.16)$$

$$\sigma'_E = \sigma_E - u_E = 121.89 - 39.24 = 82.65kPa \quad (4.5.17)$$

Graphs of total and effective in-situ stress and pore pressure are shown in Figure 4.5.1b.

4.6 SHEAR STRENGTH OF SOIL - CASE PROBLEM (K. JÓZEFIAK, A. ZBICIAK)

Problem 1: A direct shear test is run on a medium dense silty sand with the normal stress $\sigma_n = 65\ kPa$. Soil's coefficient of lateral earth pressure at rest was estimated as $K_0 = 0.5$. At failure the normal stress is still $65\ kPa$ and the shear stress is $41\ kPa$. Draw the Mohr circles for the initial conditions and at failure. Determine the principal stresses at failure.

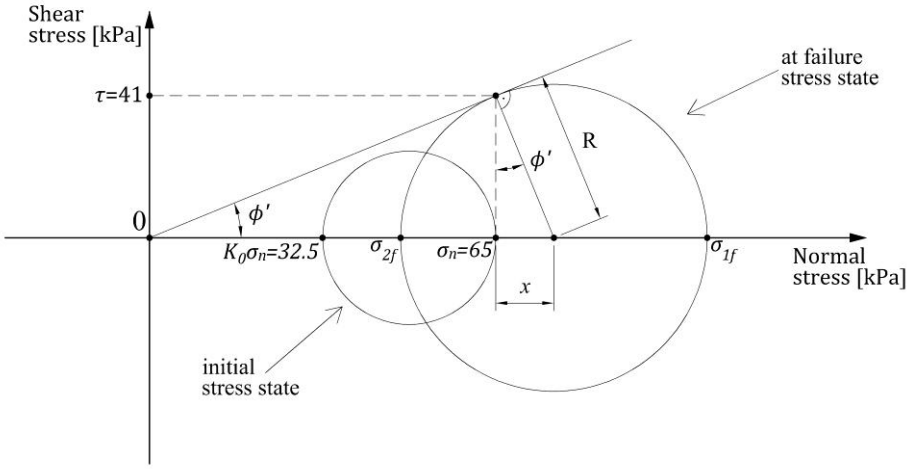

Fig. 4.6.1. Mohr circles for the initial conditions and at failure in the case problem no. 1.

Solution. The Mohr circles for the initial and at failure conditions are shown in Figure 4.6.1. The horizontal stress is related to the vertical stress σ_n by the K_0 coefficient, so that

$$\sigma_h = K_0\sigma_n = 0.5 \cdot 65\ kPa = 32.5\ kPa \tag{4.6.1}$$

According to Mohr-Coulomb failure criterion the Mohr circle at failure has to be tangent to the line defined by the function $\tau_f = c' + \sigma_n \tan\phi'$ as shown in Figure 4.6.1. Silty sand (siSa) is a granular soil (non-cohesive) so for this kind of soil we know that $c' = 0$. Hence, the effective internal friction angle $\phi' = \arctan\frac{41kPa}{65kPa} = 32°$. The distance $x = 41kPa \tan 32° = 25.62kPa$.

To calculate principal stresses at failure, first we have to determine the Mohr's circle radius at failure, R. From the Pythagoras theorem (see Fig. 4.6.1)

$$R = \sqrt{(25.62kPa)^2 + (41kPa)^2} = 48.35\ kPa \tag{4.6.2}$$

Then, the principal stresses at failure are (see Fig. 4.6.1)

$$\sigma_{1f} = 65kPa + x + R = 65 + 25.62 + 48.35 \cong \mathbf{139\ kPa} \tag{4.6.3}$$

$$\sigma_{2f} = 65kPa + x - R = 65 + 25.62 - 48.35 \cong \mathbf{42.3\ kPa} \tag{4.6.4}$$

4.7 SHALLOW FOUNDATIONS - CASE PROBLEMS (K. JÓZEFIAK, A. ZBICIAK)

Problem 1. For the rigid rectangular footing shown in Figure 4.7.1, determine the contact pressure distribution. Find the length of the footing required to achieve a uniform contact pressure if its length can be increased only beyond the right-hand side column.

Solution. First we have to calculate total vertical load

$$N = 1100kN + 500kN = 1600kN \tag{4.7.1}$$

and total momentum in the foundation centre

$$M = 580kNm + 1100kN \cdot 2.5m - 500kN \cdot 2.5m = 2080kNm \tag{4.7.2}$$

Bending moment can be replaced by a force N rotating about a certain point

$$M = N \cdot e \tag{4.7.3}$$

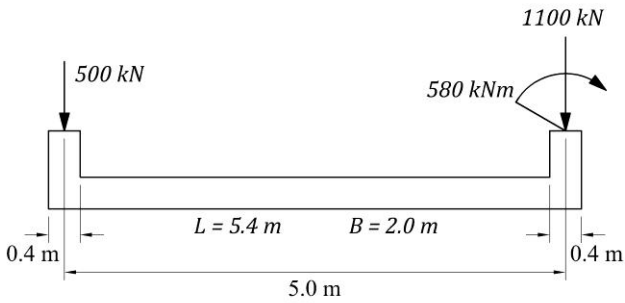

Fig. 4.7.1. Dimensions of the footing given in case problem no. 1.

Force eccentricity is equal (see Figure 4.7.2)

$$e = \frac{M}{N} = \frac{2080kNm}{1600kN} = 1.3m \tag{4.7.4}$$

Let's check if force N is applied inside cross-section's core

$$e = 1.3m > \frac{5.4}{6} \tag{4.7.5}$$

so the force is outside the core. This means some of foundation base will separate from the subgrade. This also means that stress distribution under foundation

base will be of rectangular shape. Formulating equation of equilibrium assuming that force N must be applied over triangle's geometry (mass) center (see Fig. 4.7.2)

$$\frac{1}{2}\sigma_{max} 3\ c\ B = N \tag{4.7.6}$$

we obtain

$$\sigma_{max} = \frac{2N}{3Bc} = \frac{2 \cdot 1600kN}{3 \cdot 2.0m \cdot 1.4m} = \mathbf{380.95kPa} \tag{4.7.7}$$

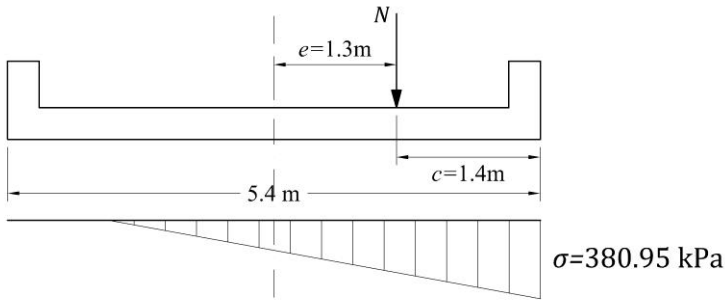

Fig. 4.7.2. Stress distribution under footing in case problem no. 1.

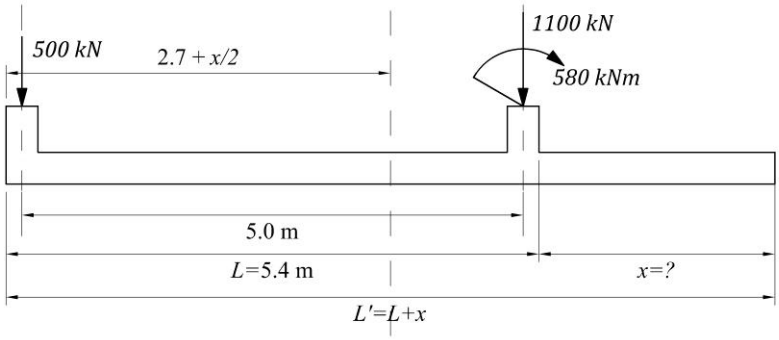

Fig. 4.7.3. Calculation of length of the footing required to achieve a uniform contact pressure in case problem no. 1.

To find the length x required to achieve a uniform contact the momentum has to be equal zero as it is shown in Fig. 4.7.3.

$$M = 0 \ \Rightarrow\ 500 \cdot \left(2.5 + \frac{x}{2}\right) = 580 + 1100 \cdot \left(5 - 2.5 - \frac{x}{2}\right) \tag{4.7.8}$$

$$1250 + 250x = 580 + 2750 - 550x \quad (4.7.9)$$

$$800x = 2080 \quad (4.7.10)$$

$$x = \mathbf{2.6m} \quad (4.7.11)$$

$$L' = L + x = 5.4m + 2.6m = \mathbf{8.0m} \quad (4.7.12)$$

and the uniform pressure is:

$$q = \frac{N}{BL} = \frac{1600}{8 \cdot 2} = \mathbf{100kPa} \quad (4.7.13)$$

Problem 2.

Check if bearing capacity of the foundation shown in Fig. 4.7.4. is exceeded according to Euro code EN 1997-1:2004, Euro code 7: Geotechnical design - Part 1: General rules, European Committee for Standardization, 2004, that is if $V \leq R_{EC7}$ and $V \leq R_{EC7}^{ud}$.

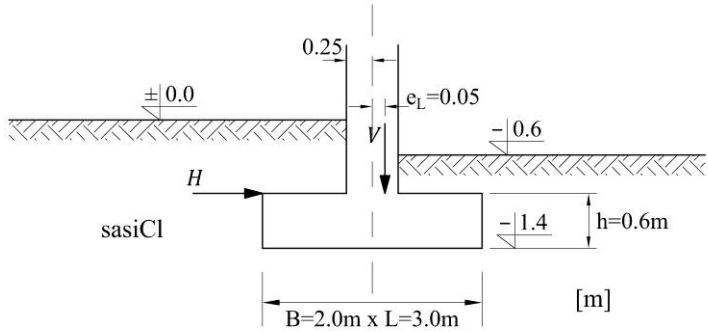

Fig. 4.7.4. Footing geometry for case problem no. 2

4.8 REFERENCES

[1] ISO 14688-1:2002, Geotechnical investigation and testing -- Identification and classification of soil -- Part 1: Identification and description, International Organization for Standardization, 2002

[R1] DIN 18218:2010-01: Pressure of fresh concrete on vertical formwork. Berlin, 2010.